DESIGN OF CABLE BOLTS USING NUMERICAL MODELLING

By

Malek Bouteldja

Department of Mining and Metallurgical Engineering

McGill University, Montréal, Canada

April 2000

A thesis submitted to the Faculty of Graduate Studies and Research in partial fulfillment of the requirements of the degree of Doctor of Philosophy

0-612-64522-3

ABSTRACT

Cable bolt supports are widely used as ground support in underground hard rock and coal mines. During the last two decades, the cable bolt technology has improved significantly and new types of cable bolts, new grouts and new installation methods and pumps have been introduced and successfully developed. The design of cable bolts is currently attempted by empirical methods based on rockmass characterization. However, until such methods do not take into account all the important parameters affecting the mechanical behaviour of cable bolts namely, the type of cable geometry, grout quality, stiffness of the host medium, the amount of confining pressure and the presence of end anchorage and pretension.

This thesis deals with the numerical modelling of cable bolts considering all of the above mentioned factors. To evaluate the shear bond stiffness of cable bolts, which simulate the interface between the cable bolt and the rockmass, a new empirical model is developed. A database with data of pull-out tests is constructed. Empirical relations were derived between the shear bond stiffness and the variation of confining pressure, the modulus of elasticity of host medium and the water:cement ratio. The relations were derived for three types of cables (standard cable, nutcase cable and garford bulb cable). A new numerical model using the finite element method is developed for the numerical simulation of cable bolts. Together with the empirical model for shear bond stiffness, the numerical model computes the load distribution along the cable bolt and thus can simulate fully grouted, partially grouted , end anchored and tensioned cable bolts. The model is implemented in an existing finite element code (e-z tools). Parametric analyses are performed on the new model, and proved useful in the demonstration of the role of each design parameter.

A new design methodology is proposed to evaluate the load distribution along the cable bolt. Two case studies are presented: a stope hanging-wall support by cable bolt

in a hardrock mine and a tailgate secondary supports in a coal mine. A comparison with measurements in the field shows good agreement with computed forces.

RÉSUMÉ

Les câbles d'ancrage sont trés utilisés comme souténement pour le contrôle de terrain dans les mines souterraines de roches dures et les mines de charbon. Durant la dernière décennie, la technologie des câbles d'ancrage a évoluée et de nouveaux types de câbles, de coulis de scellement, de méthodes d'installation et de pompes ont été développés. La conception des câbles d'ancrage peut être faite en utilisant des méthodes empiriques basées sur la classification des massifs rocheux. Cependant, jusqu'a maintenant il n'existe pas une méthode exacte pour la conception des câbles d'ancrage qui prenne en compte tous les paramètres importants affectant leur comportement : type de câble, coulis de scellement, rigidité du massif rocheux, pression de confinement, plaques d'appui et pretension.

Cette thèse traite de la modélisation numérique des câbles d'ancrage en considérant tous ces facteurs. Pour évaluer la rigidité de contact en cisaillement entre le câble et le massif rocheux, un modèle empirique a été développé. Une base de données avec des données d'essais d'arrachement a été construite. Des relations empiriques ont été trouvées entre la rigidité de contact en cisaillement et la variation de la pression de confinement qui est l'un des principaux facteurs pour la rupture des câbles sur le terrain. Des relations ont été dérivées pour trois types de câble (câble monotoron, câble à manche, câble à bulbe). Un nouveau modèle numérique utilisant la méthode des éléments finis a été développé pour la conception des câbles d'ancrage. Utilisant le modèle empirique pour l'évaluation de la rigidité de contact au cisaillement, le modèle numérique permet de simuler des câbles complétement et partiellement scellés, des câbles ancrés avec des plaques d'appui et des câbles tendus. Le modèle a été implémenté dans un code de calcul existant (e-z tools). Des analyses paramétriques ont été réalisées sur le nouveau modèle qui a permis d'identifier les paramètres les plus importants.

Une méthodologie de conception pour évaluer la distribution des forces le long des câbles d'ancrage est proposée et deux cas d'études sont présentés: un cas utilisant les câbles d'ancrage pour le soutènement des murs supérieurs des chantiers d'abattage dans les mines de roches dures et un autre exemple utilisant les câbles d'ancrage comme soutènement secondaire dans les galeries de mines de charbon. Une comparaison avec les mesures sur le terrain montre un bon accord avec les forces calculées par le modèle.

ACKNOWLEDGEMENTS

I would like to thank my supervisor Prof. Hani Mitri for his guidance through this thesis and his financial contribution. I also wish to thank the mining engineering department of McGill University for the financial support.

I also thank Mr. Steve Tadolini, of Excel mining Inc. (USA), Mr John Hennings, of Cambior, Mr Al Campoli , of Fosroc Inc. (USA) for the information about the case studies.

Finally, I want to thank the numerical modelling group for their help, especially Mr. Joseph Marwan, my friends and colleagues.

TABLE OF CONTENTS

CHAPTER 4

CHAPTER 5

LIST OF FIGURES

LIST OF TABLES

LIST OF SYMBOLS

A	Rock stress factor
A_c	Cross sectional area of the cable
a	Slope of shear bond stiffness versus confining pressure
a_0	Slope of shear bond stiffness versus modulus of elasticity
B	Joint orientation factor
$[B_b]$	Strain-displacement matrix of the bar element
[B]	Strain-displacement matrix
$[B]^T$	Transpose of B matrix
b	Intercept of shear bond stiffness versus confining pressure
b_0	Intercept of shear bond stiffness versus modulus of elasticity
BSM	Bond strength model
C	Gravity adjustment factor
D	Strain-displacement matrix
c	Cohesion
E	Modulus of elasticity
Ec	modulus of elasticity of the cable
E_{RM}	Rock mass modulus
E_R	Corrected rock mass modulus
ESR	Excavation support ratio
E.L	Embedment length
F	Load vector
F_c^0	Initial load vector
F_a	Axial force
F_i	Force acting at node i
F_j	Force acting at node j
GRC	Geomechanics Research Center
H	Depth below surface
HR	Hydraulic radius
i	Dilation angle
i_0	Apparent dilation angle
J_n	Joint set number
J_r	Joint roughness number
J_a	Joint alteration number
J_w	Joint water reduction number
k	Shear bond stiffness
k_b	Bar element stiffness matrix
k_e	Spring element stiffness matrix

k_s	Shear spring stiffness
k_c	Stiffness matric of the cable element in local coordinates
K	Stiffness matrix
K_g	Stiffness matrix of the cable element in local coordinates
K_0	The horizontal to vertical in-situ stress ratio
l	Length of cable element
L	Length of cable
M_c	Mass of hydrous cement
M_w	Mass of water
M'	Slope elastic grout
M"	Slope split grout
m	Material value for Hoek-Brown criterion
N	Stability number
[N]	Shape function matrix
$[N]^T$	Transpose of N matrix
N'	Modified stability number
NGI	Norwegian Geotechnical Institute classification
P	Axial load
P_{max}	Maximum load in cable during jacking
P_{res}	Residual load remaining in the cable after the jack is removed
P_w	Ratio of jacking load applied to wedges
p_1	Radial interface pressure
p_2	Confining pressure
Q	Rock mass quality
Q'	Modified rock mass quality
R	Reduction factor for rock mass modulus
RQD	Rock quality designation
RMR	Rock mass rating
MRMR	Mining rock mass rating
S	Slip
s	Material value for Hoek-Brown criterion
S.L	Safety level
SRF	Stress reduction factor
T	Transformation matrix from the local to global coordinates
$[T]^T$	Transpose of T matrix

t Tension force

t_i Tension force applied of node i

t_j Tension force applied of node j

u_a, u_{ax} Axial displacement

u_r, u_{lat} Radial displacement

U_s Strain energy stored in the shear springs

U_i Axial displacement of node i

U_j Axial displacement of node j

u_s Spring displacement

UCS Unconfined compressive strength

V element volume

W:C Water/cement ratio

x_i, y_j Global coordinates of node I

y_i, y_j Global coordinates at node j

$\underline{x}_i$, $\underline{y}_i$ Local cordinates of node i

$\underline{y}_i$, $\underline{y}_i$ Local cordinates of node j

α Coefficient of stretch of the cable

β Reduction coefficient of dilation angle

γ Unit weight of the rock

ΔL Short cable length

ε Strain

ϕ Internal friction of the material

ν Poisson's ratio

σ_1 Major principal stress

σ_3 Minor principal stress

σ_{all} Stress strength

σ_{max} Maximum normal stress

σ_c Uniaxial compressive strength

σ_h Horizontal stress

σ^0 Initial stress vector

σ_v Vertical stress

σ_t Tensile strength of the rock mass

$\Delta\sigma$ Variation of confining stress

σ_{lim} Limiting stress of grout

σ_{cg} Compressive strength of grout

τ Shear stress

τ_{all} Shear strength

τ_{max} Maximum shear stress

ξ Ratio of axial coordinates to length of cable element

CHAPTER 1
INTRODUCTION

1.1 General

Rock supports are used in both civil and mining engineering projects to reinforce the rock mass and to help it to support itself. Rock supports can be temporary or permanent; they can also be classified as: internal and external. Internal supports include bolting, anchoring and ground modification techniques such as ground freezing and jet grouting. External supports take many forms like backfill, shotcrete, steel arches, timber cribs and props.

Rock reinforcement by bolting and anchoring can be divided into three basic types :

- Mechanically anchored rockbolts.
- Grouted rock bolts and cable bolts
- Friction anchored rockbolts.

Generally, wire mesh and shotcrete are used in combination with rockbolts. Wire mesh is used to support small pieces of loose rock or as reinforcement for shotcrete. Two types of wire meshes are commonly used in underground excavations: chainlink mesh and weld mesh. Shotcrete is increasingly used to provide support to the rock surface between rockbolts. There are two basic types of shotcrete: the dry-mix shotcrete where the mix is transported dry and water is added at the nozzle. The wet–mix shotcrete has the same components as the dry-mix, except that the water is already added in the mix before transportation.

The history of rock anchorages dates from 1934 (Littlejohn, 1992) when Coyne pioneered their use during the raising of the Cheurfas dam in Algeria (Drouhin, 1935).

Since then, the use of rock anchors has increased all over the world. In mining, strata bolting was introduced on a large scale in American coal mines in the late 1940s. The United States Bureau of Mines (USBM) found that mechanical shell anchored roof bolts were economical and efficient support elements in coal mines, and in the late 1940s a research program was initiated to calibrate roof bolts. By 1960, roof bolts became important, safe supporting elements. In 1970, the U.S. Coal Mine Health and Safety Act enforced the law that underground openings must be supported by rock bolts and must not be operated under unsupported areas.

Cable bolt support was introduced in mining in the mid 1960's in Australia and a few years later it was applied in Canada. The first Canadian cable bolting experiment was conducted at the Noranda Geco division, Ontario, to reinforce the backs and walls of large open stope (Gramoli, 1975). Since then, much research has been carried out to better understand the behaviour of cable bolts using laboratory and field pull-out tests. Analytical and numerical models were developed (Mitri and Rajaie, 1990; Kaiser, Yazici and Nosé, 1992; Hyett and Bawden, 1992). The technology of cable bolting has made leap advances and in the last decades innovative cable bolt geometries, grout mixes, grout pumps and installation techniques have been introduced, tested and shown to give promising results. In 1996, Hutchinson and Diederichs produced a handbook and made a comprehensive review of what was done so far in the field of cablebolting. The need to monitor the behaviour of cable bolts in the field was recognized and new instrumentation methods were introduced (Choquet, 1988; Chekired et al., 1997; Bawden et al., 1997).

1.2 Classification of rock anchors

Rock anchors have been used for many years for the support of underground and surface excavations in both mining and civil engineering projects. Different types of rock anchors are used worldwide.

For mechanically anchored rockbolts, the expansion shell anchored rockbolts are the most common form of mechanically anchored rockbolt. The components of a typical expansion shell anchor are a tapered cone with an internal thread and a pair of wedges held in place by a bail. These expansion shell anchors work well in hard rock but they are not very effective in heavily jointed rocks and in soft rocks (Hoek, 1998). In such rocks, the use of resin cartridge anchors is recommended.

In permanent support applications, the use of fully resin-grouted rockbolts is recommended. The cartridges are pushed to the end of the drillhole ahead of the bolt rod that is then spun into the resin cartridges by the drill. The high unit cost of resin cartridges limits the use of fully resin grouted rock bolt.

The most commonly used grouted rock bolt is the rebar or threaded bar made of steel. Different surface geometries of this type exist on the market; cement or resin are used as grouting agents. They are used for temporary as well as permanent support under various rock condition.Grouted rebar with resin gives rapid support after installation but the disadvantage is mainly the cost. Grouted rockbolts with cement, when properly installed, provide a durable reinforcement system but the use of cement requires several days before the bolt can be considered effective and quality of grout is difficult to control (Stillborg, 1994).

More recent innovations in the grouted rockbolt include the GRP rock bolts developed by Weidman, injection bolt, self drilling bolt and resin bolt.

Another family of rockbolts is the friction anchored rockbolts , which rely on the frictional resistance to sliding between the rock and the bolt surface to provide support action. Friction is generated by a radial force against the borehole wall over the length of the bolt. This family of rockbolts is now very popular in mining because of its rapid and simple installation. Two friction anchored rockbolts types are available on the market: the Split Set and the Swellex.

Split Set rockbolts were developed by Scott (1976) and are manufactured and distributed by Ingersoll-Rand. The system consists of a slotted high strength tube and a face plate. It is installed by pushing it into a slightly undersized hole. The Split Set is very common in mining throughout the world but is seldom used in civil engineering applications. The problem with this type of rockbolt is the corrosion and it cannot be used in long term installations unless treated to resist corrosion.

Swellex rock bolts were developed and marketed by Atlas Copco, no pushing force is required during insertion and the rockbolt is activated by injection of high pressure water. Like the Split Set, corrosion is a disadvantage because the outer surface of the tube is in direct contact with the rock. Atlas Copco developed a new type with effective corrosion resistant coatings. Speed of installation is the principal advantage of the Swellex system as compared with conventional rockbolts and cement grout rock bolts. The Swellex rockbolt is commonly used in mining industry and is increasingly used in tunneling work for civil engineering applications.

Cable bolts have been used extensively in underground mines in recent years. The difference with conventional rockbolts is the increased bolt length, its flexibility and the high load bearing capacity mobilized in the cable. A conventional cable bolt is a flexible tendon consisting of a number of steel wires, which is grouted in a borehole. Modern cable bolts in hard rock mining are based on the 7-wire steel strand. The wires are made of high strength steel, and give a total ultimate tensile strength of 26 tonnes. Modified geometry cable bolts were subsequently introduced; they include the bulbed cable, steel birdcage and cable strand with buttons (Figure 1.1). During the early 1990s, glass fibre cable bolts and composite cable bolts were developed to eventually become a viable alternative to steel cable bolting; however steel conventionnal cable bolts still take the lion's share of the cable bolting market today.

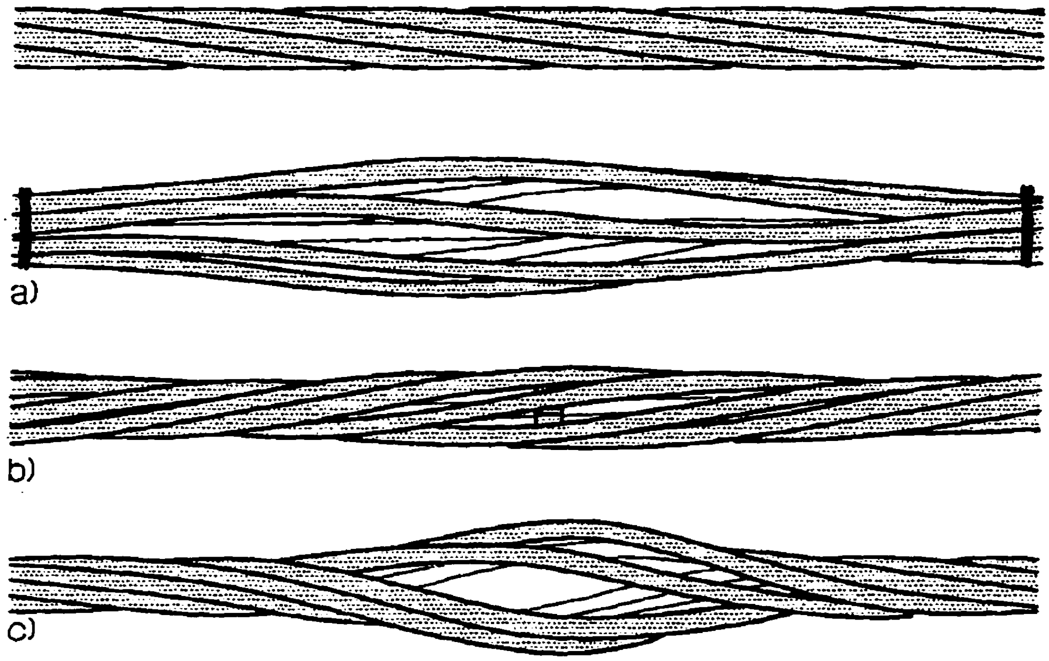

Figure 1.1 : Standard cable bolts and modified cable geometries
a) birdcaged cable b) nutcaged cable c) bulbed strand
(after Hutchinson and Diederichs, 1996)

1.3 Study problem

Since their introduction in the mining industry, cablebolts have become very popular and their applications increased in underground hard rock mines and coal mines to provide a safe working environment, to increase rock mass stability and to control ore dilution from the stope boundaries (Figure 1.2).

The natural stress conditions in the field, the interaction between the cable and host rock, the load transfer mechanisms and possible failure modes have made the design of cable bolts very difficult; some methods were developed for the design of cable bolts. In the beginning, empirical methods were used, later analytical methods and numerical methods were developed. Due to the complexity of the problem, there is no real method which will take into account all the important factors influencing the behaviour of cable bolts in the field: effect of confining pressure, effect of rockmass stiffness, effect of grout mix and additives, effect of cable bolt geometry as well as end anchoring and tensioning.

The shear stress, which resists slipping of the cable is a product of the confining pressure and the coefficient of friction between the steel wires and the grout. Shear strength increases with higher grout strength, increases in the rock stiffness and increases in confining stresses in the rock after installation of the cable. Decrease in shear strength can be expected if one of these factors decrease and causes reduction in cable capacity. Many theoretical models were developed (Yazici and Kaiser 1992, Hyett et al 1992) but these models have their own limitations as they don't take into account all the factors influencing the behaviour of cable bolts.

The objective in the design of cablebolts is the evaluation of deformations and distribution of loads in the cable which should meet the design requirement into a specified safety factor. The problem is how to determine the axial load distribution and how to design the cable bolts while taking into consideration all important design

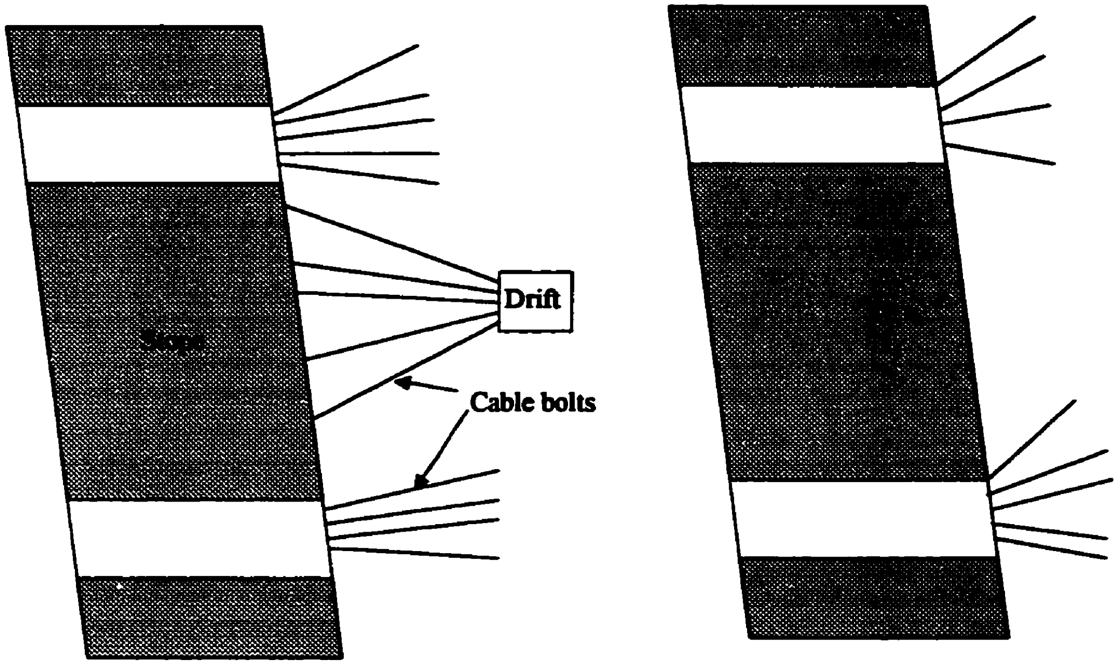

a) Open stope hanging wall support

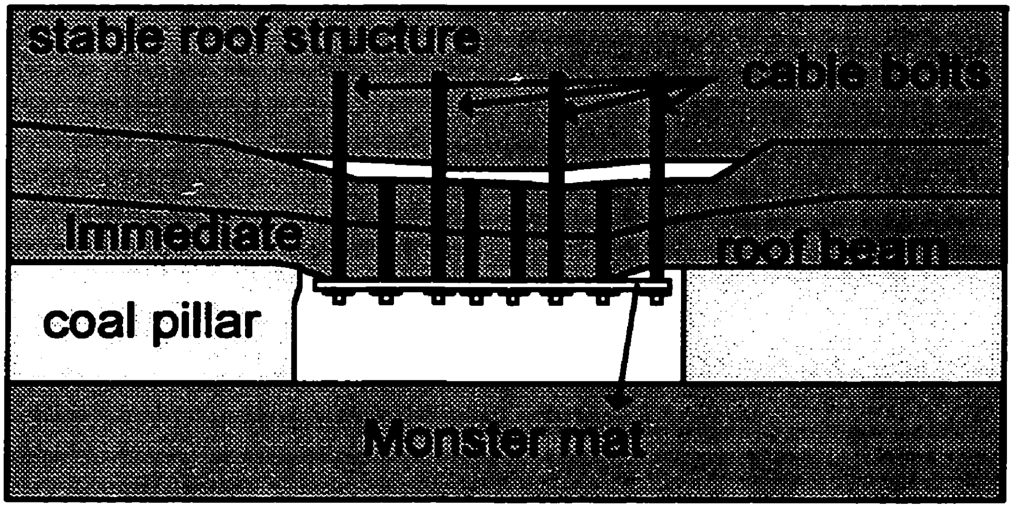

a) Gateroad support in coal mine

Figure 1.2: Application of cable bolts in underground mines

parameters: type of cables, tensioning, anchoring, properties of host rock and mining induced stress.

1.4 Scope and objectives

The primary objective of this thesis is to develop a new design/analysis method for cable bolt support systems. In particular this method will consider the effect of various parameters influencing the behaviour of cable bolts. These parameters include confining pressure, host rock medium stiffness, cable geometry, grout, end anchoring and tensioning. An empirical model for the shear bond stiffness, taking the effects of cable geometry, host medium and confining pressure will be developed. Coupled with a new numerical model for the prediction of load distribution along cable bolts which have the capability of simulating end plates and pretension, the new design method will be a key tool for the ground control engineer for the design of cable bolts and should take into account all important parameters as cable length and orientation, modified cable geometry, bonding effect of cement or resin grout, passive or tensioned bolt, effect of rock mass stiffness and effect of confining pressure.

This thesis will focus on the application of cable bolt supports in mines. For this purpose two case studies are presented. They are:

- Coal mine: gateroad support by cable bolts and rock bolts.
- Hard rock mine: hanging wall support by cable bolts.

1.5 Thesis outline

This introductory chapter is followed by a chapter focusing on cable bolt technology. Chapter 3 presents the different design methods for cable bolts. Chapter 4 presents the empirical model for cable shear bond stiffness to take into account the effect of the water:cement ratio, the stiffness of the host medium and the confining stress. Chapter

5 describes the numerical model and the formulation of the new model with its features and limitations. Chapter 6 presents a parametric study and the influence of different important design parameters. Chapter 7 is an application of the model to two case studies one for a hardrock mine and another for a coal mine. This is followed by chapter 8, which contain a summary of the main conclusion, and recommendations for further research.

CHAPTER 2
CABLE BOLTING TECHNOLOGY

2.1 Introduction

Cable bolts were first introduced in underground hardrock mines during the seventies and later they were used in underground coal mines. The technology of cable bolts was developed initially for cut and fill mining (Fuller , 1983), however, it quickly found many other applications in underground mining; see Figure 2.1. In surface excavations the systematic use of cable bolting has resulted in more stable slopes and often enabled steeper pit slopes.

The early versions of cable bolts consisted of discarded winder rope and smooth pre-stressing wires. The pre-stressing wire was readily available and was made into cable bolts consisting of seven, straight, 7mm diameter, high tensile , steel wires arranged with plastic spacers (Windsor, 1992). The load transfer characteristics of plain wires is quite poor due to their smooth, straight profile and the Poisson effect which causes radial contraction. The conversion from plain wire to strand gave startling improvements in productivity, adaptability and mechanical performance. The first use of strand cable bolts was in the early 1970's in Broken Hill, Australia.

The cable bolting technology has been greatly improved over the last decade, with the introduction of new types of cables , grouts and grout pumps.

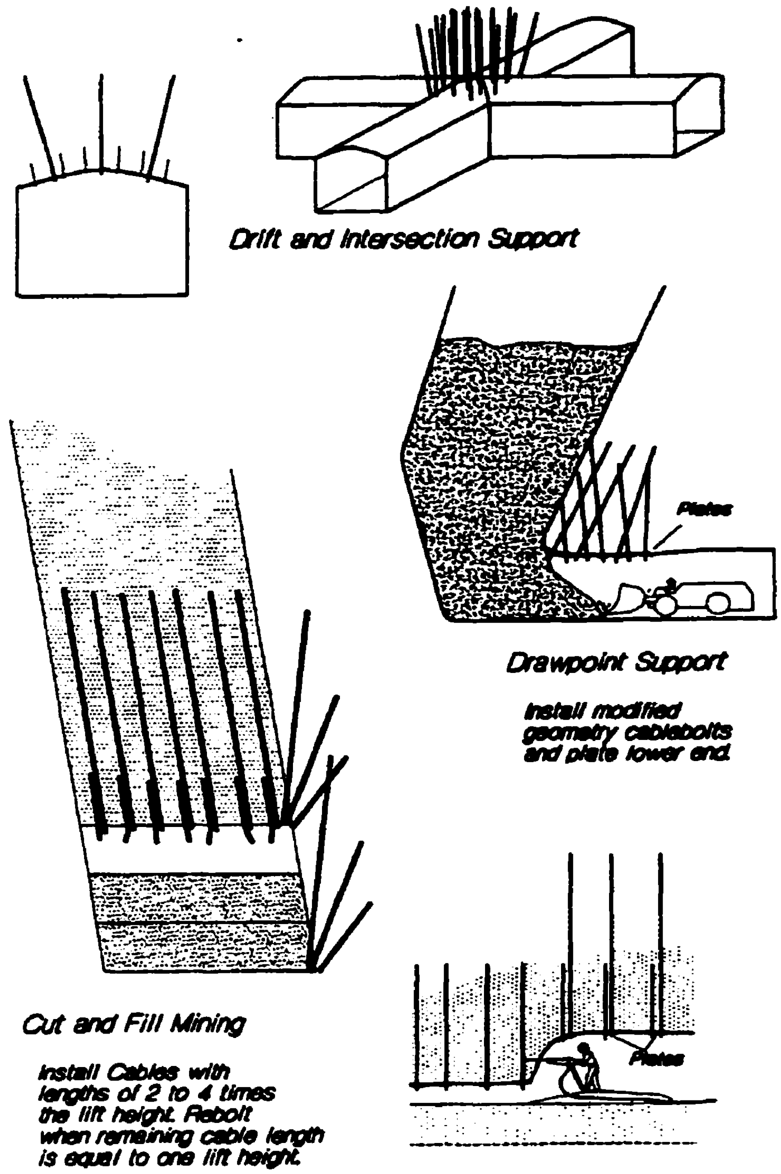

Figure 2.1: Cable bolt applications in underground mining (after Hutchinson and Diederichs, 1996)

2.2 Modified geometry cable bolts

The most common type of cable bolt used in Canadian mines is the 7 wire steel single strand cable. Other types of cable bolts which were introduced later included; double steel strand, birdcage and strand with buttons (Figure 2.2).

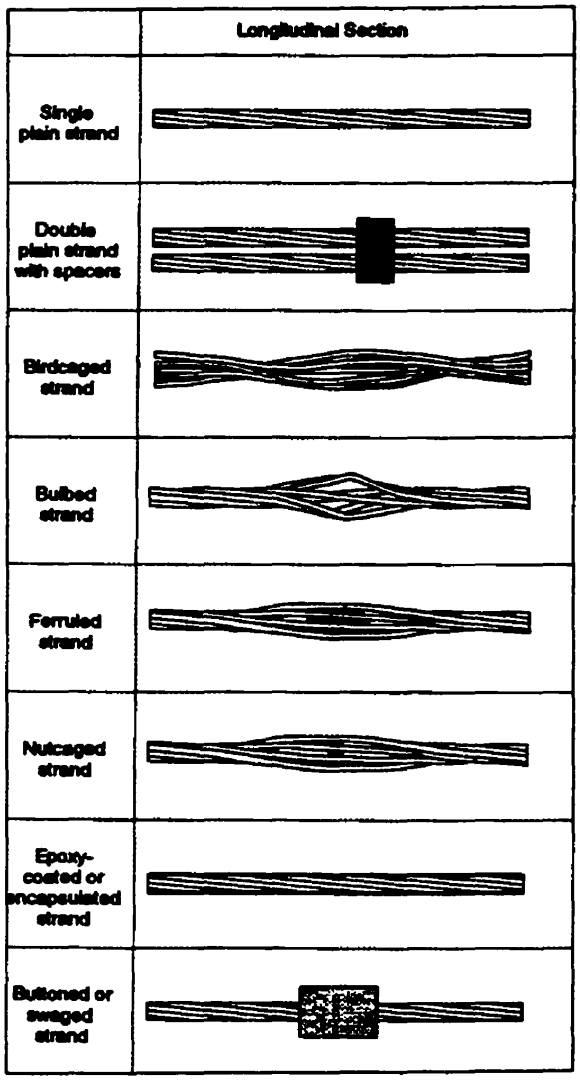

Figure 2.2: Types of cable bolts (Windsor, 1992)

Modern cable bolts for hard rock mining are primarily based on the 7-wire steel strand cable. It has a cross sectional area of 138.7 mm^2, an overall diameter of 15.2 mm, a circumference of approximately 63mm and a weight per unit length of 1.1 Kg/m. The wires are made of high strength steel, and give an ultimate tensile strength of 26 tonnes.

In 1983 the birdcaged cable bolt was developed for use in cut and fill mining at Mount Isa mine in Australia (Windsor, 1992). In the last few years a number of other modified strands have appeared in the form of 'bulbed' strand and 'ferruled' strand. The performance (pull out tests) of modified geometry cable bolts is generally higher than the performance of the 7 wire steel single strand.

A new type of cable bolt was developed during the early 1990s the glass fibre cable bolt (Pakalnis, 1994). Approximately 70% of the composites's volume consists of reinforcement fibre which provide 98% of the tensile strength. When a load is applied to a composite, it is transferred by the matrix material to the reinforcement fibre through interfacial shear (Figure 2.3). The surface coating of the cable can be changed in order to prevent severe corrosion and to alter the cable bolt's pull out resistance. Pull-out tests and direct-shear tests were conducted on this type of cable by Miller and Ward (1998). The ultimate tensile strengths of grouted fiberglass cable bolts were approximately 260 kN for the 7-tendon bundle and 408 kN for the 10-tendon bundle. Another type of cable bolt was recently introduced by Atlas Copco (Hoek, 1998) the hollow cable and this could reduce some of the grouting problems.

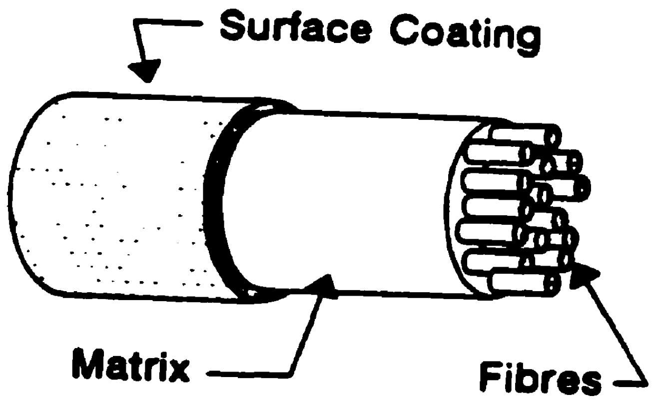

Figure 2.3: Fibre glass cable bolt (after Pakalnis, 1994)

2.3 Installation methods

In situ installation methods are numerous. The selection of the best method depends on the type of grout used. The cable bolt installation methods most commonly used for cement grout are : the breather tube method and the grout tube method (Hutchinson and Diederichs, 1996). The breather tube method (Figure 2.4) is used for upholes only with grout of 0.375-0.45 water:cement (w:c) ratio. The optimum grout for this method is one with w:c ratio of 0.4. This method should be used with caution in areas with open fractures which may cause grout loss with thinner grouts and may prevent complete filling of the hole. The main problem with this method is that it is difficult to detect when the hole is full of grout. It is preferable to stop grouting the bore hole only when grout returns along the bleed tube. In loose, thinly laminated ground, caution is required to avoid pressuring fractures causing the laminations to separate and rupture.

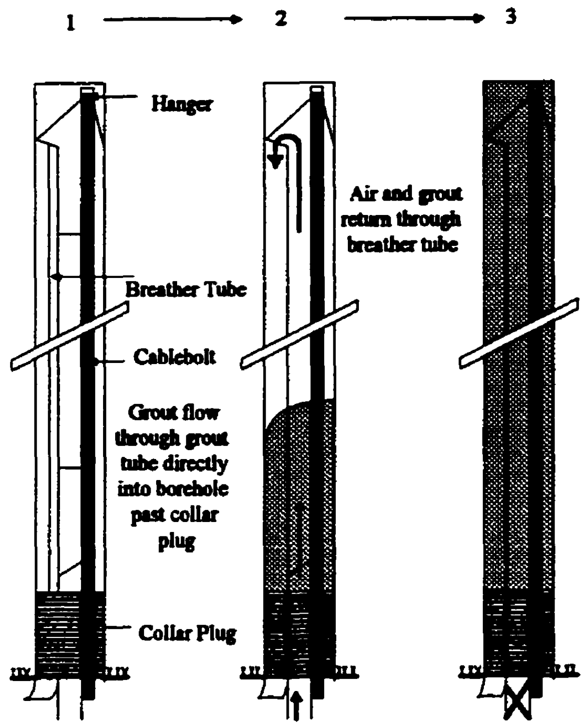

Figure 2.4: Breather tube method

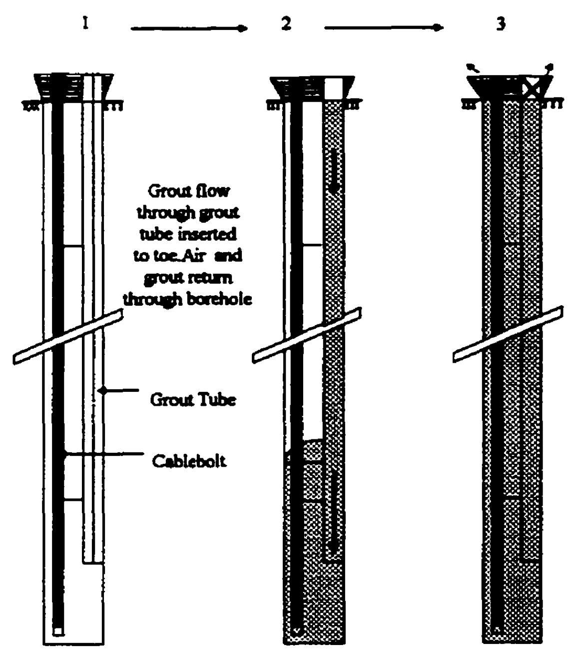

Figure 2.5: Grout tube method

The grout tube method (Figure 2.5) can be used for any hole orientation and with grout of 0.3 to 0.375 w:c ratio. The optimum grout for this method should have a w:c ratio of 0.35. These thicker grouts may cause pumping difficulties when less powerful pumps in long holes are used. The grout will have to be pumped into borehole and there is little danger of slump voids being formed. A higher water/cement ratio mix will certainly result in air voids in the grout column as a result of slumping of the grout. Modified cable, such as birdcage, ferruled or bulbed strand, should be grouted using a 0.4 water/cement ratio mix to ensure that the grout is fluid enough to fill the cage structure of the cable. Therefore the breather tube method must be used for these types of cables (Hoek, 1998).

For resin cable bolt, the installation is different (Figure 2.6). After drilling the desired hole based on the correct depth, resin cartridges are inserted into the drilled hole. The cable is inserted under rotation and after the resin cable bolt has been spun for the specified time, plates and nuts are mounted. Resin cartridges consist of two compartments separated by a physical barrier. One compartment contains a unsaturated polyester resin mastic and the other an organic peroxid catalyst. The rotation of the bolt during installation ruptures the cartridge, shreds the film, and mixes the two components, thus causing a chemical reaction which transforms the resin mastic to a rock solid anchor.

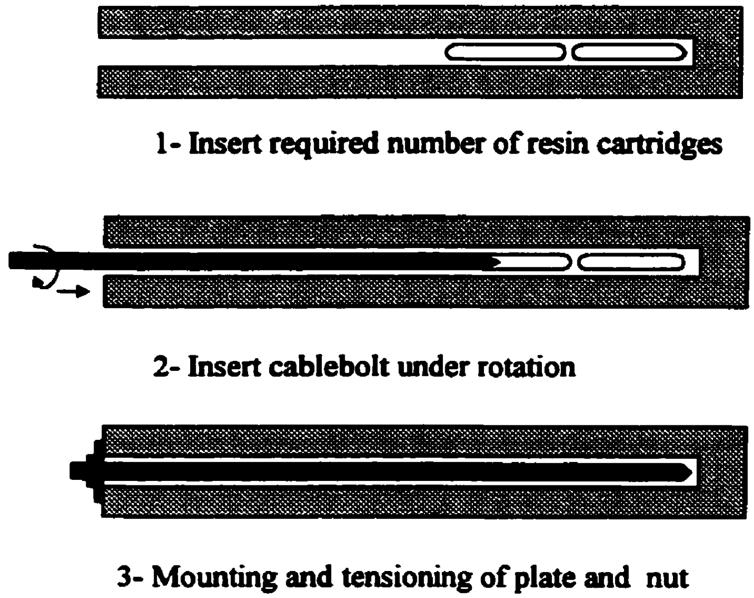

Figure 2.6: Resin-grouted cable bolt installation

2.4 Grout and resin mixes

Generally speaking, two groups of cable grouts are currently in use: cement- based grout and resin- based grout.

2.4.1 Cement -based grout

Cement grout consists of water and Portland cement with occasional use of additives such as sand, silica fume and plasticizers .

The most commonly used grout is from Portland cement type 10, and type 30. Type 30 is less attractive in practical mining than type 10 because of its higher cost and its lower uniaxial compressive strength.

The design of the grout for cable bolt applications depends on installation considerations (installation method, pumping rate, mixing time) and performance considerations (bond strength and load transfer mechanics, grout performance with time).

Three factors affect the physical and mechanical properties of the grout:
- The water:cement ratio.
- The use of additives.
- The pumping system.

These factors contribute to the ultimate cable bolt capacity.

The most important property of cement is the water:cement (w:c) ratio. It is defined as the ratio of the mass of water (M_w) used to create the fresh cement paste mix, to the mass of any hydrous cement (M_c) used in the same mix:

$$w{:}c = M_w(Kg) \, / \, M_c(Kg) \qquad (2.1)$$

The results of an experimental study done by Hyett et al. (1992) on Portland cement grouts showed that the properties of grout with water/cement ratios of 0.35 to 0.4 are better than those with ratios in excess of 0.4 (Figure 2.7). The ideal water/cement ratio for use with cable bolts lies in the range of 0.35 to 0.4. The influence of different additives on the physical and mechanical properties of cement grout was studied by Benmokrane et al. (1992). The introduction of aluminium-based, silica fume, and sand to the standard grout appears to improve the bond strength characteristics.

There are a number of different grouting equipment. The mixer selected must be able to completely mix a given volume of design consistency grout in a reasonable amount of time. The grout mixers currently in use in cablebolting applications include drum mixers, colloidal mixers and paddle mixers.

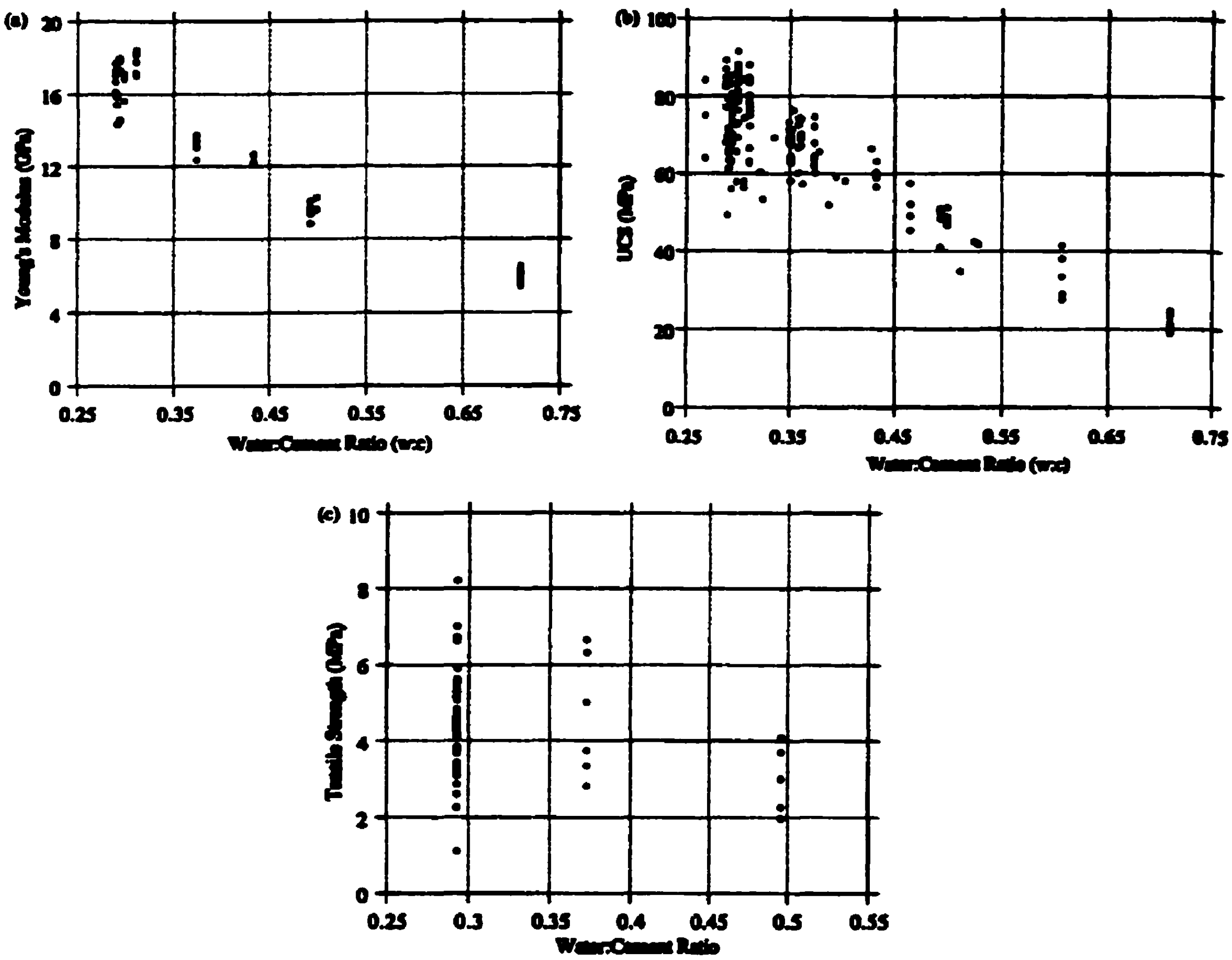

Figure 2.7: Variation of mechanical properties of cement grout with water:cement ratio (after Hyett et al., 1992)

2.4.2 Resin-based grout

Chemical grout is a new technology. The chemical grout is largely associated with roof control in longwall mining operations. The first chemical grout introduced in the mining industry was the polyurethane grout in 1971. The utilization of polyurethane grout is restricted by its limited range of physical and mechanical properties. A new type of chemical grout that was developed and became more popular is the polyester resin grout.

Resin-grouted cable bolting was initiated in the United States in 1992 and the procedure is new for underground coal mines (Tadolini, 1999). The mechanical properties of polyester grout would be particularly effective where the roof material is weak and under heavy loading (Campoli, 1999). Laboratory and field results indicate that keeping the resin at the top of the hole can be the difference between adequate and inadequate anchorage for resin-grouted cable.

An experimental work done by Kafarkis et al. (1998) showed that various resin formulations exhibited somewhat different responses. In the testing program of polyesters-based grouts, five resins, identified as Resins A through E, were used. Resin A and B provided initial indications of mechanical properties and pumpability characteristics of polyester-based grouts. Resin C, D and E were tested in formulations both with and without additive. Grout formulations with Resin E were designed to improve on the cohesion, deformability, pumpability, variable gel times and water resistance of the grout from the previously tested grouts. Among all of the formulations tested, it appears that grout formulations with Resin E exhibit the best laboratory deformability and strength characteristics for field testing (Figure 2.8). The range of properties identified with the various formulations suggests that polyester grout may prove to be a versatile ground support means for many applications in difficult ground conditions.

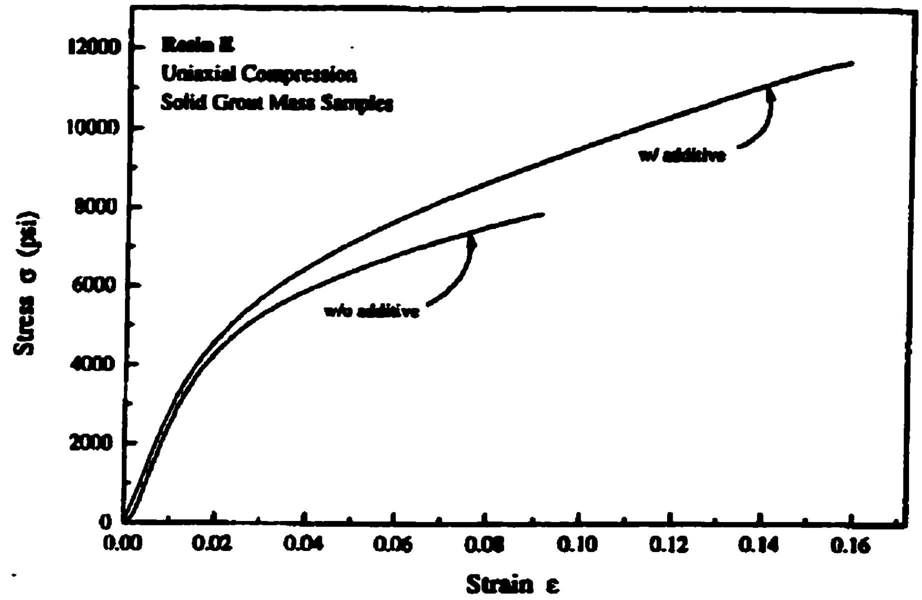

Figure 2.8: Stress-strain curves for Resin E grout formulations (after Kafarkis et al., 1998)

Resin grout is often preferred when effective reinforcement is required from cables in a short period of time after installation. Resin grouts usually set in two hours and achieve appreciable bond strength in 12 hours, whereas cement based grouts may require 24 to 48 hours to achieve equivalent bond strength. Until now the limitation of using resin grout is mainly the cost.

2.5 Pumping

The grout pump must be able to pump the thickest grout into the longest cablebolt borehole that will be used on the site. This depends on the water-cement ratio of the grout. Grout pumps commonly used in cablebolting can be classed into two groups on the basis of their pumping mechanism: piston pumps and progressing cavity pumps.

2.5.1 Piston pumps

The pumping action of a piston pump is shown in Figure 2.9. The grout is pushed into the hose on the up-stroke alone. Double-acting pumps push grout on both strokes. The capabilities of piston pumps vary widely, depending upon the design of the piston, valves, the pump chamber, the consistency of the grout, and the power of the motor.

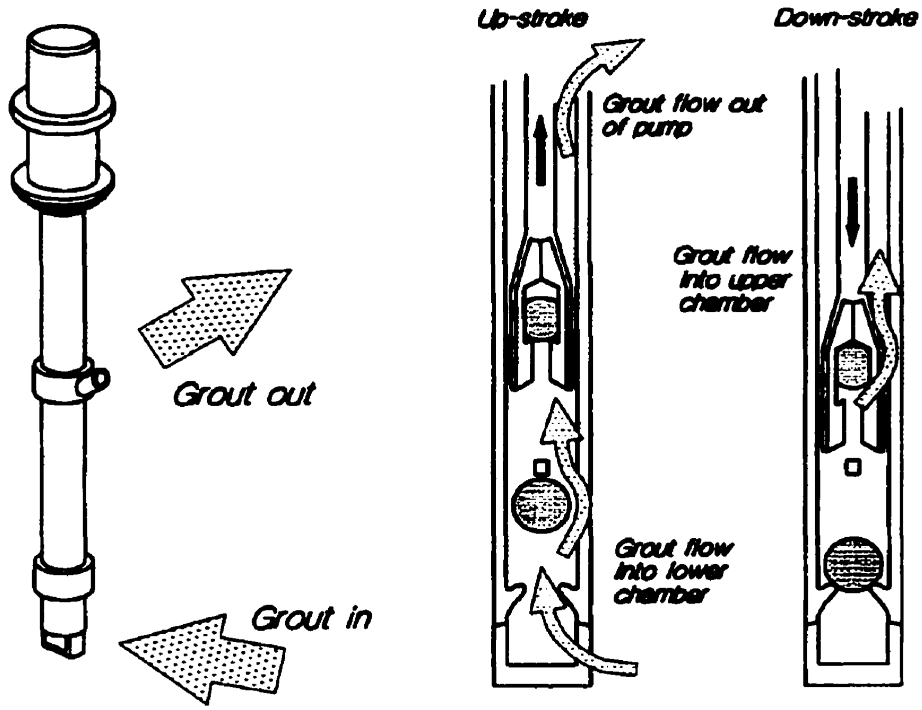

Figure 2.9: Single acting piston pump (after Hutchinson and Diederichs, 1996)

2.5.2 Progressing cavity pumps

The rotor and stator are the two key elements of a progressing cavity or eccentric screw pump (Figure 2.10). As the rotor turns, it rotates concentrically around its own axis, and moves eccentrically as well, creating both a complete seal along the length of the stator at all times and cavities which progress continuously (in a non-pulsating manner) along the length of the pump.

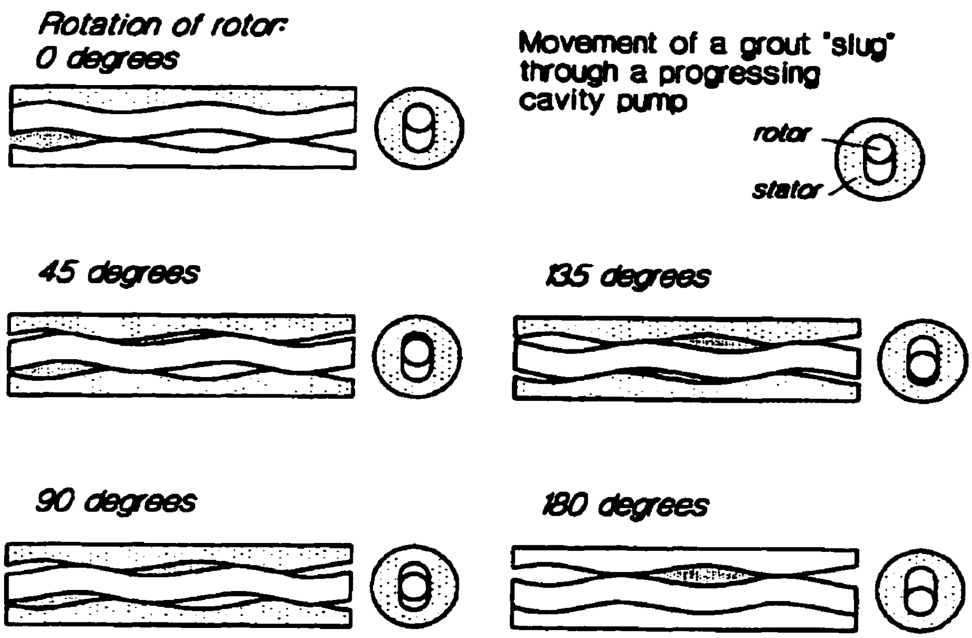

Figure 2.10: Progressing cavity pump for continuous grout flow
(after Hutchinson and Diederichs, 1996)

The hydraulic properties of grouts influence the pumpability of grouts. The flow rate of grout depends on the type of pump and the w:c ratio (Figure 2.11). One of the critical factors has been the evolution of grout pumps capable of pumping grouts with a low water:cement ratio to achieve adequate strengths. Now, there is a range of grout pumps on the market which will pump very viscous grout.

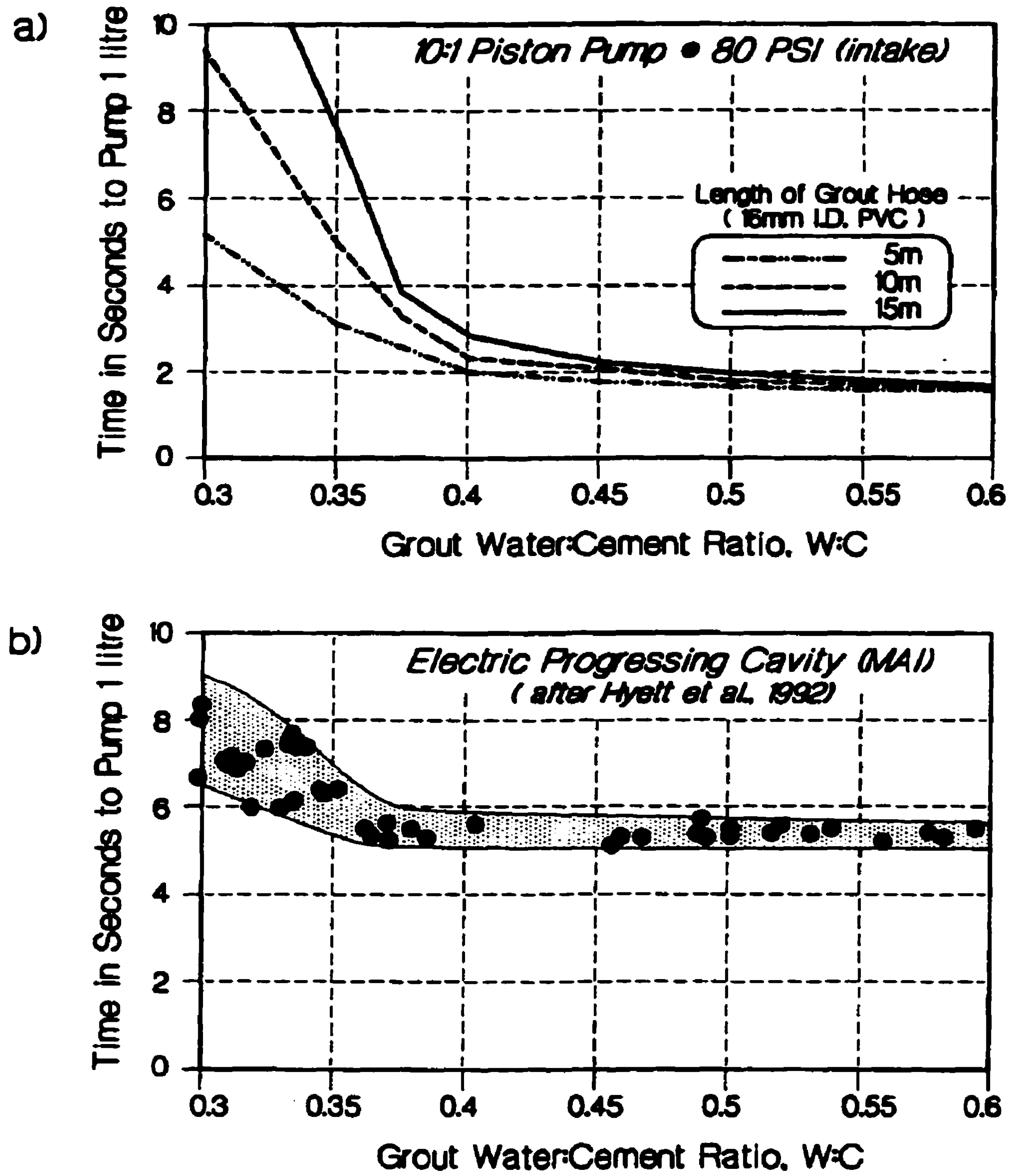

Figure 2.11: Typical flow rates vs w:c ratio for a) piston and b) progressing cavity pump (after Hutchinson and Diederichs, 1996)

2.6 Plates and anchorage devices for cable bolts

2.6.1 Plates

A face plate is designed to distribute the load at the bolt head uniformly into the surrounding rock. They are predominantly used when little loading will develop near the exposed end of the cables. There are two classes of plates that are generally used: thin and thick (Figure 2.12). Thinner plates can be deformed during manufacture to increase the initial displacement in high-stress or dynamic conditions. In highly fractured ground, thicker plates must be used which have load capacities equivalent to the tensile strength of the cable bolt (Table 2.1). The choice of the face plate is important for the load transfer between the rock and the bolt. The commonly used face plates for cable bolts are: flat plate and domed plate. The flat plate can be used when the rock surface is smooth and the bolt is installed perpendicular to the surface of the rock. The flat plate, when loaded, is supported only at a few highly stressed points at the rock surface. Under sufficiently high pressure, the rock mass may crush at these points. This shortcoming in the flat plate is greatly reduced with the domed plate, which have larger supporting areas.

Table 2.1: Typical dimensions and capacities of bolt face plates
(after Douglas and Arthur, 1983; in Hutchinson and Diederichs, 1996)

Working Load Bolt (kN)	Size of Plate (Length or Diameter) (mm)	Thickness (mm)
80	125 to 150	7
150	150 to 200	10
300	200 to 250*	12*

- Recommended for cablebolting in fractured ground

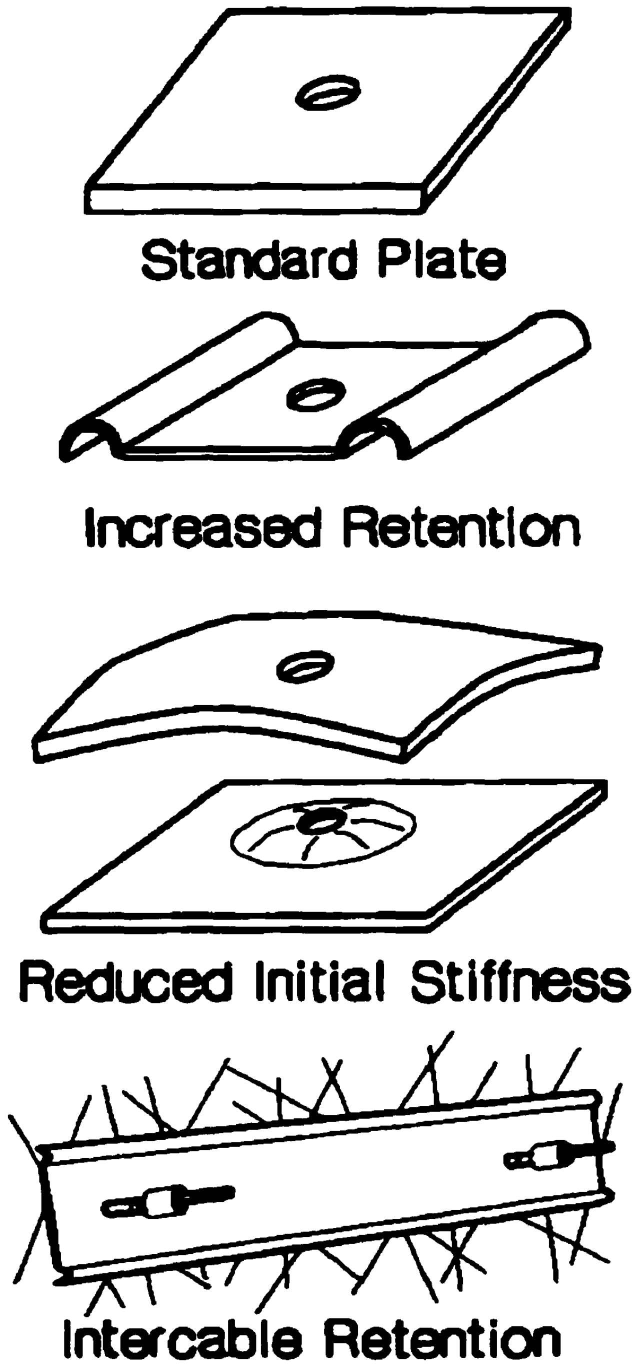

Figure 2.12: Typical face plates (after Hutchinson and Diederichs, 1996)

2.6.2 Pretension

The mechanics of installing cables with an initial pre-tension are complex due to the interactions between the various components of the system. The tensioning procedure for cables consists of two phases. The first is the stressing of the cable while at the same time pushing the surface hardware, including the anchor, tightly against the rock face. The second is the relaxation of the system following removal of the external force.

Thompson (1992) showed that three key considerations determine the correct reaction configuration: P_w (the ratio of jacking load applied to wedges), P_{max} (maximum load in cable during jacking) and P_{res} (the residual load remaining in the cable after the jack is removed). The relation between the residual load in cable P_{res} and the free cable length is shown in Figure 2.14.

When the reaction load is applied directly to the wedges (A: P_w=100%), the peak cable load behind the plate will be 30 to 50 % of the peak load registered by the jack. When a partial load is applied to the wedges (D: P_w=10%) the peak load in the cable behind the anchor approaches the maximum total load registered by the jack. Jacking systems which apply 100% of the load solely to the barrel (B: P_w=0%) are unacceptable for plating, the residual load in the cable can approach zero in this configuration. Jacking systems which apply 50% of the load (C: P_w=50%) can be effective for tensioning applications.

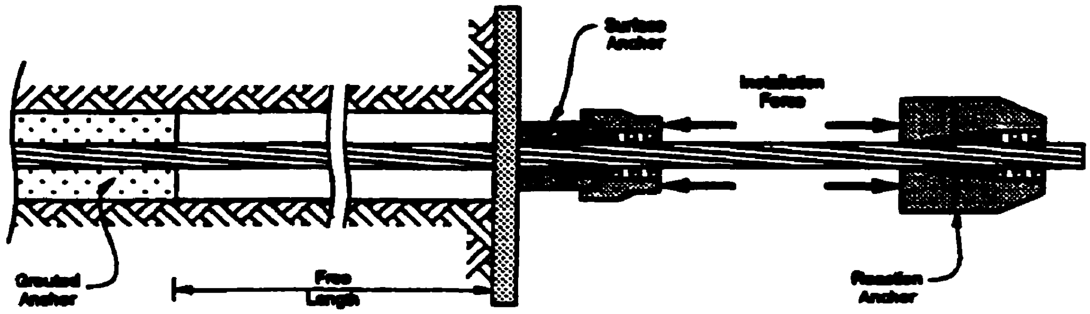

Figure 2.13: Tensioning configuration (after Thompson, 1992)

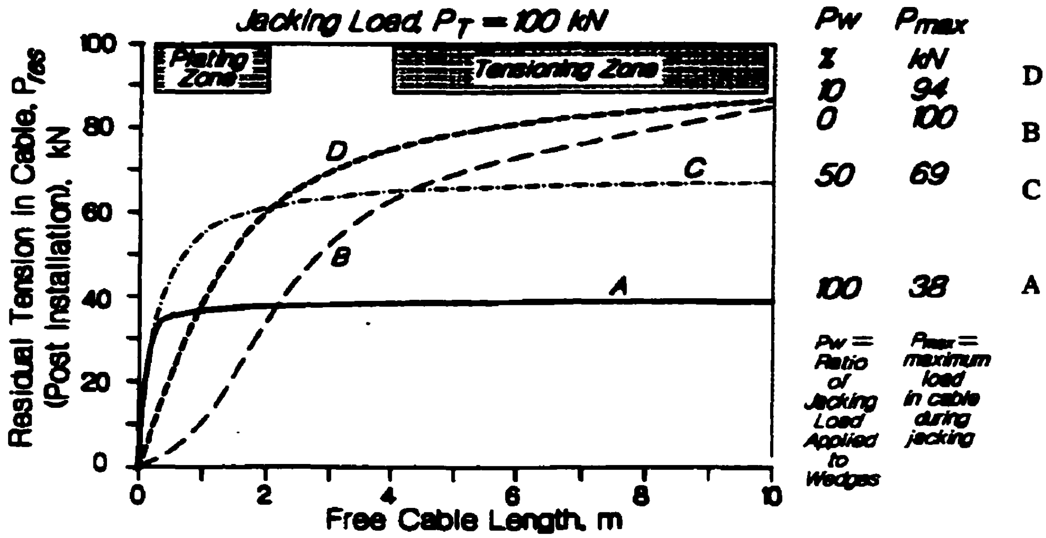

Figure 2.14: Relationships between P_w, P_{max} and the P_{res}
(in Hutchinson and Diederichs , 1996, after Thompson,1992)

Hutchinson and Diederichs (1996) gave some recommendations :

- For plate installation jacks which apply full load to the wedges during installation are recommended for barrel and wedge anchorage of surface fixtures where a residual cable load of 4 tonnes is required.
- For tensioning, jacks which apply a partial load to the wedges by means of a nose cone spring are recommended for tensioning applications where high residual loads are required and most importantly, where long free lengths are present.

2.7 In-situ monitoring of cable bolt performance

To see how cables behave in the field and to compare with results from laboratory tests and numerical modelling, an instrumentation program is needed to measure axial deformations and loads in the cable to improve the cable bolt design (Hutchinson, 1992; Hutchinson and Grabinsky, 1992).

The data collected from these instruments can help the engineer to change cable bolt pattern, add more cable bolts, change length of cable bolts, determine if the cables are being loaded, verify the specified bond strength and change the type (plain to birdcage) of cable bolts.

The instruments available on the market are based on the variation of wire resistance during axial loading. Gauge type measuring device and cell type load measuring device are used. An available spiral strain gauge (Tensmeg gauge) manufactured and marketed by Roctest inc. consists of a set of plastic sheathed wires that are wrapped around the cable bolt (Choquet and Miller, 1988). The gauge is a patented device for monitoring of strains. Using the calibration curve, provided by the manufacturer, the load can be monitored. Many factors and effects may invalidate the results and the gauge life. This type of instrument is not recommended for long term monitoring.

Environmental conditions in the field (temperature, humidity, corrosion) are not ideal and have an influence on the instrumented cable in the long term.

Anwyll (1996) from McGill University developed an instrument called the Cable Bolt Grout Displacement Meter or cable-GDM. The cable-GDM is a multi-point wire extensometer that monitors the movement of the grout column surrounding a cable bolt. The limitations of this instrument is that it assumes that the grout will remain in contact with the surrounding rock mass regardless of the condition of the cable/grout interface and it doesn't measure the cable displacement to get the tension in the cable.

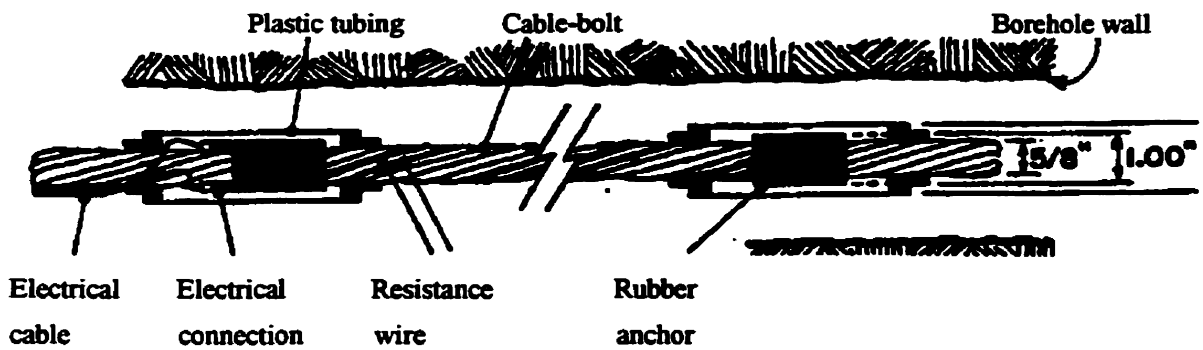

Figure 2.15: The Tensmeg gauge (after Choquet and Miller, 1988)

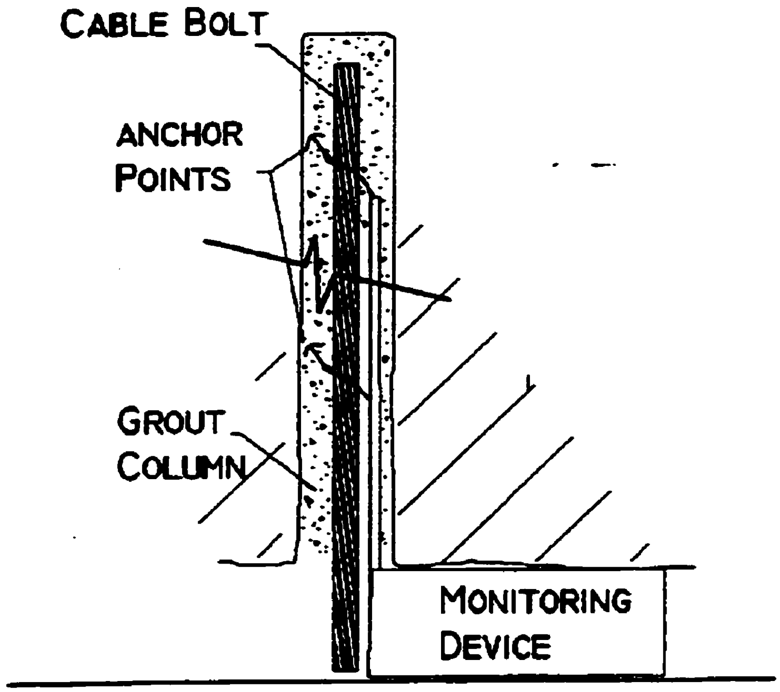

Figure 2.16: The cable-GDM, a wire extensometer cable bolt grout displacement (after Anwyll, 1996)

Another instrumentation device developed at the University of Sherbrooke in collaboration with McGill University (Chekired et al., 1997) is the CTMD (Cable Tension Measuring Device). The CTMD consists of a vibrating wire strain gauge and is designed specifically for the 7 wire steel cable which is 15.2 mm diameter (Figures 2.17 and 2.18). The configuration of the installed CTMD has an approximate length of 120 mm and can be installed at any point of the cable. To record cable bolt tension the vibrating wire strain gauge frequency must be adjusted using a readout data logger before the screwing step. The CTMD may cause grout pumping difficulties and doesn't capture large strains. Small range of strain is limited by the strain limit of vibrating wires.

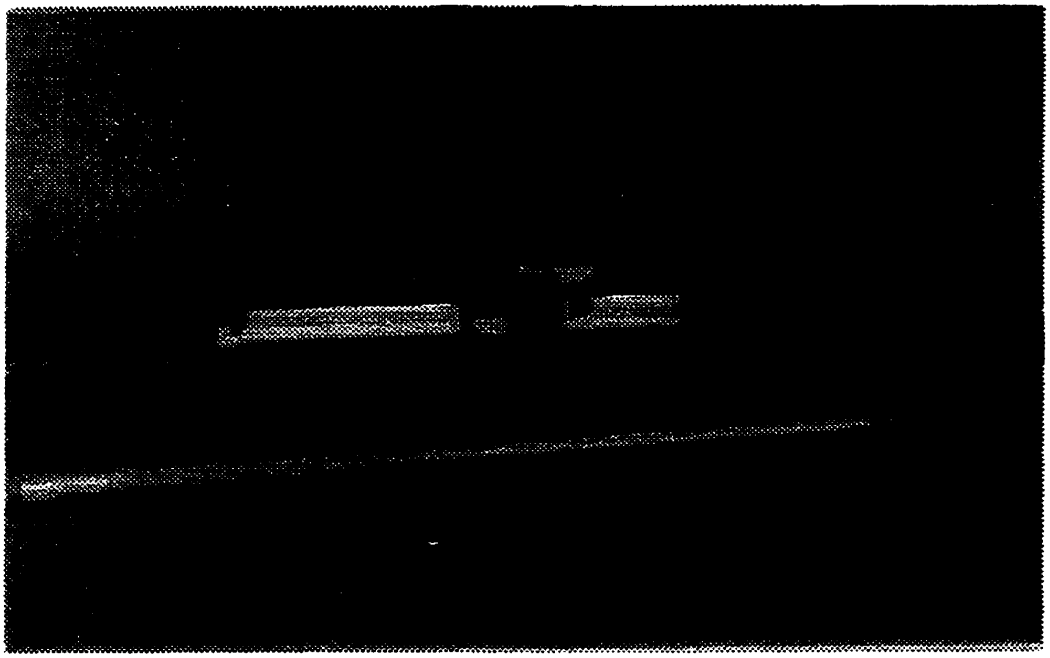

Figure 2.17: CTMD installed on cable bolt (after Chekired et al., 1997)

Figure 2.18: Different components of the CTMD (after Chekired et al., 1997)

Bawden et al. (1997) developed a new instrument integrated in the cable : the SMART cable (Stretch Measurement to Assess Reinforcement Tension). It consists of a Multi-Point Borehole Extensometer (MPBX). It involves instrumenting the king wire of the cable with fixed reference anchors and the originality of this instrument compared to others is the integration of the instrument inside the cable to avoid the contact with the grout and the external conditions.

The concept of SMART cable (Bawden et al. 1997) is if the extension or stretch (d^i-d^{i+1}) between two known locations (L^i+L^{i+1}) along a 7-wire strand cable can be measured, the strain (often referred to as elongation) may be written:

$$\varepsilon = \frac{d^i - d^{i+1}}{L^i - L^{i+1}} \quad \text{(m/m)} \qquad (2.2)$$

For 15.8 mm diameter low relaxation 7-wire strand the corresponding tension is

$$F = \alpha . \varepsilon \text{ (kN)} \qquad (2.3)$$

where for the elastic response:

α = 25000 kN/m/m (0<F<225kN)

and for the strain hardening response after yield:

α = 600 kN/m/m (F>225kN ε<0.035 m/m or 3.5%)

Thus the average load in the cable can be calculated from the strain between adjacent anchor points, and by using multiple anchor points the load along the whole cable bolt is determined.

Experimental tests in the field using SMART cable at Bousquet mine (Québec) (Hyett et al. 1997) and Callinan mine (Manitoba) (Bawden et al. 1999) showed that SMART technology may be used as a valuable tool in cable design verification. The main limitation of the SMART cable is that the readings are temperature sensitive. Temperature changes can lead to erroneous measurements of displacements, and hence strains and cable axial load. A second limitation of the SMART cable is the necessity of unwinding the cable and rewinding it before installation. This complication adds cost and does not make the instrument readily available for any cable bolt installation.

2.8 Performance of cable bolts

2.8.1 Effect of water cement ratio

Hassani et al. (1992) showed that water:cement ratio (w:c) dictate both workability and pull out strength (Figure 2.19) . Excessive amount of water in grout decreases the density of grout as a result a poor grout is obtained.

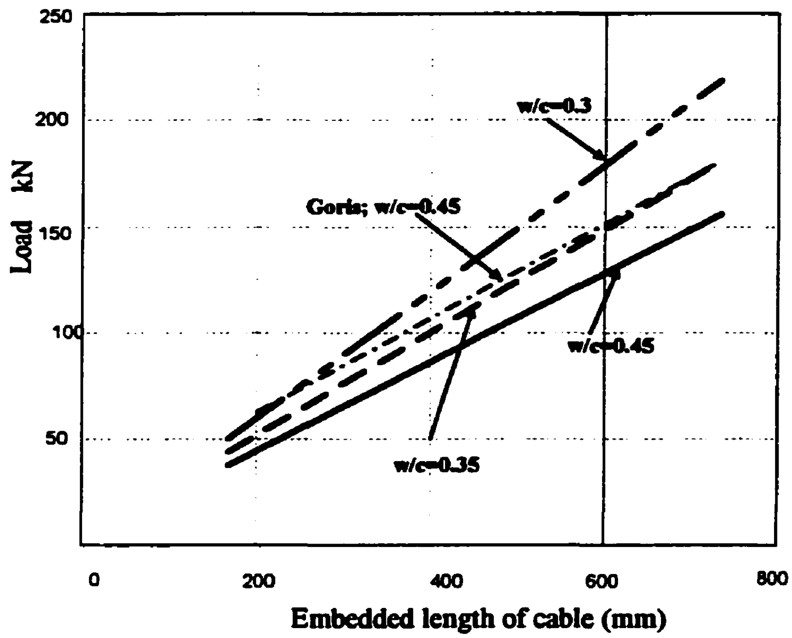

Figure 2.19 : Effect of water:cement ratio on the capacity of cable bolt (after Hassani et al., 1992)

Reichert et al. (1992) conducted laboratory and field programs to investigate the major factors influencing bond capacity of grouted cable bolts. They gave the variation of the mechanical properties of the grout (uniaxial compressive strength, Young's modulus) with water:cement ratio(w:c) . They concluded that the range of w:c=0.35 to 0.4 provides the optimum balance of strength.

2.8.2 Cable embedment length

The embedment length for a cable is determined by the joint spacing along the axis of cable bolt. It is used to describe the active length of grouted cables. The effect of embedment length on the behaviour of cable bolts has been studied in the laboratory and in the field by several authors.

Hyett et al.(1992) conducted several laboratory and field tests at different embedment lengths. They showed that the cable bolt capacity increased almost linearly over the range of embedment lengths tested .

Figure 2.20 shows the results of pull-out tests conducted on cable bolts of embedment lengths from 15 cm to 75 cm. As can be seen, cable capacity increases with embedment lengths (Hassani et al, 1992). The longer the embedment length the stronger the system should be.

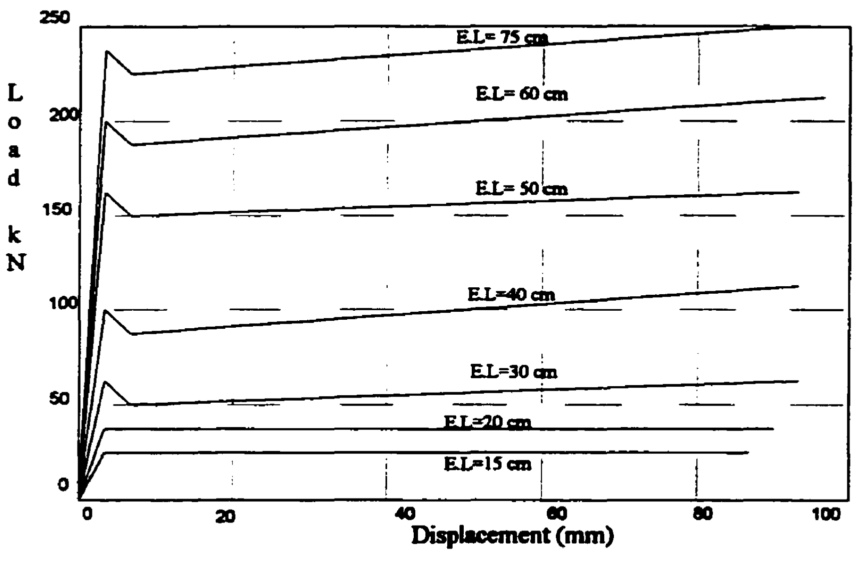

Figure 2.20 : Effect of the embedment length (E.L) on the capacity of cable bolts (after Hassani et al., 1992)

2.8.3 Mechanical properties of host medium

While the cable geometry and grout are controllable design parameters, the properties of the rock mass in which the cable bolt is inserted is not. The modulus of elasticity of the host rock appears to greatly influence the capacity of cable bolts.

Hyett et al. (1992) made a comparison between the radial confinement provided by the steel, aluminium and PVC pipes in the laboratory (Figure 2.21) and with the granite, limestone and shale rock masses in the field and concluded that:

- when the radial stiffness of the confinement is accounted for, a good correlation exists between laboratory and field test results.
- the effect of radial confinement is most evident for high strength grouts (0.3 and 0.4, UCS > 65 MPa).
- for low strength grouts the peak cable bolt capacity depends primarily on just how strong the grout is.
- for the granite, high variability in the radial stiffness correlates to high variability in the cable capacities.

Hassani et al.(1992) in a laboratory investigation using pull-out tests with the radial confinement of steel pipe, concrete block, weak block and PVC pipe showed that rocks with higher modulus of elasticity increase confinement or radial stresses on the grout and as a result improves the cable bolt capacity (Figure 2.22).

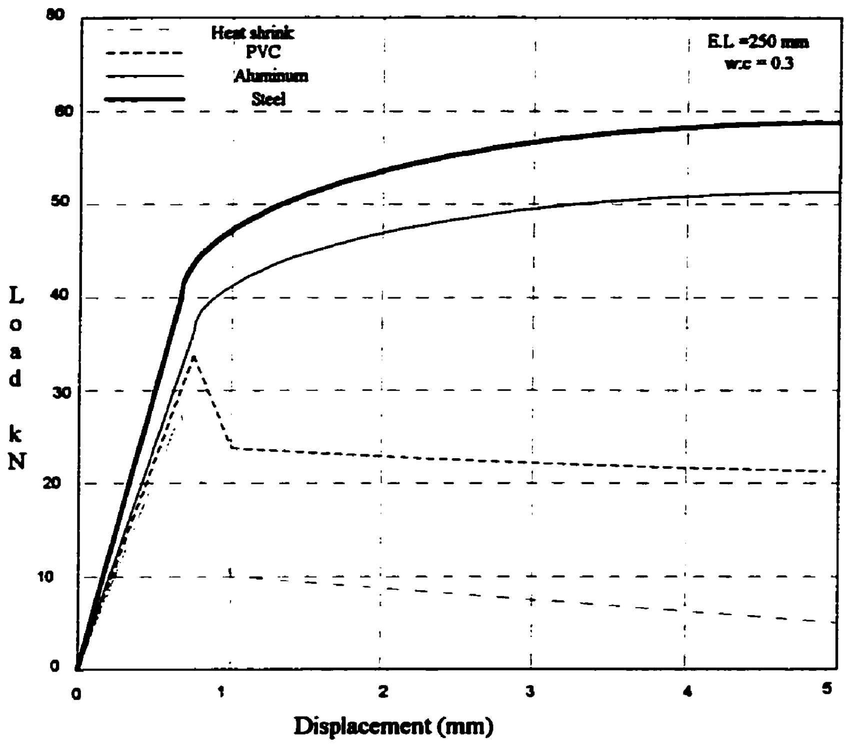

Figure 2.21: Effect of confining media on the capacity of cable bolts (after Hyett et al, 1992)

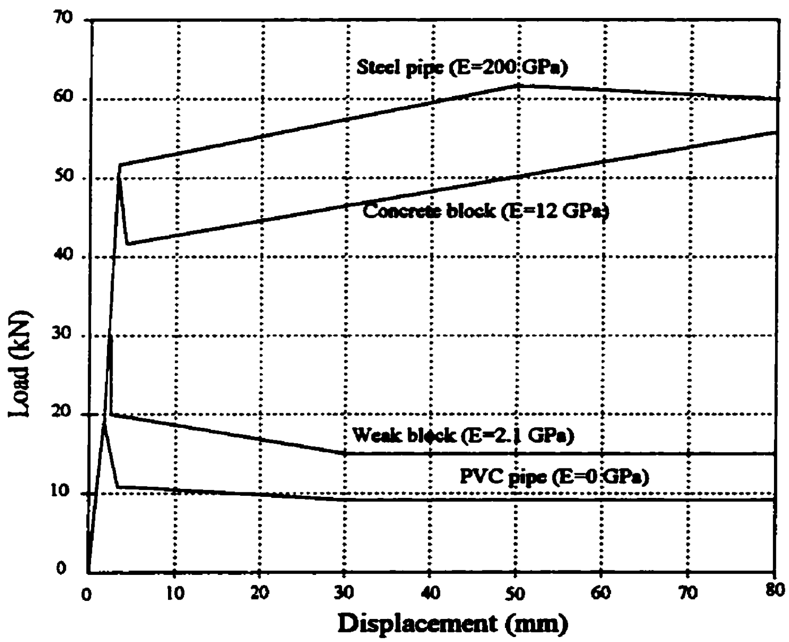

Figure 2.22: Effect of modulus of elasticity on cable pull-out resistance (after Hassani et al., 1992)

2.8.4 Confining stress

The behaviour of cable bolt depends also on the stress state in the field. This factor must be taken into account in the design of cable bolts. The problem is how to simulate this effect.

An experimental work in the laboratory was conducted by Hyett et al. (1995) and it consists of a series of pull tests using fully-grouted seven-wire strand cable, in which the confining pressure at the outside of the cement annulus was maintained constant using a modified Hoek cell. The bond strength was shown to increase with confining pressure. The results (Figure 2.23) show that the shape of the load-displacement plots is pressure dependent. For low confining pressure, peak capacity was attained during the initial 10 mm of axial displacement whereas for higher confining pressure it usually occurs after 40-50 mm. The data were used to develop a frictional-dilational model for cable bolt failure

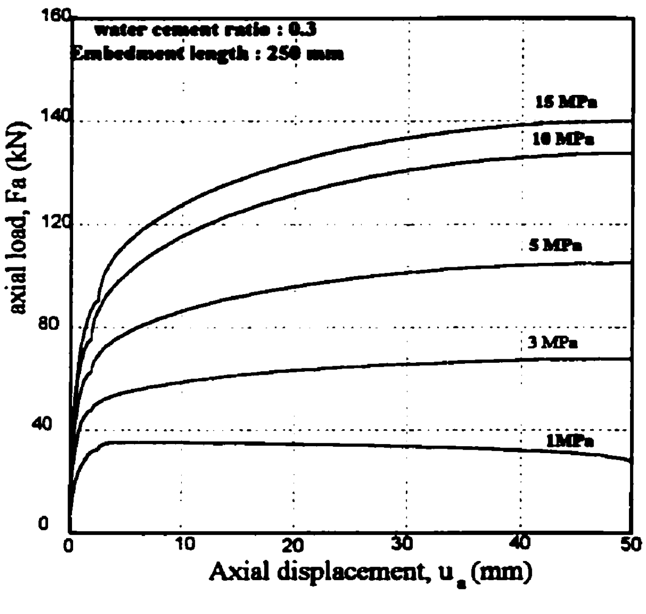

Figure 2.23: Effect of confining stress on the cable capacity
(after Hyett et al., 1995)

The concept of bond stress and load transfer is complex in the behaviour of cablebolting. Cable bolt research , in the laboratory and field, confirmed that the most prevalent mode of failure for a cement grouted seven wire strand involves frictional slip at the grout cable interface. Cables behave like a frictional support system. This implies that the pull out resistance of a cable depends primarily on the radial pressure exerted by the grout on the steel thus on the confinement of the grout column by the surrounding rock mass. The pull-out resistance or cable bond strength is directly linked to the confinement pressure at the steel-grout interface.

Yazici and Kaiser (1992) studied the bond strength of grouted cable bolts and the effect of stress change and they concluded that the bond strength increases with the stiffness ratio (rock-to-grout), the strength of the grout, the friction coefficient between bolt and grout, and decreases with the diameter of the borehole. They developed a conceptual model, the bond strength model (BSM), to take into account all these factors . For the stress change, it is concluded that mining induced stress change is one of the most important parameters controlling the cable bond strength. Stress reductions, often measured in deep mine, can cause the cables to lose most of their bond strength in low to medium stiffness rocks.

2.9 Summary

The technology of cable bolts has seen leap advancements over the last two decades. Cable geometry, pumping and grouting play an important role in the installation and effectiveness of a cable bolt support system. Plating and tensioning increase the cable efficiency. Instrumented cables were developed to measure the maximum loads supported by the cable in the field. The mechanical performance of cable bolts is influenced by the water-cement ratio, the stiffness of the host rock as well as the confinement pressure around the cable.

CHAPTER 3

DESIGN OF CABLE BOLTS - LITERATURE SURVEY

3.1 Introduction

Due to the complex nature of the problem of designing of cable bolt support system, it is virtually impossible to follow a rigorous design procedure. However, a global approach is needed to take into account all important parameters affecting the behaviour of cable bolts. The key aspects of modern cable bolt design include the choice of some parameters (Windsor, 1992): the cable bolt element and its arrangement, the cable bolt array geometry, the cable bolt installation procedure, pre- or post-reinforcement and pre- grout properties, cable bolt geometry and surface fixtures, rock mass effects and mining induced effects. Bawden et al. (1992) proposed a methodology for the design of cable bolts describing the critical factors controlling the capacity of grouted cable bolts: cable design parameters (grout properties, cable bolt geometry and surface fixtures), rock mass effects and mining induced effects.

This chapter presents a thorough review of the currently available design methods for cable bolt support systems in hard rock mines.

3.2 Empirical methods

The most widely used classification systems in rock mechanics are: RMR system and Q system. Empirical support design are based on these systems.

3.2.1 RMR method

The Rock Mass Rating (RMR) system, known as the Geomechanics classification was developed by Bieniawski (1973). It was modified over the years as more case histories became available (Bieniawski, 1989 and 1993). Six parameters are used to classify a rock mass using the RMR system:

- Uniaxial compressive strength (UCS) of rock material: 0 - 15.
- Rock quality designation (RQD): 3 - 20.
- Spacing of discontinuities: 5 - 20.
- Condition of discontinuities: 0 - 30.
- Groundwater conditions: 0 - 15.
- Orientation of discontinuities (penalty parameter): (-12) - 0.

For each parameter we have a rating depending on in-situ conditions and the RMR is the total ratings. A classification of the rock mass is given based on this parameter (Table 3.1).

Table 3.1: The Rock Mass Rating System (RMR) (after Bieniawski, 1973)

Ratings	100-81	80-61	60-41	40-21	<20
Class no.	I	II	III	IV	V
Desription	very good rock	good rock	fair rock	poor rock	very poor rock

Unal (1983) used RMR classification method for the design of cable bolts and gave semi empirical support guidelines. Tunnel support pressure, cable bolt length and density are determined as a function of the span and the RMR (Figure 3.1). The design of cable bolts using RMR method is suited for moderate to large openings in blocky ground under low to moderate stress. The method don't take into account the effect of stress in the field, for massive rocks at high stresses and highly fractured rocks.

The RMR method is widely used in rock engineering field but is limited for civil engineering applications (tunneling). For applications in mining Laubscher (1977) modified the method as MRMR method (Mining Rock Mass Classification). The classification uses the same parameters as Bieniawski but involves differences in the detail. Each of the five classes is divided into subclasses, A and B. the RMR rating is further adjusted to take into account joint orientation, weathering, field and induced stresses, stress changes due to mining and the effects of blasting.

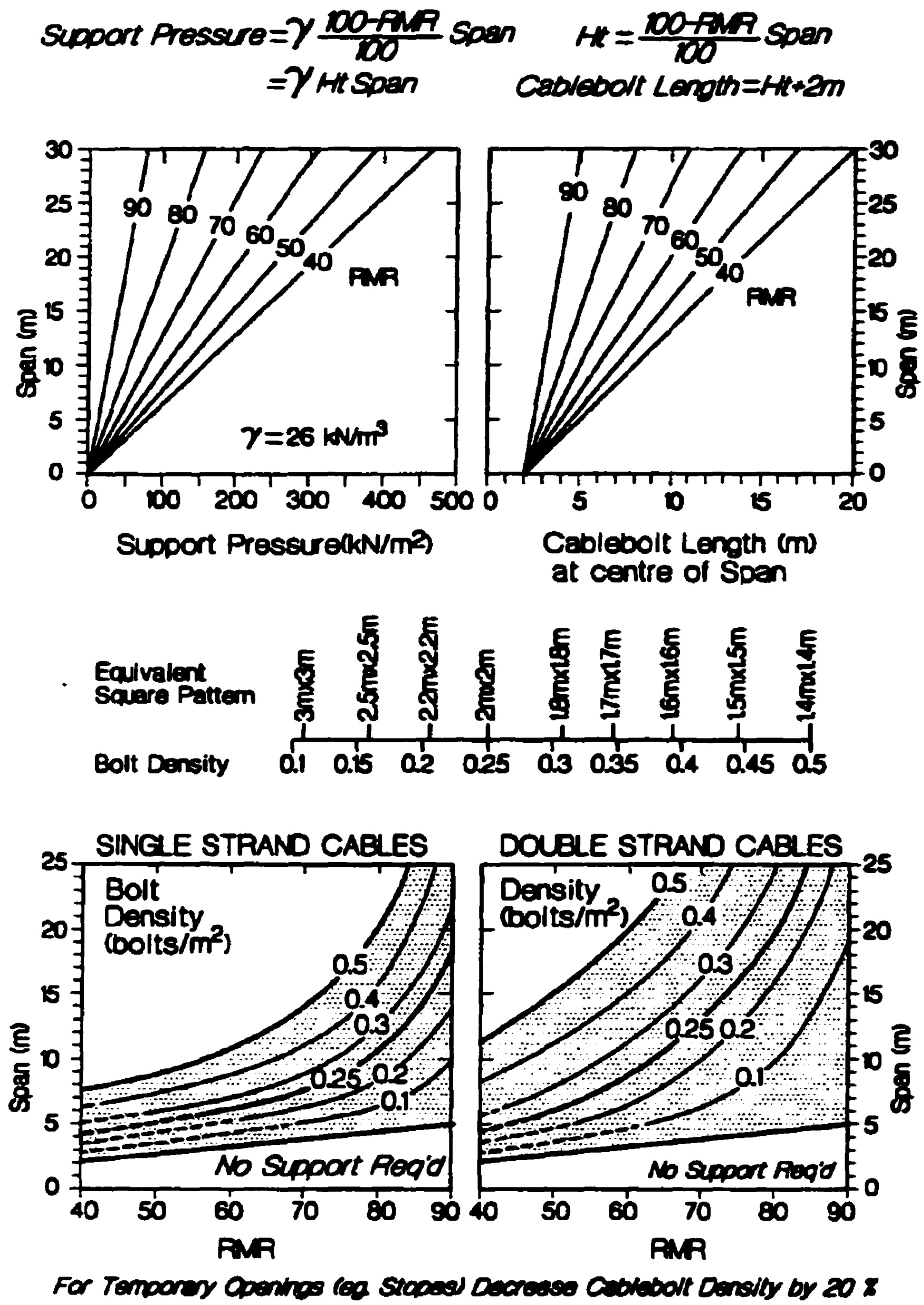

Figure 3.1: Design of cable bolts using RMR system (after Unal, 1983)

3.2.2 Q method (NGI classification)

Barton, Lien and Lunde (1974) developed the Norwegian Geotechnical Institute (NGI) engineering classification of rock masses. The classification was based on an analysis of some 200 tunnel case histories from Scandinavia.

The Q-system is based on a numerical assessment of the rock mass quality using six different parameters:

- RQD.
- Number of joint sets.
- Roughness of the most unfavorable joint or discontinuity.
- Degree of alteration or filling along the weakest joint.
- Water inflow.
- Stress condition.

These six parameters are grouped into three quotients to give the overall rock mass quality Q as follows:

$$Q = (RQD.J_r.J_w) / (J_n.J_a.SRF) \qquad (3.1)$$

Where:

RQD = rock quality designation (0 - 100).
J_n = joint set number (0.5 - 20).
J_r = joint roughness number (1 - 4).
J_a = joint alteration number (0.75 - 20).
J_w = joint water reduction number (0.05 - 1.0).
SRF = stress reduction factor (0.5 - 10).

The numerical value of each of the classification parameters is given by Barton et al. (1974). The classification was adapted for tunnel reinforcement and design of cable bolts (Barton, 1988; Grimstad et al., 1993). The Q value is related to tunnel support requirements by defining the equivalent dimensions of the excavation (Figure 3.2). This equivalent dimension which is a function of both the size and the purpose of the excavation, is obtained by dividing the span, diameter, or the wall height of the excavation by a quantity called the excavation support ratio (ESR). The ESR is related to the use for which the excavation is intended and the degree of safety demanded.

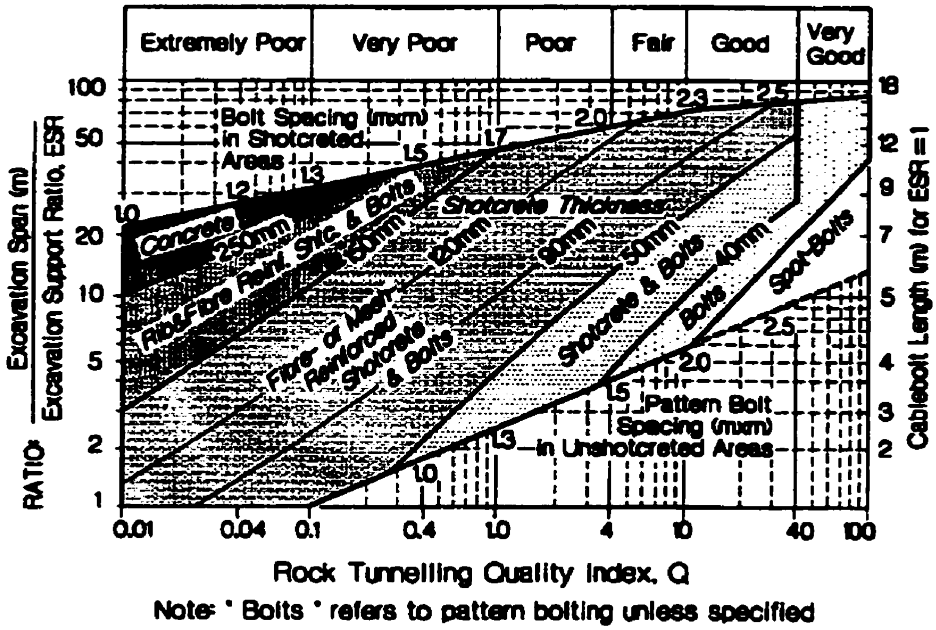

Figure 3.2: Design of cable bolts using Q-system

(after Grimstad et al., 1993)

The method was modified by Mathews et al. (1981) and Potvin (1988) for applications in mining. It is to be noted that RMR and Q are related by the equation (Bieniawski, 1989)

$$RMR = 9 \ln Q + 44 \qquad (3.2)$$

Like the RMR method, the Q method is not suited for massive rocks at high stress levels and for highly fractured rocks. Hoek showed the limits of cable bolt application using RMR and Q method (Figure 3.3).

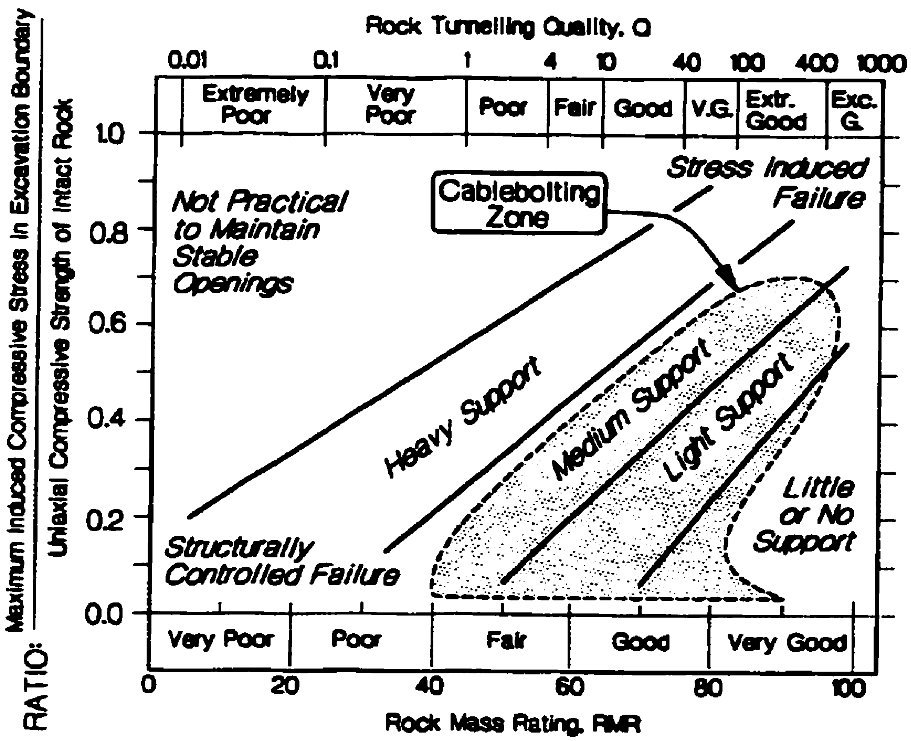

Figure 3.3: Limits of cable bolt application

(in Hutchinson and Diederichs, 1996 , after Hoek, 1981)

3.2.3 Mathews/Potvin stability graph method

The Mathews/Potvin was initially proposed by Mathews (1981) and then modified by Potvin (1988).

3.2.3.1 Mathew's Stability Graph Design Method

Developed by Mathews et al. (1981), the method uses an adjusted NGI "Q" rating to determine stable excavations dimensions. The first four parameters of the NGI system are unchanged and the quotient of the final two parameters is arbitrarily set to one.

Thus, Q is then adjusted to Q' for induced stresses, orientation of joint structure and orientation of the surface being examined:

$$Q' = (RQD x J_r) / (J_n x J_a) \qquad (3.3)$$

Q' is called the modified Q classification value. This value is the same as the standard Q classification value except for the SRF (stress reduction factor) which is set to 1.0. In all applications of this technique design, the joint water reduction J_w factor is equal to 1.0, representing the conditions commonly found in deep Canadian mines.

The Stability Graph Design approach consists of assessing the rock mass strength based on Q', and three factors introduced to account for the stress, structure and surface orientation. The resulting value, based on these four parameters, is called the stability number (N) and is plotted against the shape factor (S) which is the surface area divided by the perimeter. The graph relating the resulting stability number versus shape factor or hydraulic radius delineate zone of "potentially stable", "potentially unstable" and "potentially caving" (Figure 3.4). The stability number (N) is calculated after equation 3.4 (Mathews et al., 1981)

$$N = Q' \times A \times B \times C \qquad (3.4)$$

Where :

A is a factor designed to account for the influence of high stresses.
B is a factor designed to take into account the influence of the orientation of discontinuities.
C is a factor designed to consider the orientation of the surface being analysed.

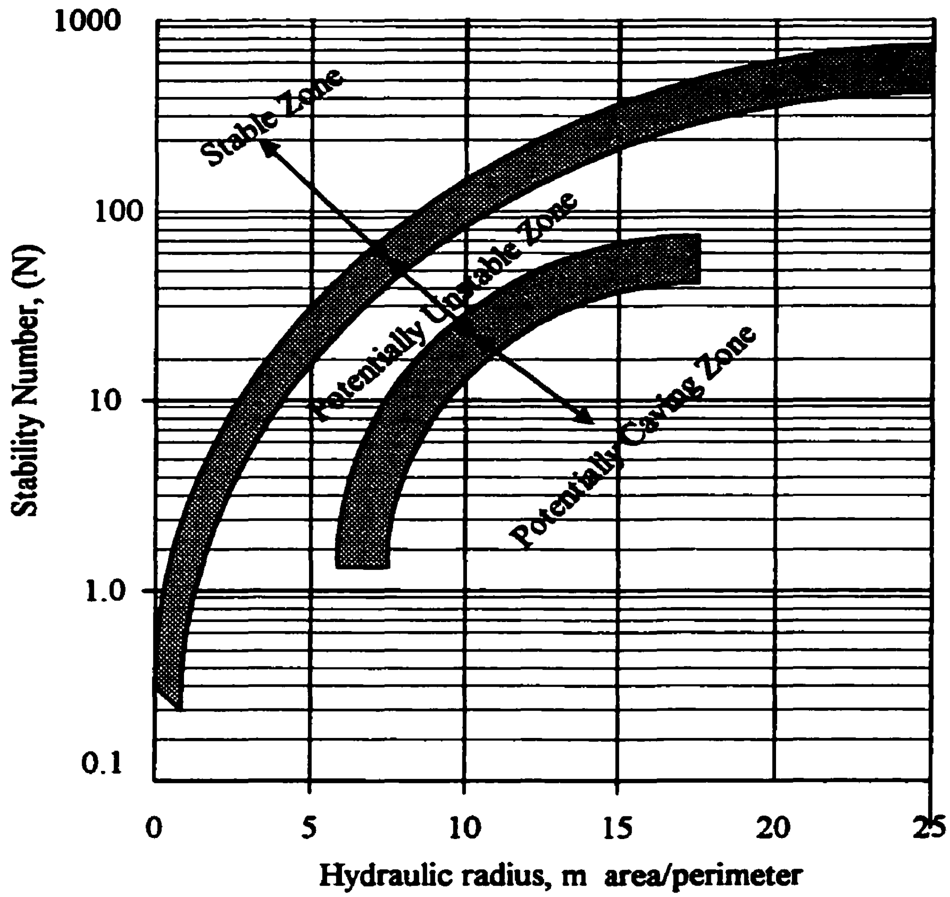

Figure 3.4: Stability Graph Method (after Mathews, 1981)

3.2.3.2 Potvin modifications: The Modified Stability Graph Method

Potvin et al. (1988) modified the Mathews's stability graph by redefining some of the rating adjustment factors. The modification was based on the collection of a large number of case histories in Canadian mines. 176 case histories by Potvin (1988) and 13 by Nickson (1992) of unsupported open stopes were plotted on the stability graph. The modified stability graph relates the modified stability number (N') to the hydraulic radius (HR) which is the surface area divided by the perimeter. The design graph (Figure 3.5) has essentially two main zones: "stable and caved" separated by three narrower zones: "unsupported transition zone, stable with support, and supported transition zone".

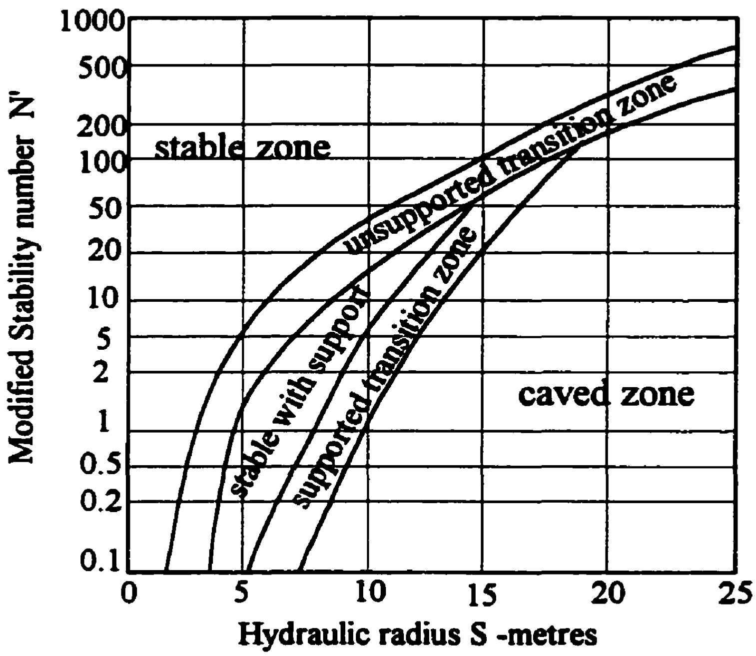

Figure 3.5: Modified Stability Graph Method (after Nickson, 1992)

$$N' = Q' \times A \times B \times C \qquad (3.5)$$

Where :

N' is the modified stability number

Q' is the modified Q classification value (as described before).

A is a factor measuring the ratio of intact rock strength to induced stress.

B is a factor measuring the relative orientation of dominant jointing with respect to the excavation surface.

C is a factor measuring the influence of gravity on the stability of the face being considered.

Potvin and Milne (1992) introduced a "cable bolting " line and gave cable support recommendations. They proposed design charts for cable bolt density and cable bolt length. For cable bolt density the key empirical parameter is $(RQD/J_n)/HR$ and for cable bolt length the key parameter is the hydraulic radius (Length = 1.5 x HR) (Figure 3.6).

Stewart and Forsyth (1993) proposed the updated Mathew's stability graph method with new data points from open stoping mines. It has four zones: potentially stable, potentially unstable, potentially major collapse and potentially caving. Hadgigeorgiou et al. (1995) augmented the database with new case of footwall instability.

The Stability Graph method is very widely used in Canadian mines but it has some limitations because it doesn't take into account some important parameters like mining induced stresses over the stope face considered (only the point at the centre is considered for the evaluation of stability). Others limitations are observed in the use of the method for stope and support design: corners design, intersections design, discrete wedges, delamination zones and discrete shear structures design.

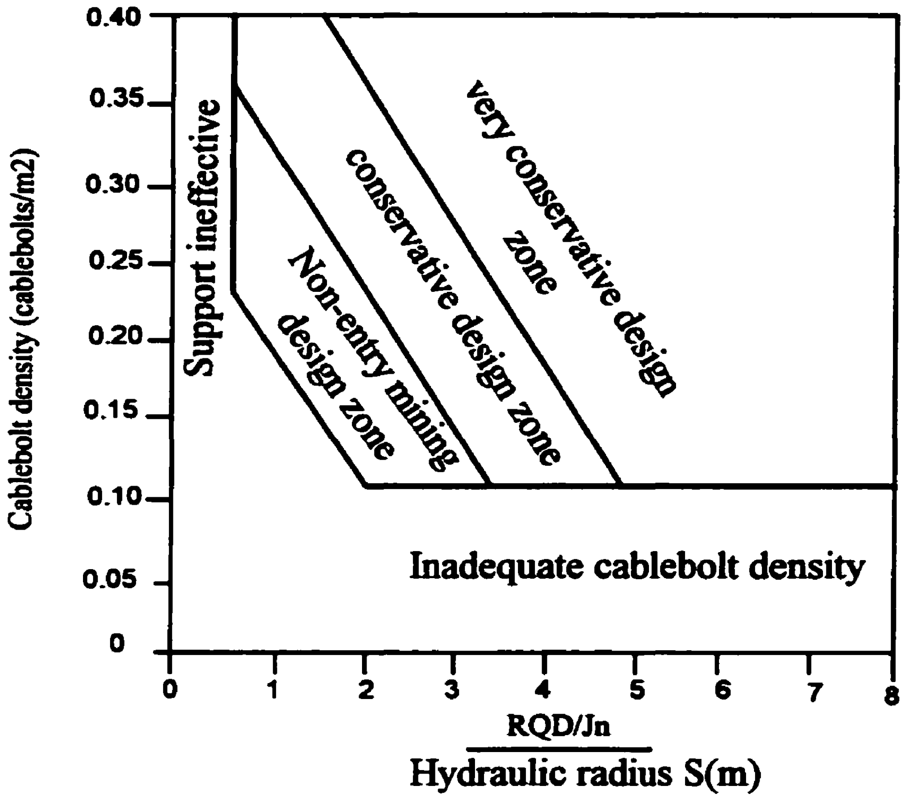

Figure 3.6: Empirical estimate of required cable bolt density (after Potvin and Milne, 1992)

3.3 Analytical methods

Farmer (1975) developed an analytical model for rock anchors by assuming that the host rock is rigid and conducted pull out tests of rock anchors using concrete, limestone and chalk as host medium. He concluded that if boundary conditions were satisfied, then the shear distribution along the embedded length was non linear for hard rock prior to tendon yielding. St.John and Van Dillen (1983) developed a new one-dimensional element allowing yielding only at the bolt-grout interface. This one-dimensional element can be incorporated as a rock bolt in any general purpose, non-linear finite element computer code suitable for rock modelling. The limitation of this element is that it does not consider any radial stress around the borehole and, no consideration was given to the dilatancy of the interface. Other analytical models were developed for rock bolts (Aydan et al. 1985; Peng and Guo, 1992). For cable bolts, two analytical models were developed during the recent years: GRC-Cable bond strength model and CABLE model.

3.3.1 GRC-Cable bond strength model (Yazici and Kaiser, 1992)

The GRC cable bond strength was developed to determine the capacity of fully grouted bolts and cables. It predicts the load at which radial grout cracking initiates; whether stable or unstable splitting of the grout occurs; and the ultimate bond strength at a point along a cable. The theory behind the bond strength model has been tested against laboratory studies at Laurentian University and cable bolt pull-out test data produced by Queen's University (Reichert et al., 1992). Thick cylinder equations (Obert and Duvall, 1967; Popov, 1978) are used to simulate the combined cable-grout-rock system.The rock is approximated by a cylinder of infinite outer radius. The model involves four main components: axial and lateral displacements, pressure at bolt-grout interface and bond strength (Figure 3.7).

- The first quadrant shows the variation of bond strength τ with axial displacement.
- The second quadrant relates the pressure p_1 at the bolt-grout interface to the bond strength using the equation:

$$\tau = \sigma \tan\{i_0 [1-(\sigma/\sigma_{\lim})^{\beta}]+\phi\} \qquad (3.6)$$

where τ = shear or bond strength.

σ = radial stress at the bolt-grout interface.

ϕ = friction angle between the bolt and grout.

i_0 = apparent dilation angle.

β = reduction coefficient of dilation angle (β=0.25, Ladanyi and Dominique, 1980).

$\sigma_{\lim}$ = limiting stress , $\sigma_{\lim} = \sigma_{cg}$ and σ_{cg} = compressive strength of grout.

- The third quadrant shows the relation between axial and lateral displacements:

$$u_{lat} = u_{ax} \tan i \qquad (3.7)$$

where

u_{lat} = lateral displacement at the bolt-grout interface.

u_{ax} = axial displacement of the bolt.

- The fourth quadrant shows the relation between lateral displacement and the interface pressure p_1 . In the BSM model the grout is elastic, fully or partially split with an elastic portion.

The bond strength model explains the development of the bond strength at the bolt-grout interface of grouted bolts and cables. Several factors influence the bond strength of cables but the effect of stress change is very important. Mining induced stress change is one of the most important parameters controlling the cable bond strength. Stress increases confine the grout and increase the bolt-grout interface pressure, whereas stress decreases reduce the interface pressure and the bond strength. The model is limited in its application to a single cable of the standard type because it also doesn't take into account the length of cables and the interaction between the rock mass and cables, all of which are important aspects for design purposes.

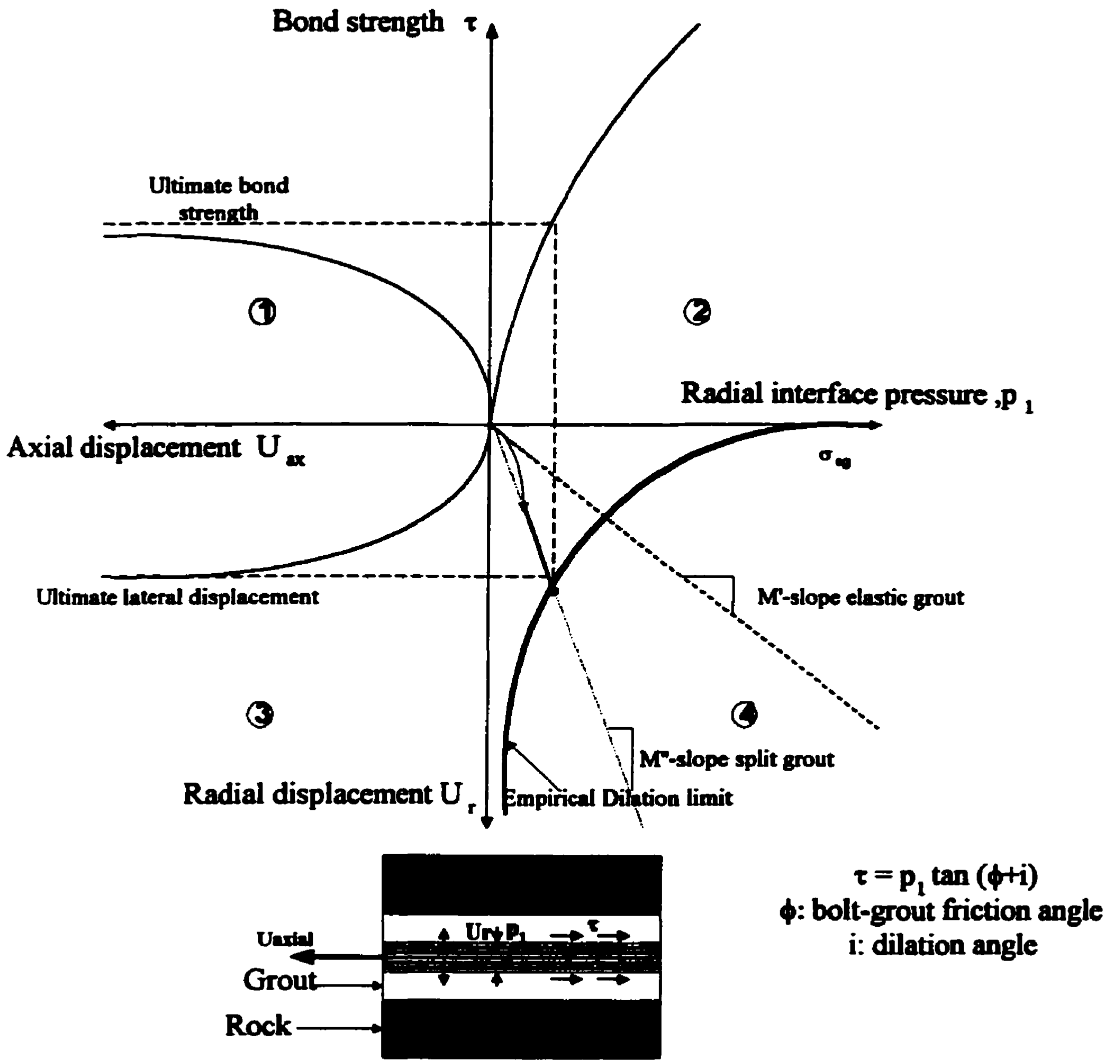

Figure 3.7: Bond Strength Model (BSM) (after Yazici and Kaiser, 1992)

3.3.2 CABLE model

Using experimental results with a modified Hoek cell, Hyett et al. (1995) developed a frictional-dilational model for cable bolt failure. This model was developed using the approach adopted for rock joints by Goodman and Boyle(1983) and Saeb and Amadei (1985), the mechanical response of any rough interface to shear loading depends most critically on the surface morphology, the strength of the irregularities and the boundary conditions applied normal to the surface. The graphical model is similar to that presented by Yazici and Kaiser (1992) for cable bolts.

The graphical model (Figure 3.8) represents the variation of axial load and radial displacement with axial displacement and confining pressure. An analysis of the cable-grout interface was done. Load distribution along one cable bolt was investigated both analytically and numerically (Figure 3.9). All the data were implemented into a software program called CABLE (Computer Aided Bolt Load Estimation). This program is designed for one cable only and for field situations involving a group of cables with interaction with rock masses the model needs to be implemented into numerical models, such as finite element, finite difference or discrete element computer programs

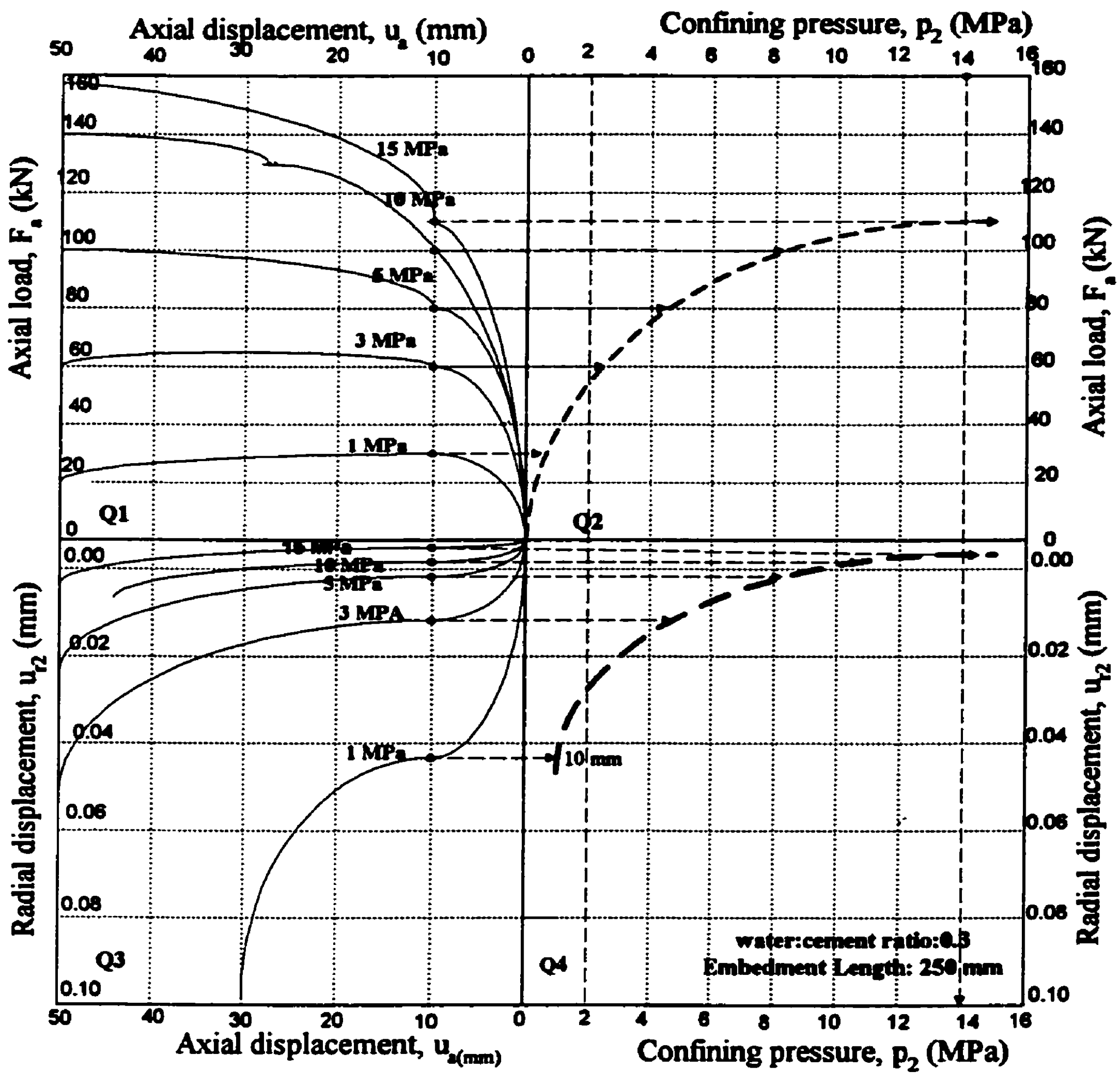

Figure 3.8: CABLE Model (after Hyett et al., 1995)

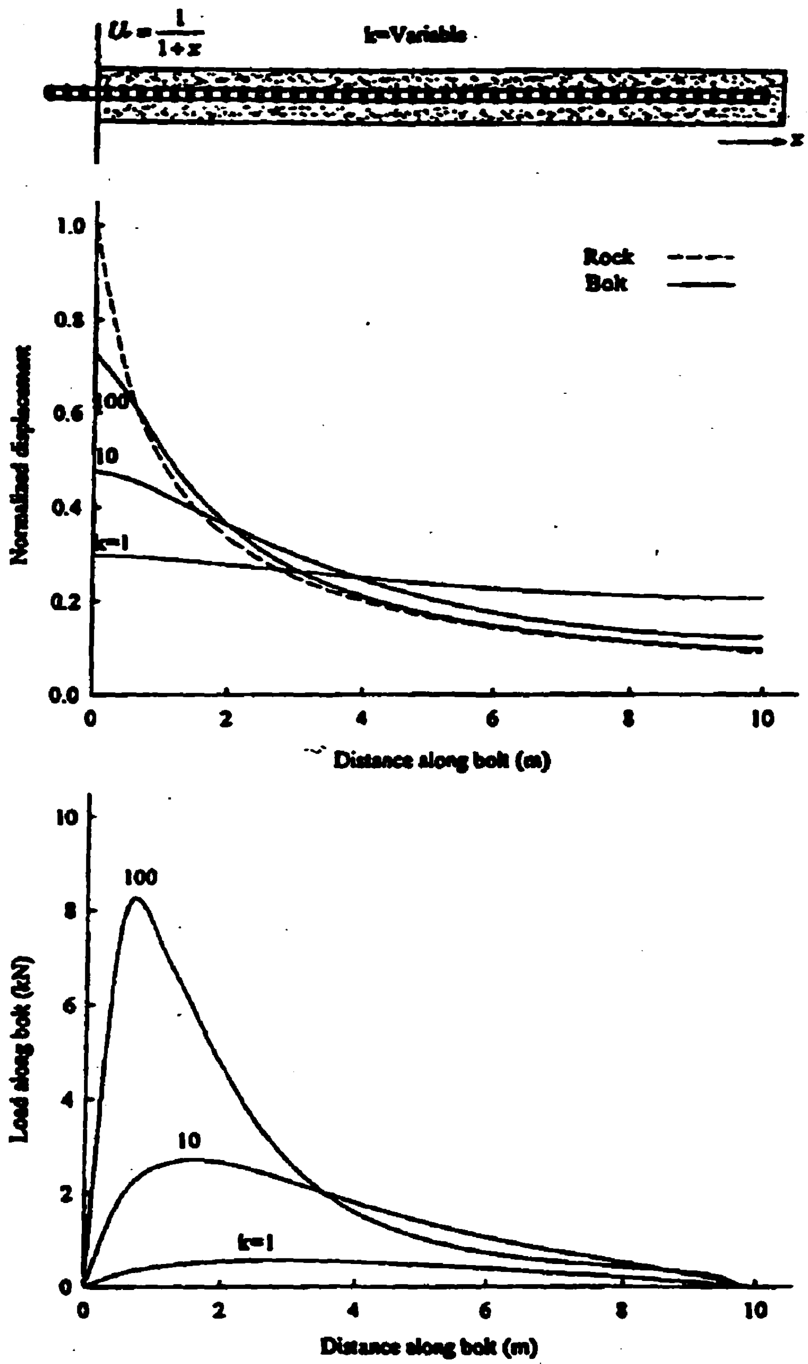

Figure 3.9: Analytical solutions for axial displacement and axial load for a bolt with two free ends (after Hyett et al. 1996)

3.4 Numerical modelling

The development of numerical models for mining engineering applications has been increasing during the recent years in order to help predict the stability of underground openings. Today, numerical modelling has became an indispensable engineering tool for ground control and mine planning. Initially, the finite element method was used. Later, boundary and distinct element methods for modelling jointed rock masses were adopted. Table 3.2 shows the advantages and disadvantages of each method.

Table 3.2: Advantages and disadvantages of numerical methods (after Hoek et al.,1991)

	Advantages	Disadvantages
Boundary element method	Far-field conditions inherently represented Only boundaries require discretization	Coefficient matrix fully populated Solution time increases exponentially with number of elements used
Finite-element and finite-difference methods	Material heterogeneity easily handled Material and geometric non-linearity handled efficiently with explicit solution techniques Matrices are banded with implicit solution techniques When explicit solution techniques are used, less skill is required from user	Entire volume must be discretized Far-field boundary conditions must be approximated For linear problems, explicit solutions techniques are relatively slow Solution time increases exponentially with number of elements used for implicit solution techniques
Discrete-element method	Data structures well suited to model systems with high degree of non-linearity from multiple intersecting joints Very general constitutive relations may be used with little penalty in terms of computational efforts Solution time increases only linearly with number of elements used	Solution time seem much slower than for linear problems Results can be sensitive to assumed values of modeling parameters

Hollingshead (1971) modelled rock bolts using finite element technique as three phase material systems (steel tendon, grout and host rock). He used an elastic-perfectly plastic analysis assuming each of the three materials to yield according to the Tresca yield criteria. Yap and Rodger (1984) used finite element technique to evaluate the mechanism of the transfer of load in the pull out tests of fully grouted tendons. Other finite element models (Wang and Garga, 1992; Marence and swoboda, 1995) and finite difference models (Brady and Lorig, 1988) were developed for numerical modelling of rock anchors. Most of the work done in numerical modelling of rock anchors is limited to the behaviour of fully grouted rebars. The mechanism of 7-wire or cable has not been exclusively analyzed and it is not differentiated from the rock bolt.

3.3.1 FLAC and UDEC

FLAC (Fast Lagrangian Analysis of Continua) is a commercially available finite difference program for modelling soil and rock behaviour which is developed by Itasca Ltd. It has a large range of applications to geomechanical problems (Cundall et al. 1988). Using the concept of one-dimensional element of St. John and Van Dillen (1983), Itasca incorporated a rock bolt element in their finite difference software. Tan (1993) in his Ph.D thesis developed a new cable bolt load displacement relationship and implemented this into FLAC. Equations for two critical cable bolt loads –the linear elastic limit load and the ultimate bond load – are given. The load – displacement for the standard cable bolts is derived based on these loads and analysis of displacement (Tan et al. 1993). The latest version of FLAC is FLAC^{3D} Version 2.0.

UDEC (Universal Distinct Element Code) is a commercially available distinct element program for geomechanical analysis in which the performance of the rock mass may be dominated by discontinuities (joints, faults, bedding planes). Since 1983, Itasca has completed a number of modifications to the code which expand its range of applicability and the last version is UDEC version 3.0. UDEC has the capability to model cable bolts and as for FLAC Tan (1993) implemented a cable bolt load displacement relationship.

3.3.2 Phase^2

Phase^2 is a two dimensional finite element program for calculating stresses and displacements around underground or surface excavations. It was developed in the Department of Civil Engineering at the University of Toronto and is currently marketed by Rocscience Inc. It has the ability to model underground openings with rock support . The analytical model developed by Hyett (1996) was implemented in the program for the determination of the load distribution along one bolt. The limitation of the modelling technique is that bolts are simulated as bar elements passing through triangular elements which simulate the rock mass and this doesn't take into account the shear bond characteristics along the cable, which is an important factor for the simulation of cable bolts. Other parameters such as the type of cables and the induced stresses are not accounted for.

3.3.3 e-z tools

The software was developed at McGill University by the numerical modelling group (Mitri, 1993) for 2-dimensional stress and stability analysis of surface and underground excavations in rock and soil materials. It uses a linear elastic finite element model. The model predicts stresses, displacements and safety factors around excavations.

A simplified cable support finite element was formulated to simulate bolts. The cable element formulation is based on the assumption that the grouting material can be idealized by a continuous Winkler-type spring running parallel to the cable and connecting the cable surface to the borehole wall.

The limitations of the model is that it doesn't take into account tensioning and anchoring nor does it account for the effect of different types of cables other than standard.

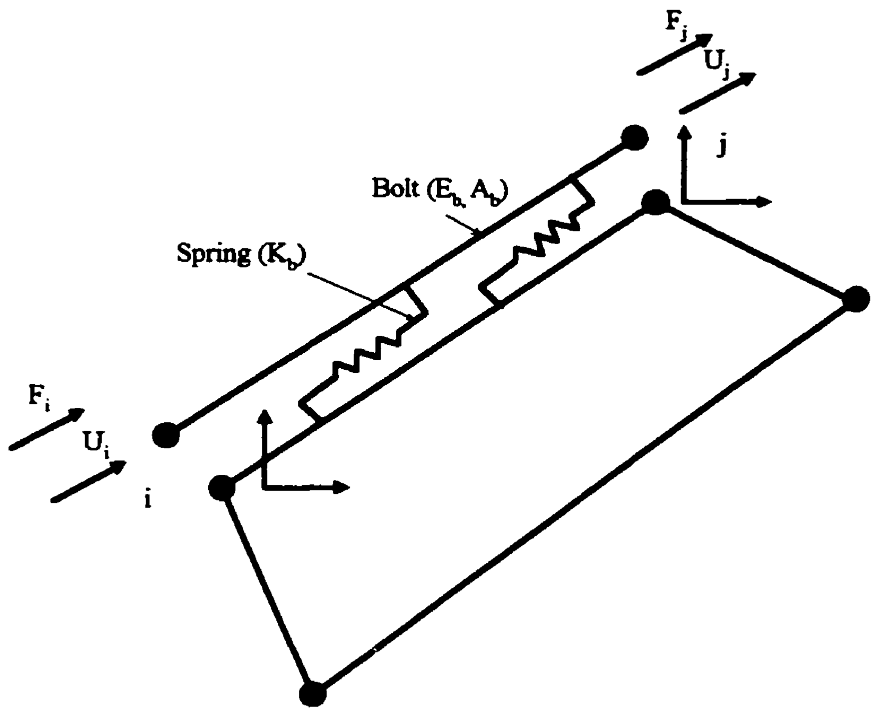

Figure 3.10: Modelling of bolts in e-z tools

3.5 Summary

The most commonly used design methods for cable bolts are the empirical methods, which are based on rock mass classification. They include the RMR system and the Q system. More recently, the Stability Graph Method for open stope design was proposed by Mathews et al. (1981) and subsequently modified by Potvin (1988). The Modified Stability Graph is quite popular in Canadian hard rock mines. Although, the use of analytical models and numerical model has been increasingly popular in recent years, no particular method has been suggested for the design of cable bolts.

CHAPTER 4
EMPIRICAL MODEL FOR THE SHEAR BOND STIFFNESS OF CABLE BOLTS

4.1 Introduction

The load transfer in cablebolting from the cable bolt and the rock mass and vice versa is done through the grout column. The axial force in the cable is transmitted to the grout by the shear bond stress. It is necessary to understand the process by which the load is transferred from the rock mass to the cable via the shear resistance at the cable-grout interface. Bond stress may be defined as the shear per unit length, which acts parallel to the cable axis at the grout-cable interface.

Generally pull-out tests are used in the laboratory or in the field to determine the cable bolt bond strength (Stillborg, 1984; Bawden et al. 1992), see Figure 4.1a. From the load-slip curve of Figure 4.1b, the bond stiffness, K, of the cable bolt at its loaded end, in the prepeak range can be obtained by assuming that the behaviour is linear elastic. Thus, K=P/S, where P is the applied load, and S is the corresponding tip displacement, and should have the units MN/m. The cable axial load and the slip distributions are shown in Figures 4.1c and 4.1d respectively. As can be seen, the axial load is transferred to the test cylinder through the grout material by shear bond action. The distribution of shear bond stress along the cable bolt is shown in Figure 4.1e. This load transfer mechanism has been previously explained by several other authors for bond in concrete (Gambarova, 1982; Tognon, 1982) and for cable bolts (Kaiser, 1992; Hyett, 1995).

As will be seen later, the numerical model defines the cable-rock interface by a Winkler shear spring. The stiffness of such spring, k, is defined per unit length of the cable i.e. (MN/m)/m length. For this reason, the following expression is used to calculate k:

$$k = \frac{P}{S.\Delta L} = \frac{K}{\Delta L} \qquad (4.1)$$

where k: shear bond stiffness per unit length of the cable (MN/m/m)

P: load (MN)

S: slip (m)

ΔL: short length of the grouted cable (m)

K: bond stiffness (MN/m)

Cables behave like a frictional support system and cohesive or adhesive strength components due to chemical bonding have been traditionally neglected because they are not mobilized simultaneously with the friction components (Yazici and Kaiser, 1992; Stillborg, 1984).

Many analytical models have been developed to simulate the effect of the bond stress as was mentioned in chapter 3 (Bond Strength Model, CABLE model) but they have their own limitations.

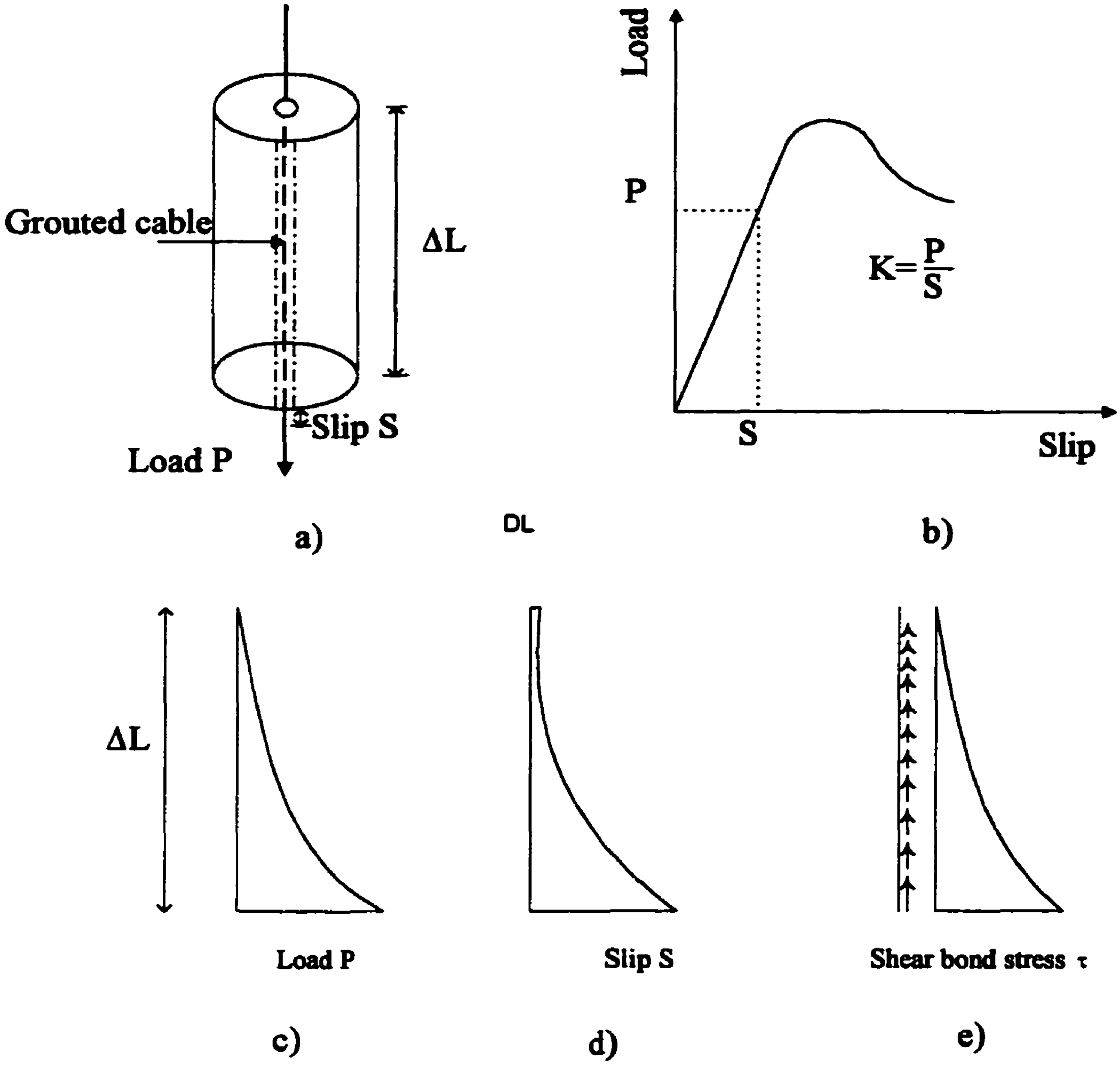

$$k = \frac{P}{S.\Delta L}$$

Figure 4.1: Definition of shear bond stiffness per unit length k from pull-out tests

4.2 Compilation of data

Laboratory pull-out tests (Figure 4.2) and field pull-out tests (Figure 4.3) have been performed with varying cable bolt geometry, grout type, host medium and confining stress, in order to examine the effect of these parameters on the behaviour of cable bolts.

Rajaie(1990) carried out a series of laboratory pull out tests on standard cable bolts for his Ph.D thesis at McGill University. Conventional grout and grout aggregate mixture were used with different embedment lengths. The host rock was modeled with concrete blocks.

Goris (1990) for the U.S.Bureau of Mines used conventional single cable, double cable and birdcage cables for laboratory pull out tests with steel pipes as confining medium . Water cement ratio (w:c) varied from 0.3 to 0.45 and the embedment length from 0.2 to 0.75 m.

Reichert (1992) conducted a laboratory and field research program in his thesis at Queen's University to determine the major factors influencing bond capacity of grouted cable bolts. Standard cable bolts were used. In the laboratory 'Split-pipe' tests were conducted using PVC, aluminum and steel pipes to provide radial confinement, and field tests were chosen in granite, limestone and shale rock masses. A normal (type 10) Portland cement grout was used. Water-cement ratio varied from 0.3 to 0.5 and embedment length from 0.25 m to 0.5 m.

Bawden and Hyett (1992) conducted a field cable bolt pull test program at Bousquet mine (Val-d'Or, Québec). Standard, birdcage and nutcase cable bolts were used in schist and ryolite medium.

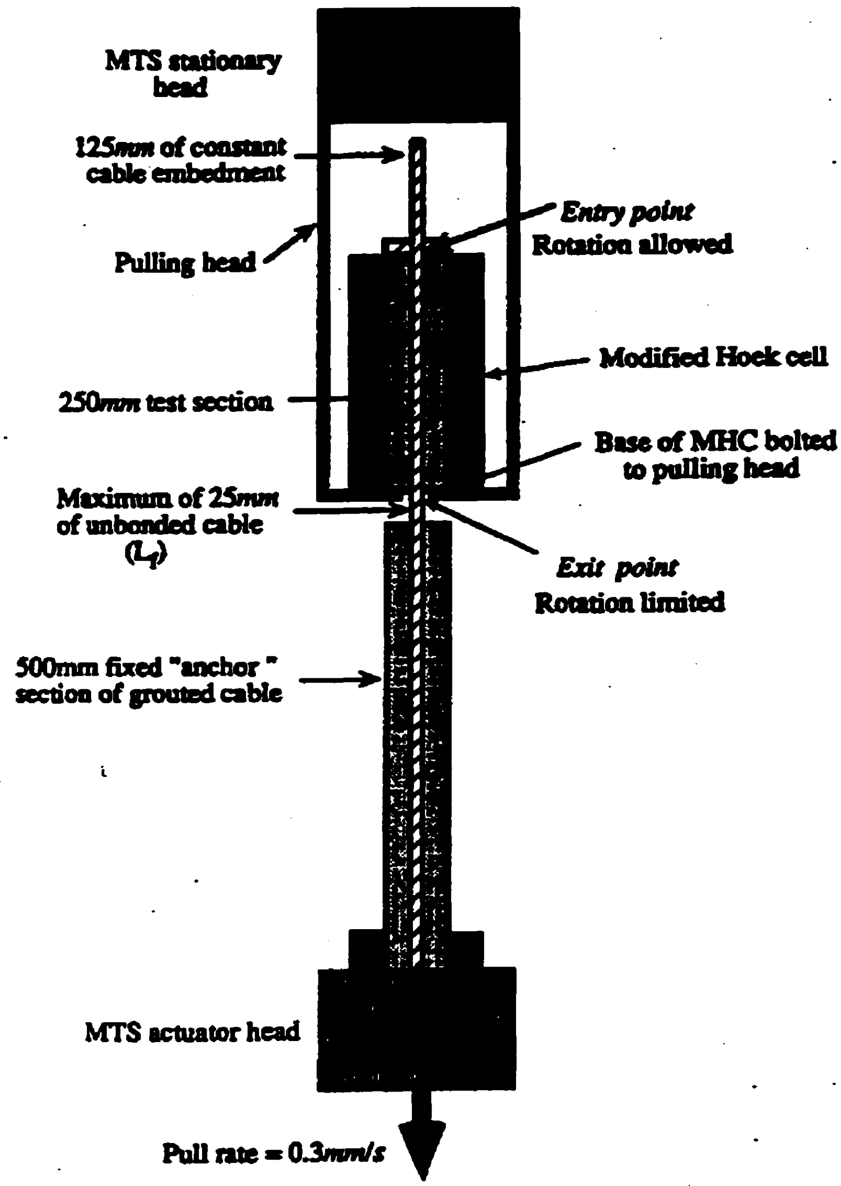

Figure 4.2: Laboratory pull test set-up (Hyett et al., 1995)

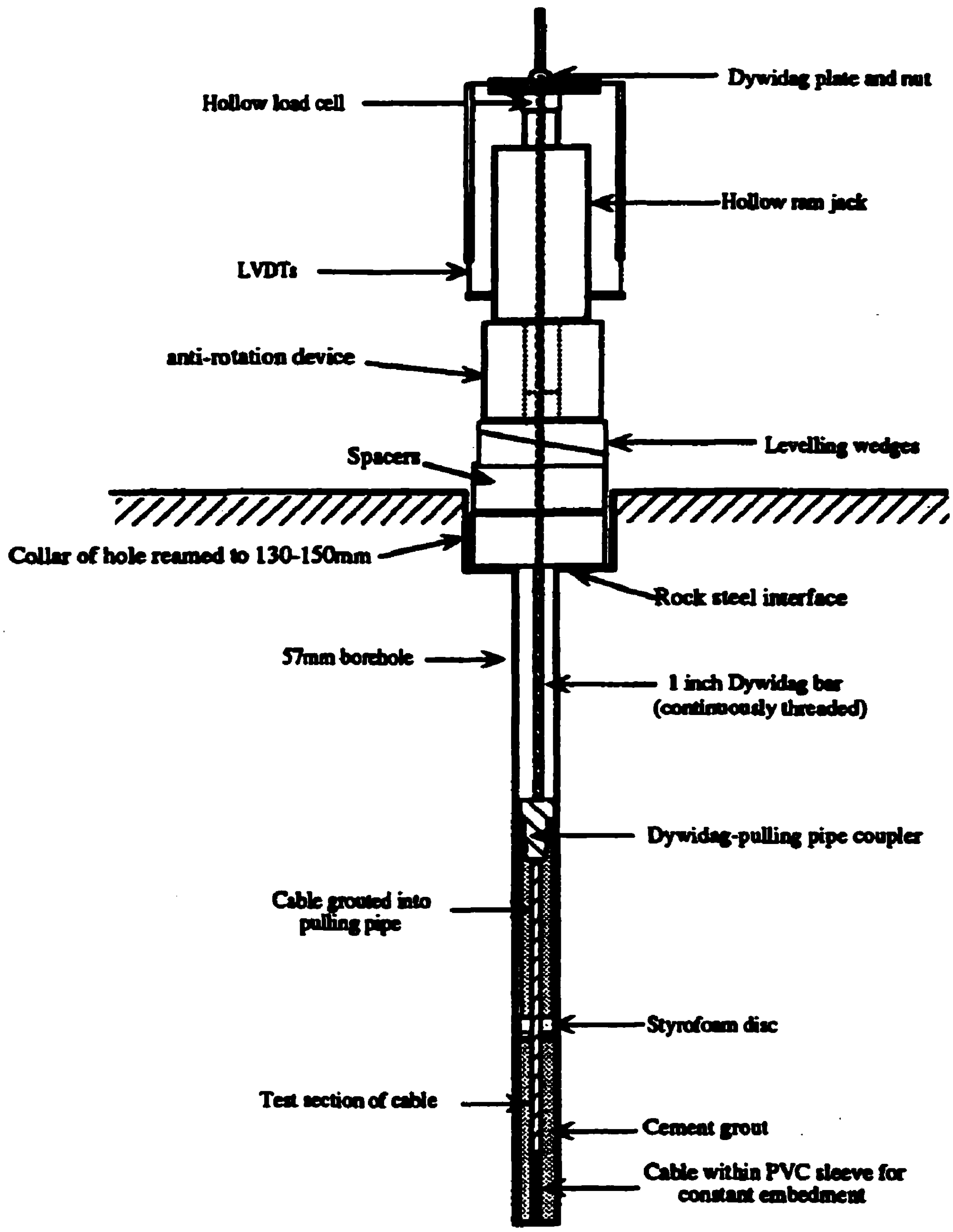

Figure 4.3: The field pull test apparatus (Bawden et al., 1992)

McSporran (1992) at Queens University used the conventional cable bolt and a series of pull out tests was performed under constant radial confinement in a pressure vessel to simulate the effect of confining pressure on the cable bolt capacity using steel pipes as confining medium.

Khan (1995) for his Ph.D thesis at McGill University conducted laboratory pull-out tests on conventional cable bolts and composite material tendons. For cable bolts, high strength cement grout, shotcrete grout and conventional grout were used with variation of stiffness and stress, water cement ratio, embedment length and rate of displacement.

Moossavi (1997) for his Ph.D thesis at Queen's University continued the work of McSporran (1993) with modified geometry cable bolts (Garford bulb and nutcase). A new modified Hoek cell was designed and pull out tests under different confining pressure were conducted.

A compilation of data has been done by the author using all the results collected and integrated in a database using Microsoft Access (see Appendix). Data are shown for each type of cable in Tables 4.1, 4.2, 4.3 and 4.4. Conventional cement grout is considered with water:cement ratio varying from 0.3 to 0.5. The effects of three parameters on the shear bond stiffness are analyzed. They are:

- Type of cable.
- Modulus of elasticity of host medium.
- Confining pressure.

4.3 Factors influencing shear bond stiffness

The effect of host medium and confining pressure after installation are shown in Figures 4.4 to 4.13 for each type of cable.

4.3.1 Modulus of elasticity of host medium

The rock mass itself exerts a major influence on the capacity of cable bolts through the modulus of elasticity of host medium.

4.3.1.1 Standard cable

Figures 4.4 and 4.5 show the effect of this parameter on the shear bond stiffness *k*. The shear bond stiffness increases linearly with the modulus of elasticity of the host medium. When the confining stress ($\Delta\sigma$) increases the shear bond stiffness increases (Figure 4.4) and it appears from the comparison of Figures 4.4 and 4.5 that when the water cement ratio decreases the shear bond stiffness increases.

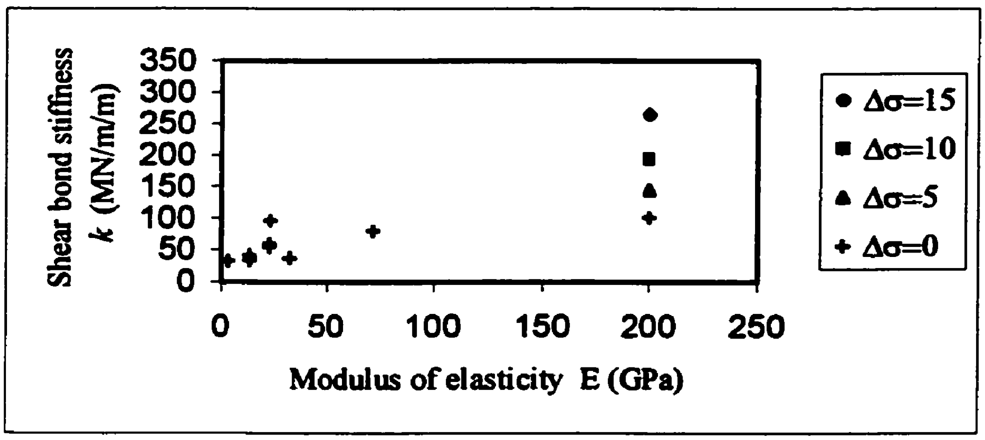

Figure 4.4: Effect of modulus of elasticity (E) of host medium on the shear bond stiffness (standard cable, w:c = 0.3)

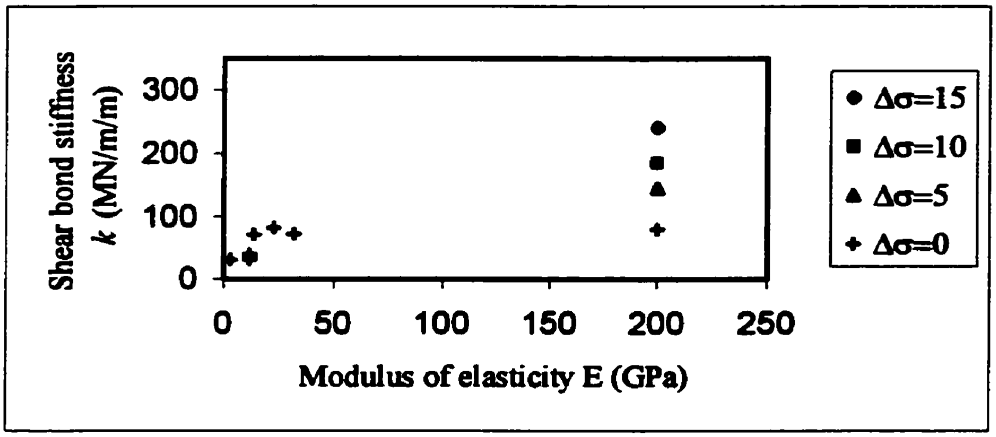

Figure 4.5: Effect of modulus of elasticity (E) of host medium on the shear bond stiffness (standard cable, w:c = 0.4)

4.3.1.2 Modified cable geometries

Figures 4.6, 4.7 and 4.8 show the variation of the shear bond stiffness k with the rock modulus for the birdcage cables, the nutcase cables and the garford bulb cable. The shear bond stiffness varies linearly with the modulus of elasticity and is higher than for the conventional cable bolts. Nutcase cables (Figure 4.9) show higher shear bond stiffness than for garford bulb cables and birdcage cables for the same values of the modulus of elasticity.

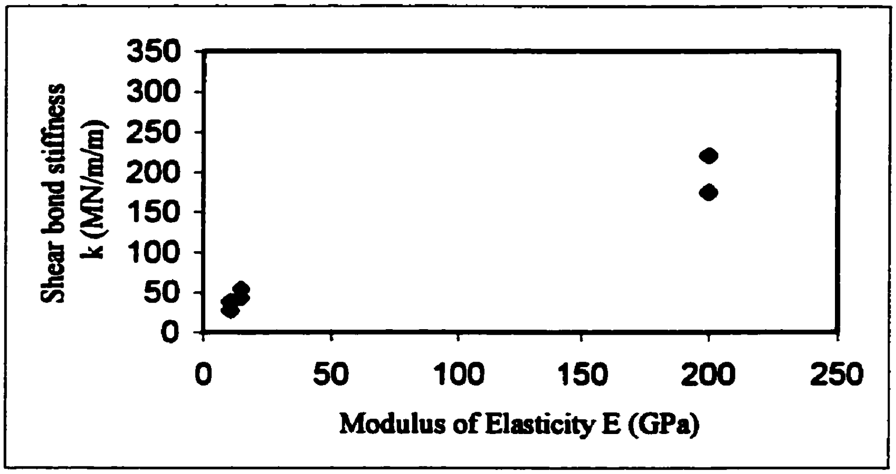

Figure 4.6 : Effect of modulus of elasticity E of host medium on the shear bond stiffness (birdcage cable , w:c ratio=0.35)

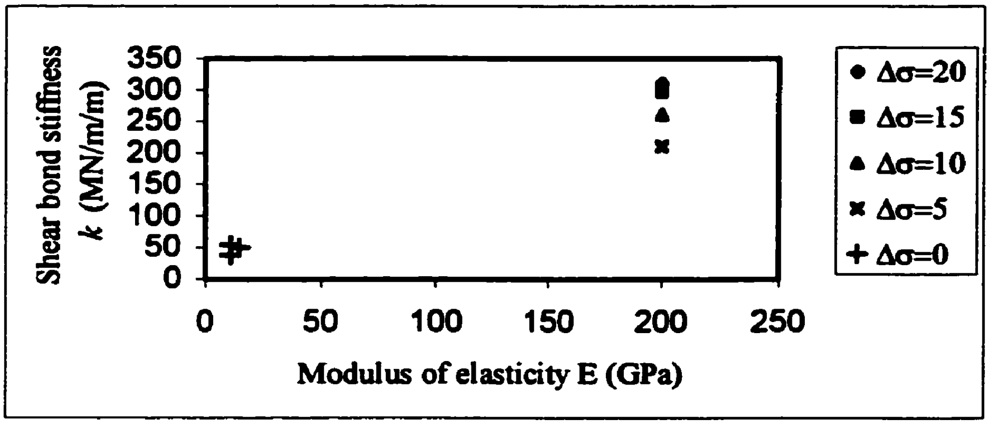

Figure 4.7: Effect of modulus of elasticity of host medium on the shear bond stiffness (nutcase cable, w:c =0.4)

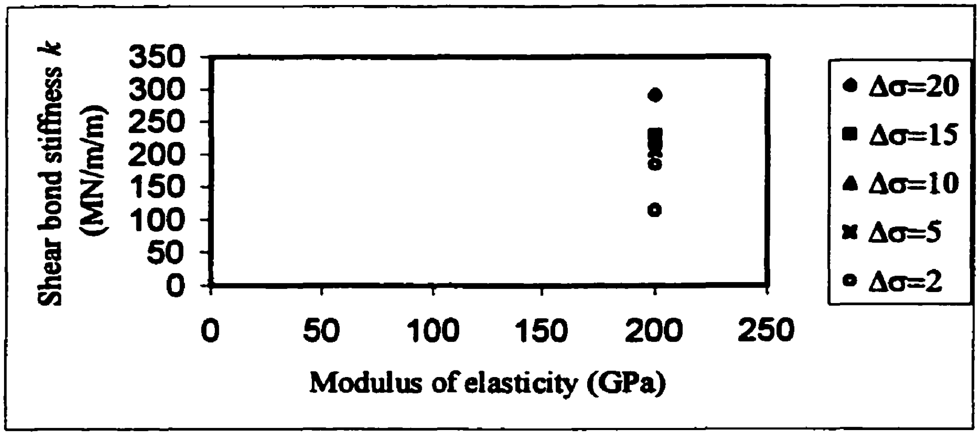

Figure 4.8: Effect of modulus of elasticity of host medium on the shear bond stiffness (garford bulb cable, w:c = 0.4)

4.3.2 Confining pressure

Mining induced stress change in the field is one of the most important factors which can lead to cable failure. A stress decrease in a direction radial to the cable bolt hole will result in a decrease in cable capacity and can lead to a cable failure (Kaiser et al., 1992). Stress change may cause a change in the rock mass modulus due to the stress dependent stiffness of the rock joints and microfractures (Bandis et al., 1983).

4.3.2.1 Standard cable bolts

McSpooran (1993) for conventional cable bolts used a Modified Hoek cell to simulate this effect in the laboratory. Figures 4.9, 4.10 and 4.11 show the variation of the shear bond stiffness with the confining pressure for a water cement ratio of 0.3, 0.4 and 0.5.

From the figures, the shear bond stiffness varies linearly with variation of confining pressure. As for the modulus of elasticity of host medium, when the water : cement ratio increases the shear bond stiffness decreases. For a water cement ratio of 0.3 (Figure 4.9) the values are higher than for a water:cement ratio of 0.4 and 0.5 (Figures 4.10 and 4.11).

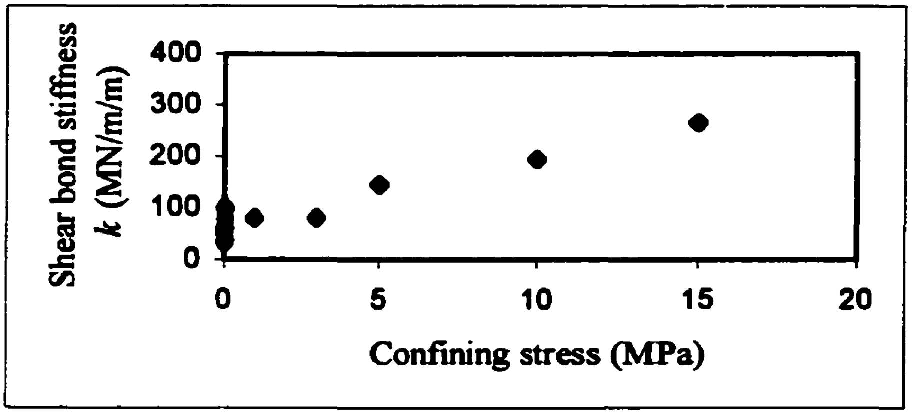

Figure 4.9: Effect of confining stress on the shear bond stiffness (standard cable, w:c = 0.3)

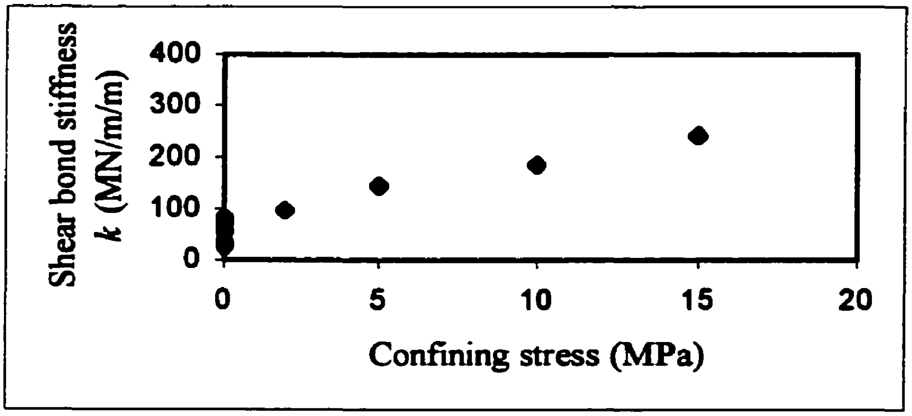

Figure 4.10: Effect of confining stress on the shear bond stiffness (standard cable, w:c = 0.4)

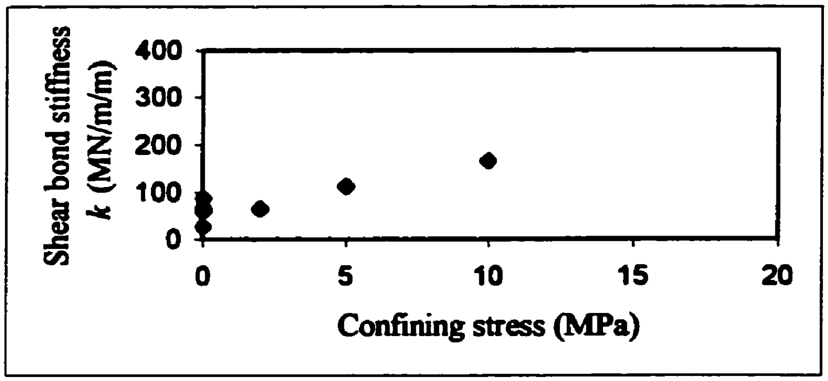

Figure 4.11: Effect of confining stress on the shear bond stiffness (standard cable, w:c = 0.5)

4.3.2.2 Modified cable geometries

As shown for conventional cable bolts, variation of confining pressure is a critical parameter in the design of cable bolts. For modified cable geometries the simulation of variation of confining stress in the laboratory was done by Moossavi (1997).

Figures 4.12 and 4.13 show the effect of confining stress on the shear bond stiffness *k* for garford bulb and nutcase cable bolts. The shear bond stiffness increases linearly with the confining pressure until a certain value of the pressure and then becomes constant. The mobilized load in the cable increases linearly with confining pressure to reach a constant value at higher pressures. In comparison with conventional cable bolts, modified cable geometries are less sensitive for stress change than the standard cable bolts.

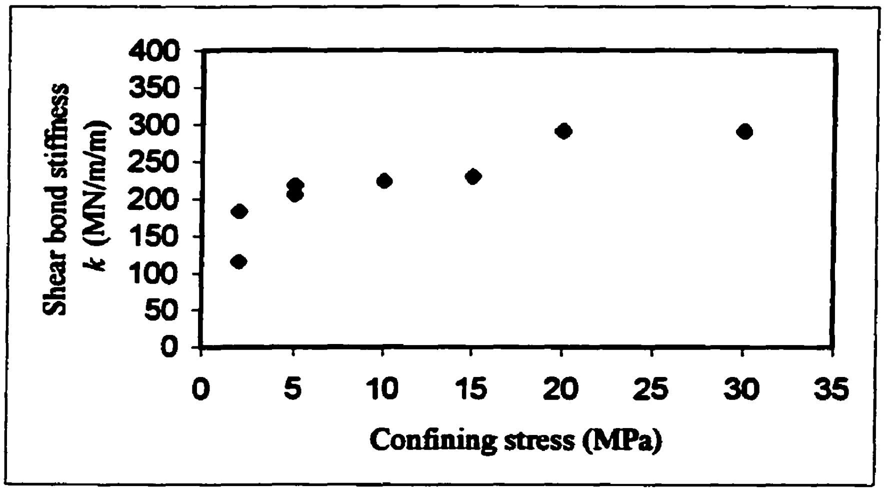

Figure 4.12: Effect of confining stress on the shear bond stiffness
(garford bulb cable, w:c=0.4)

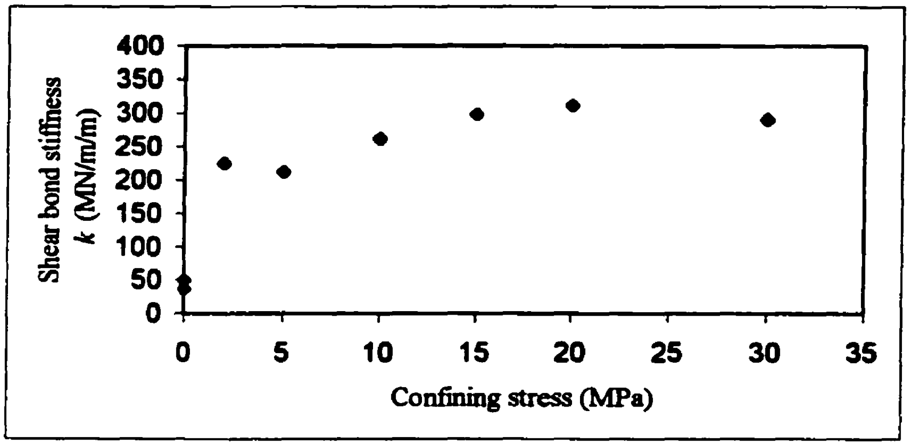

Figure 4.13: Effect of confining stress on the shear bond stiffness
(nutcase cable , w:c=0.4)

4.4 Empirical model

As shown before, the shear bond stiffness is a function of type of cable, modulus of elasticity, variation of the confining pressure and water:cement ratio, i.e.

$$k = f(\Delta\sigma).\ f(E).\ f(w{:}c) \qquad (4.2)$$

$k = k_0$ when the variation of confining pressure is equal to zero ($\Delta\sigma$=0 MPa).

4.4.1 Variation of shear bond stiffness with modulus of elasticity

From Figures 4.4, 4.5 and 4.6 the empirical relations between the shear bond stiffness and the modulus of elasticity of host medium were established for a confining pressure equal to zero using the database and statistical analysis. The shear bond stiffness varies linearly with the modulus of elasticity .

$$k_0 = a_0\, E + b_0 \qquad (4.3)$$

Where:

k_0: shear bond stiffness for $\Delta\sigma$=0 (MN/m/m).
a_0 and b_0: coefficients depending on cable geometry and water:cement ratio.
E: Modulus of elasticity of host medium (GPa).

4.4.1.1 Standard cable bolts

Figures 4.14 and 4.15 show the variation of shear bond stiffness k_0 with the modulus of elasticity with water:cement ratios w:c=0.3 and w:c=0.4. The correlation factor is R^2=0.43 for w:c=0.3 and R^2= 0.64 for w:c=0.4. Empirical relations established using regression analysis are:

$$k_0 = 0.22\,E + 59.03 \quad w{:}c = 0.3\,, \quad 0 \le E \le 200\ \text{GPa} \qquad (4.4)$$

$$k_0 = 0.24\,E + 41.12 \quad w{:}c = 0.4, \quad 0 \le E \le 200\ \text{GPa} \qquad (4.5)$$

From the empirical relations the shear bond stiffness increases when water:cement ratio decreases.

4.4.1.2 Birdcage cable

Figure 4.16 shows the variation of shear bond stiffness k_0 with the modulus of elasticity with a water:cement ratio w:c=0.35. The correlation factor is R^2=0.98. A good correlation was found and the empirical relation is:

$$k_0 = 0.83\,E + 32.58 \qquad w{:}c = 0.35, \quad 0 \le E \le 200\ \text{GPa} \qquad (4.6)$$

The shear bond stiffness k_0 when the variation of confining pressure is equal to zero is higher for birdcage cable bolts than for standard cable bolts.

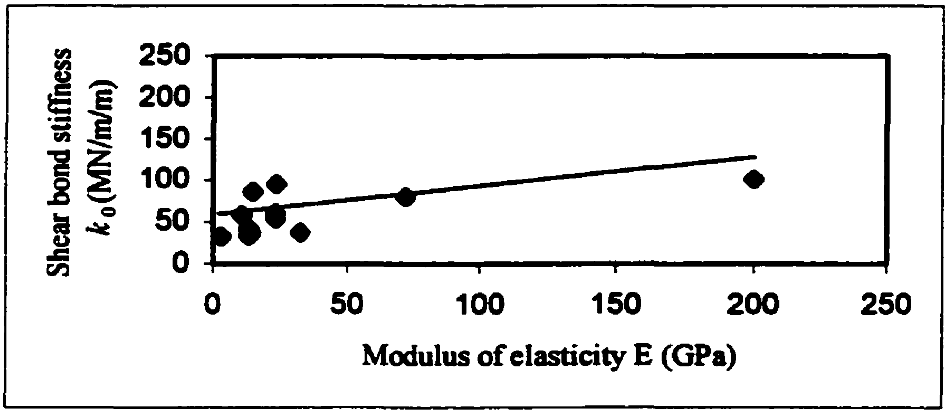

Figure 4.14: Variation of shear bond stiffness with modulus of elasticity (standard cable, w:c=0.3, Δσ=0)

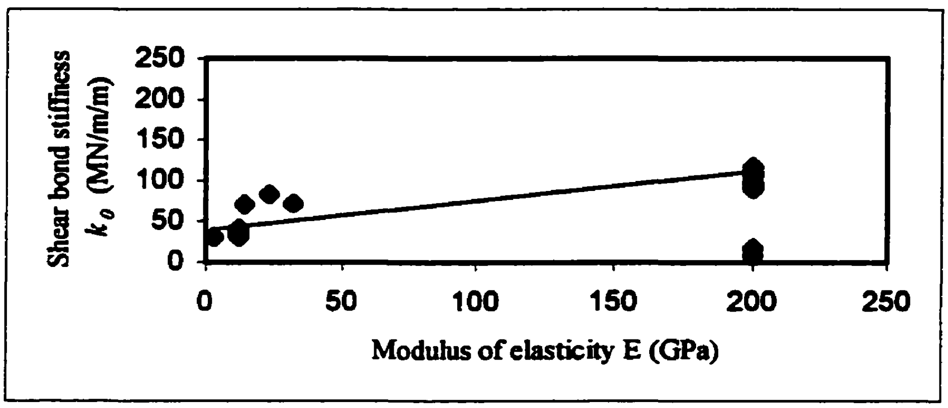

Figure 4.15: Variation of shear bond stiffness with modulus of elasticity (standard cable, w:c=0.4, Δσ=0)

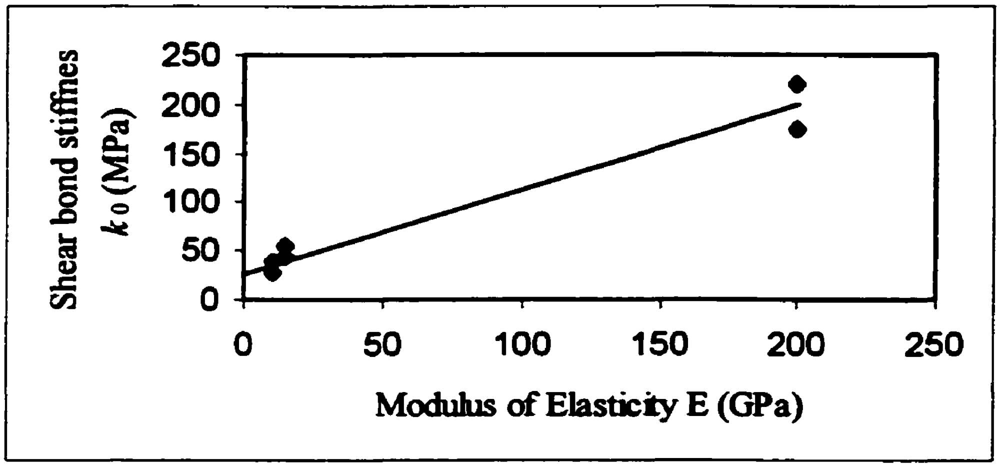

Figure 4.16: Variation of shear bond stiffness with modulus of elasticity (birdcage cable, w:c=0.35, $\Delta\sigma$=0)

4.4.2 Variation of shear bond stiffness with confining pressure

From Figures 4.9, 4.10,4.11, 4.12 and 4.13, the empirical relations between the shear bond stiffness and the variation of confining pressure were established by the author for 3 types of cable bolts (standard cable, nutcase cable and garford bulb cable) using the database and statistical analysis.

The shear bond stiffness varies linearly with confining pressure :

$$k = a\,\Delta\sigma + b \qquad (4.7)$$

Where :

k: shear bond stiffness (MN/m/m)

a and b: coefficients depending on cable geometry and water:cement ratio

$\Delta\sigma$: variation of confining pressure (MPa)

4.4.2.1 Standard cable bolts

For standard cable bolts, Figure 4.17 shows the variation of shear bond stiffness k with confining pressure for different water:cement ratios (w:c=0.3-0.5).

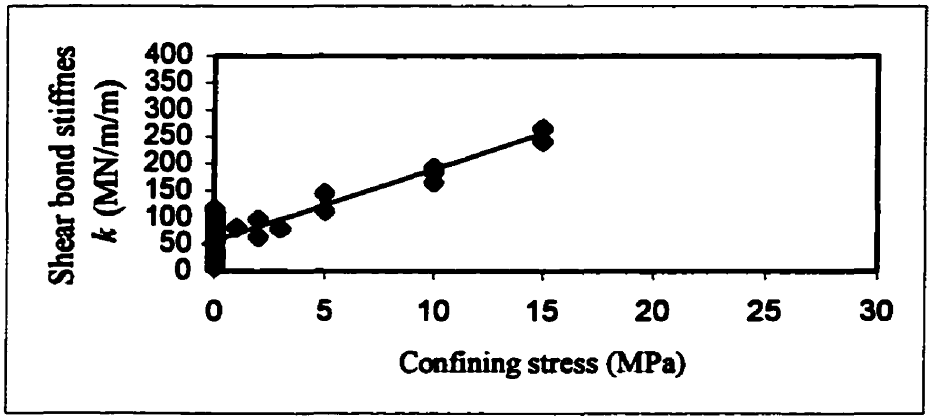

Figure 4.17: Variation of shear bond stiffness with confining pressure (standard cable)

An empirical relation from the data was established using statistical analysis. The correlation coefficient using regression analysis is $R^2 = 0.924$. A good correlation was found with coefficients "a" (slope) = 12.31 and "b" (intercept) = 63.7. Thus,

$k = 12.31\Delta\sigma + 63.7 \qquad 0 < \Delta\sigma \leq 15$ MPa, $0 \leq E \leq 200$ GPa (4.8)

4.4.2.2 Garford bulb cable

From the Figure 4.18, an empirical relation was established for garford bulb cables. The correlation coefficient is $R^2 = 0.893$ and coefficients "a" and "b" are: a = 5.74 and b = 175. For values higher than 20 MPa the shear bond stiffness is constant.

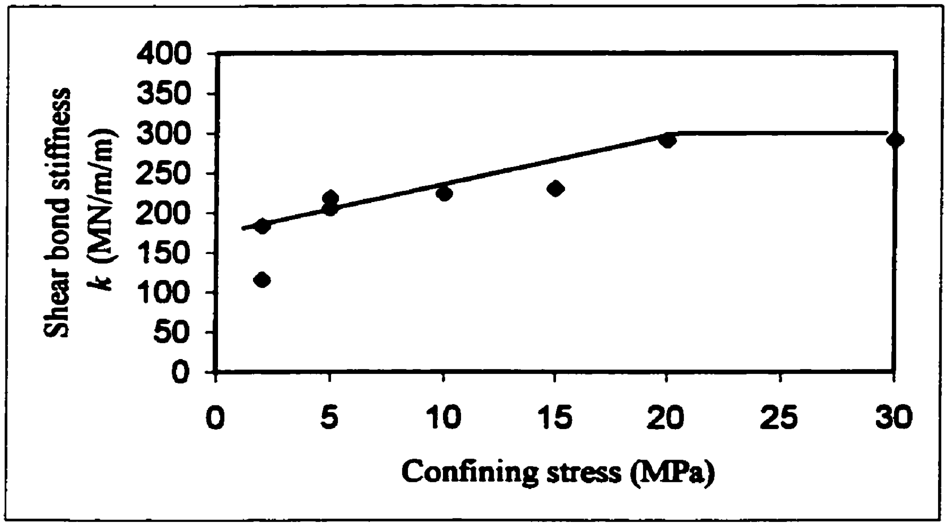

Figure 4.18: Variation of shear bond stiffness with confining pressure (garford bulb cable)

$k = 5.74\Delta\sigma + 165$ $\quad$ $0<\Delta\sigma<20$ MPa , E= 200 GPa, w:c=0.4 $\quad$ (4.9)

$k = 280$ MN/m/m $\quad$ $\Delta\sigma\geq 20$ MPa, E= 200 GPa, w:c=0.4

4.4.2.3 Nutcase cable

Figure 4.19 shows the variation between the shear bond stiffness and confining pressure for nutcase cable bolts. The correlation coefficient is $R^2 = 0.957$. Coefficients "a" and "b" are equal to: a=5.74 and b=202.5. For values higher than 20 MPa the shear bond stiffness is constant.

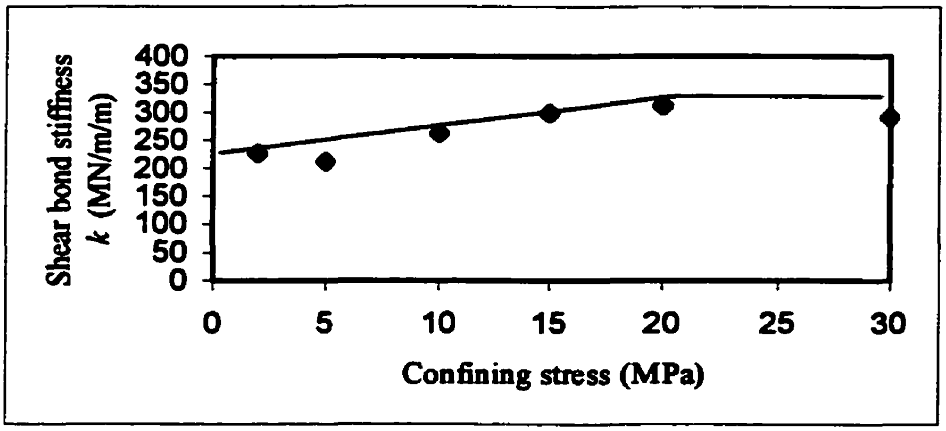

Figure 4.19: Variation of shear bond stiffness with confining pressure (nutcase cable)

$k = 5.74\Delta\sigma + 202.5$ $\quad$ $0<\Delta\sigma<20$ MPa, E= 200 GPa, w:c=0.4 $\quad$ (4.10)

$k = 317$ MN/m/m $\quad$ $\Delta\sigma \geq 20$ MPa, E=200 GPa, w:c=0.4

Figure 4.20 shows a comparison for the three types of cable bolts. The shear bond stiffness for modified cable geometries is higher than for standard cable bolts.

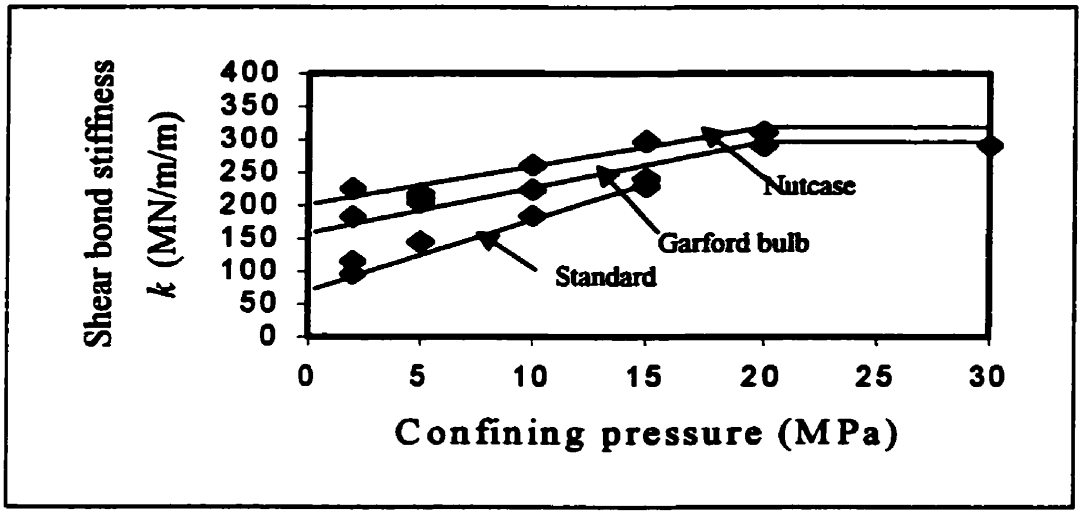

Figure 4.20: Variation of shear bond stiffness with confining pressure for different types of cable bolts

4.4 Summary

The compilation of data for the empirical model was carried out using laboratory tests with all uncertainties and errors resulting from the laboratory testing.

As many parameters affect the design of cable bolts, the empirical model is sensitive to the type of cable geometry, host medium stiffness and variation of confining pressure. Water cement ratio of the cement grout varied from 0.3 to 0.5 for standard cable bolts. For nutcase and garford bulb cables the water:cement ratio was kept constant (w:c= 0.4).

It should be noted that the model is limited only for three types of cables (standard, garford bulb, nutcase). Another limitation of the model is that only steel pipes were used to simulate the host medium in the laboratory pull-outs test using modified Hoek cell and the effect of variation of confining pressure. Only the reported values of the modulus of elasticity of the host medium were used. No statistical variation of this data was found. More data are needed to extend the range of validity of the database and to include the effect of resin grout and new types of cable bolts under different confining pressures.

Table 4.1: Data for shear bond stiffness (standard cable bolts)

Water:cement ratio (w:c)	Host medium	Modulus of elasticity E (GPa)	Confining pressure $\Delta\sigma$ (MPa)	Calculated shear bond stiffness k (MN/m/m)
0.3	Steel	200.0	0	101.0
0.3	Aluminum	72.0	0	80.0
0.3	PVC	3.0	0	32.4
0.3	Granite	23.3	0	96.0
0.3	Limestone	32.3	0	37.32
0.3	Shale	13.5	0	41.68
0.4	Steel	200.0	0	79.8
0.4	PVC	3.0	0	30.8
0.5	Steel	200.0	0	64.6
0.5	PVC	3.0	0	27.0
0.4	Granite	23.0	0	82.8
0.4	Shale	14.0	0	71.2
0.4	Limestone	32.0	0	72.0
0.5	Granite	23.0	0	59.2
0.5	Shale	14.0	0	66.8
0.5	Limestone	32.0	0	87.6
0.3	Granite	23.0	0	60.0
0.3	Shale	14.0	0	36.3
0.3	Granite	23.0	0	54.4
0.3	Shale	13.5	0	34.0
0.35	Schist	14.9	0	86.8
0.35	Schist	14.9	0	86.8
0.35	Schist	14.9	0	86.8
0.35	Schist	14.9	0	86.8
0.35	Schist	14.9	0	86.8
0.35	Ryolite	10.6	0	58.8
0.35	Ryolite	10.6	0	58.8
0.35	Ryolite	10.6	0	58.8
0.35	Ryolite	10.6	0	58.8
0.35	Ryolite	10.6	0	58.8
0.35	Ryolite	10.6	0	58.8
0.45	Steel	200.0	0	8.33
0.45	Steel	200.0	0	16.67
0.45	Steel	200.0	0	116.65
0.45	Steel	200.0	0	104.96
0.45	Steel	200.0	0	110.17

Table 4.1: Data for shear bond stiffness (standard cable bolts)

0.45	Steel	200.0	0	97.2
0.45	Steel	200.0	0	97.25
0.45	Steel	200.0	0	105.6
0.45	Steel	200.0	0	108.8
0.45	Steel	200.0	0	96.9
0.45	Steel	200.0	0	99.2
0.45	Steel	200.0	0	95.45
0.45	Steel	200.0	0	97.5
0.45	Steel	200.0	0	89.8
0.30	Steel	200.0	0	65.88
0.35	Steel	200.0	0	62.12
0.40	Steel	200.0	0	21.6
0.45	Steel	200.0	0	13.96
0.40	Concrete	12.0	0	33.3
0.40	Concrete	12.0	0	40.6
0.40	Concrete	12.0	0	35.4
0.40	Concrete	12.0	0	34.4
0.40	Concrete	12.0	0	33.3
0.40	Concrete	12.0	0	30.8
0.40	Concrete	12.0	0	30.7
0.30	Steel	200.0	1.0	80.48
0.30	Steel	200.0	1.0	80.48
0.30	Steel	200.0	1.0	80.48
0.30	Steel	200.0	3.0	80.12
0.30	Steel	200.0	3.0	80.12
0.30	Steel	200.0	3.0	80.12
0.30	Steel	200.0	3.0	80.12
0.30	Steel	200.0	3.0	80.12
0.30	Steel	200.0	5.0	144.8
0.30	Steel	200.0	5.0	144.8
0.30	Steel	200.0	5.0	144.8
0.30	Steel	200.0	10.0	193.2
0.30	Steel	200.0	10.0	193.2
0.30	Steel	200.0	10.0	193.2
0.30	Steel	200.0	15.0	265.6
0.30	Steel	200.0	15.0	265.6
0.30	Steel	200.0	15.0	265.6
0.30	Steel	200.0	15.0	265.6
0.4	Steel	200.0	2.0	96.56
0.4	Steel	200.0	2.0	96.56

Table 4.1: Data for shear bond stiffness (standard cable bolts)

0.4	Steel	200.0	5.0	144.8
0.4	Steel	200.0	5.0	144.8
0.4	Steel	200.0	5.0	144.8
0.4	Steel	200.0	10.0	185.12
0.4	Steel	200.0	10.0	185.12
0.4	Steel	200.0	10.0	185.12
0.4	Steel	200.0	10.0	185.12
0.4	Steel	200.0	15.0	241.4
0.4	Steel	200.0	15.0	241.4
0.4	Steel	200.0	15.0	241.4
0.5	Steel	200.0	2.0	64.4
0.5	Steel	200.0	2.0	64.4
0.5	Steel	200.0	2.0	64.4
0.5	Steel	200.0	5.0	112.16
0.5	Steel	200.0	5.0	112.16
0.5	Steel	200.0	5.0	112.16
0.5	Steel	200.0	5.0	112.16
0.5	Steel	200.0	10.0	165.6
0.5	Steel	200.0	10.0	165.6
0.5	Steel	200.0	10.0	165.6

Table 4.2: Data for shear bond stiffness (nutcase cable bolts)

Water:cement ratio (w:c)	Confining medium	Modulus of elasticity E (GPa)	Confining pressure $\Delta\sigma$ (MPa)	Calculated shear bond stiffness *k* (MN/m/m)
0.35	Schist	14.9	0	50.0
0.35	Schist	14.9	0	50.0
0.35	Schist	14.9	0	50.0
0.35	Schist	14.9	0	50.0
0.35	Ryolite	10.6	0	37.50
0.35	Ryolite	10.6	0	37.50
0.35	Ryolite	10.6	0	37.50
0.35	Ryolite	10.6	0	37.50
0.35	Ryolite	10.6	0	54.20
0.35	Ryolite	10.6	0	54.20
0.35	Ryolite	10.6	0	54.20
0.40	Steel	200.0	2.0	226.0
0.40	Steel	200.0	2.0	226.0
0.40	Steel	200.0	2.0	226.0
0.40	Steel	200.0	2.0	226.0
0.40	Steel	200.0	5.0	211.7
0.40	Steel	200.0	5.0	211.7
0.40	Steel	200.0	5.0	211.7
0.40	Steel	200.0	5.0	211.7
0.40	Steel	200.0	10.0	261.7
0.40	Steel	200.0	10.0	261.7
0.40	Steel	200.0	10.0	261.7
0.40	Steel	200.0	10.0	261.7
0.40	Steel	200.0	15.0	297.7
0.40	Steel	200.0	15.0	297.7
0.40	Steel	200.0	15.0	297.7
0.40	Steel	200.0	15.0	297.7
0.40	Steel	200.0	20.0	311.5
0.40	Steel	200.0	20.0	311.5
0.40	Steel	200.0	20.0	311.5
0.40	Steel	200.0	20.0	311.5
0.40	Steel	200.0	30.0	291.3
0.40	Steel	200.0	30.0	291.3
0.40	Steel	200.0	30.0	291.3

Table 4.3: Data for shear bond stiffness (garford bulb cable bolts)

Water:cement ratio (w:c)	Confining medium	Modulus of elasticity E (GPa)	Confining pressure $\Delta\sigma$ (MPa)	Calculated shear bond stiffness k (MN/m/m)
0.40	Steel	200.0	2.0	183.7
0.40	Steel	200.0	2.0	115.7
0.40	Steel	200.0	2.0	183.7
0.40	Steel	200.0	2.0	183.7
0.40	Steel	200.0	5.0	205.3
0.40	Steel	200.0	5.0	205.3
0.40	Steel	200.0	5.0	205.3
0.40	Steel	200.0	5.0	205.3
0.40	Steel	200.0	10.0	224.0
0.40	Steel	200.0	10.0	224.0
0.40	Steel	200.0	10.0	224.0
0.40	Steel	200.0	10.0	224.0
0.40	Steel	200.0	15.0	230.0
0.40	Steel	200.0	15.0	230.0
0.40	Steel	200.0	15.0	230.0
0.40	Steel	200.0	15.0	230.0
0.40	Steel	200.0	20.0	291.3
0.40	Steel	200.0	20.0	291.3
0.40	Steel	200.0	20.0	291.3
0.40	Steel	200.0	20.0	291.3
0.40	Steel	200.0	30.0	291.3
0.40	Steel	200.0	30.0	291.3
0.40	Steel	200.0	30.0	291.3

Table 4.4: Data for shear bond stiffness (birdcage cable bolts)

Water:cement ratio (w:c)	Confining medium	Modulus of elasticity E (GPa)	Confining pressure $\Delta\sigma$ (MPa)	Calculated shear bond stiffness k (MN/m/m)
0.45	Steel	200.0	0	220.8
0.45	Steel	200.0	0	175.0
0.35	Ryolite	10.6	0	27.8
0.35	Ryolite	10.6	0	27.8
0.35	Ryolite	10.6	0	38.7
0.35	Ryolite	10.6	0	38.7
0.35	Ryolite	10.6	0	38.7
0.35	Schist	14.9	0	54.3
0.35	Schist	14.9	0	54.3
0.35	Schist	14.9	0	54.3
0.35	Schist	14.9	0	54.3
0.35	Schist	14.9	0	43.3

CHAPTER 5
FINITE ELEMENT MODEL

5.1 Introduction

With the rapid advancement of computer hardware technology in the last two decades, the use of numerical modelling software as a design tool in geotechnical engineering has become both affordable and popular. Methods like finite elements, boundary elements and distinct elements have all been used extensively in the design and analysis of geotechnical structures. Numerical methods have certain advantages over other methods; notably they will account for the complex geometry of an excavation, the deformation properties of the rock and the presence in situ (virgin) stresses.

A number of numerical models were developed especially for the simulation of rockbolts and cable bolts such as those reported by Mitri (1990), Wang (1992), Peng (1992) and Tan (1993). This chapter presents a specialized finite element modelling technique developed to simulate the mechanical behaviour of cable bolts performance. The technique is implemented in a finite element code (e-z tools) developed at McGill University.

5.1 Model assumptions

The cable bolt formulation presented here employs the following assumptions:

- A cable bolt can be represented by any number of 2-node bar elements. The cross sectional area and modulus of elasticity of the bar element are those of cable material (Figure 5.1).

- If the cable bolt is partially or fully grouted, the bonding effect of the grout as well as the shear slip occurring at the rock-grout and grout-cable interfaces can be represented by continuous shear springs acting along the anchor length. The stiffness of those springs, k, represents the shear bond stiffness per unit length of the grouted cable bolt as defined in chapter 4.

- The bar element representing the cable bolt is connected to quadrilateral isoparametric elements representing the host rock via the shear springs ; see Figure 5.1.

- Based on this formulation, only the axial load exerted on the cable bolt is considered. Bending load that may develop along a fully grouted cable bolt is not accounted for.

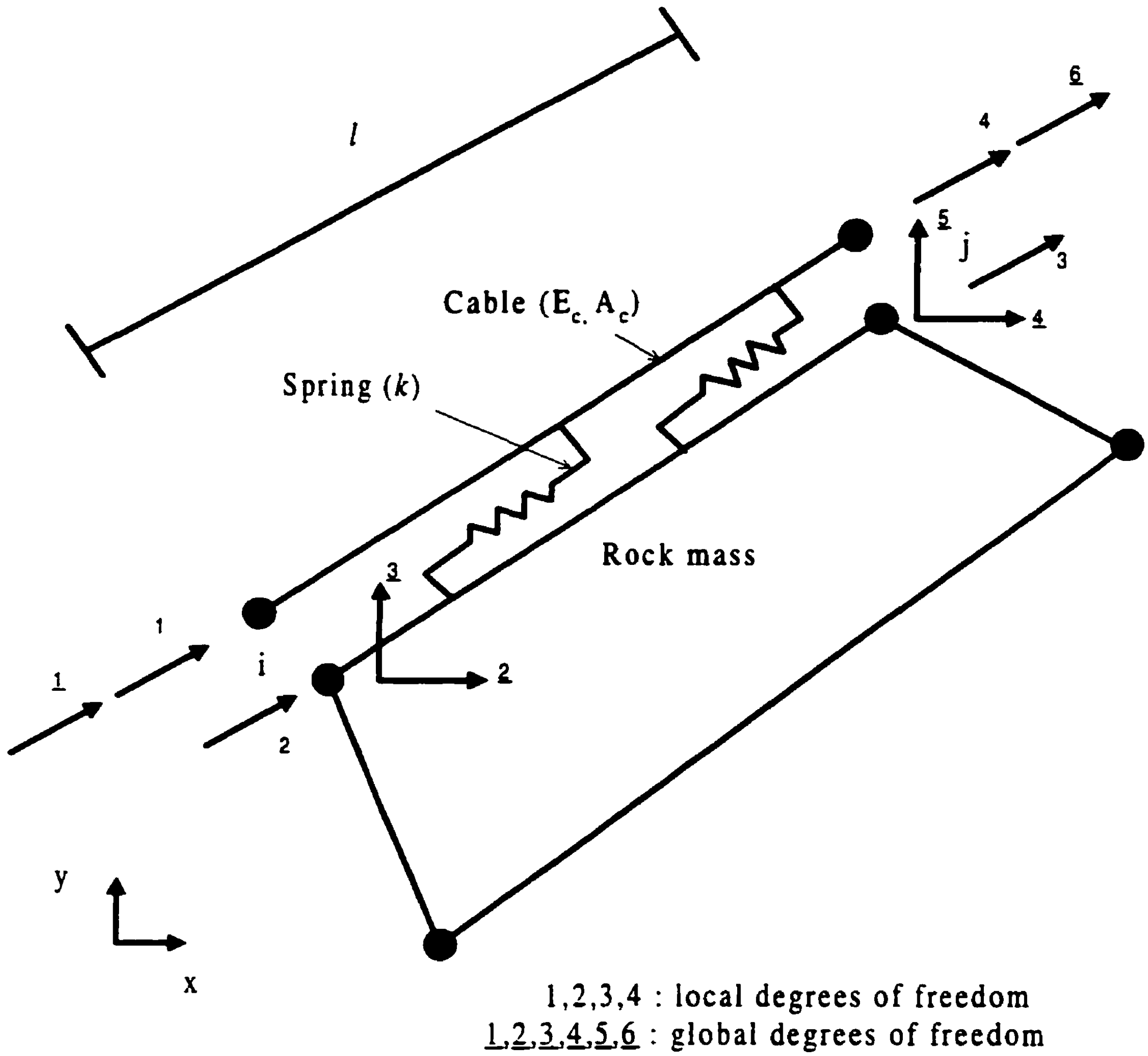

Figure 5.1: Geometry and degrees of freedom of a cable element

5.2 Finite element formulation

5.2.1 Equations

The 4-node quadrilateral, isoparametric element is used to represent the rock domain. The stiffness matrix K is given by:

$$K = \int_V B^T D\, B\, dV \qquad (5.1)$$

Where B is the strain-displacement matrix, and D is the stress-strain elasticity matrix. In rock mechanics problems, the load vector F is generally defined as follows.

$$F = -\int_V B^T \sigma^0 dV + \int_V \gamma N^T dV \qquad (5.2)$$

Where,

V = element volume

σ^0 = initial stress vector

N = the shape function matrix

γ = unit weight of the rock

Details of the above mentioned equations can be found in textbooks on finite elements (Cook, 1995; Pande et al., 1990).

For the new cable element, the total stiffness matrix k_c is obtained by adding up the stiffness contributions from the bar element k_b and the shear springs k_e. Thus,

$$k_c = k_b + k_e \qquad (5.3)$$

Where,

$$k_b = \begin{bmatrix} E_c A_c / l & -E_c A_c / l \\ -E_c A_c / l & E_c A_c / l \end{bmatrix} \qquad (5.4)$$

In the above, E_c is the modulus of elasticity of the cable, A_c is its cross sectional area, and l is the element length.

The shear spring stiffness, k_s, is assumed to vary linearly along the anchor element. This variation can be expressed in terms of the nodal values k_i and k_j as follows.

$$k_s = (1-\zeta)k_i + k_j \qquad (5.5)$$

Where $0 \le \zeta = x/l \le 1$

k_i and k_j : stiffness of continuous spring at nodes i and j respectively

Likewise, the spring displacement, u_s, can be expressed in terms of the nodal values as

$$u_s = (1-\zeta)u_{si} + u_{sj} \qquad (5.6)$$

The shear spring stiffness matrix is calculated from the strain energy stored in the shear springs of stiffness, k_s over the element length, l, as follows.

$$U_s = \frac{l}{2}\int_0^1 k_s u_s^2 d\zeta \qquad (5.7)$$

The stiffness matrix of the spring element is:

$$k_e = \int_0^l [N]^T . [k_s][N] dl \qquad (5\text{-}8)$$

After integration the resulting spring element stiffness matrix is:

$$k_e = \frac{l}{12} x \begin{bmatrix} 3k_i + k_j & -3k_i - k_j & -k_i - k_j & k_i + k_j \\ & 3k_i + k_j & k_i + k_j & -k_i - k_j \\ & & k_i + 3k_j & -k_i - 3k_j \\ \mathit{symmetric} & & & k_i + 3k_j \end{bmatrix} \qquad (5.9)$$

The total stiffness matrix of a cable element, k^c, is obtained from the algebraic addition of its two components: the spring element stiffness matrix and the truss element stiffness matrix.

The spring stiffness k is measured as the shear force per unit length of the bolt causing unit displacement and this information is derived from the load-slip curves obtained by means of laboratory or field pull-out tests as reported in chapter 4.

The above equation represents the local stiffness of the cable element. To transform this to global coordinates, we use the transformation matrix T:

$$[K^g] = [T]^T . [k_c] . [T] \qquad (5.10)$$

where :

- $[K^g]$ = stiffness matrix of the cable element in global coordinates.
- $[k_c]$ = stiffness matrix of the cable element in local coordinates.
- $[T]$ = transformation matrix from the local to global coordinates.

The transformation matrix [T] is defined by:

$$T = \begin{bmatrix} 1 & 0 & 0 & 0 & 0 & 0 \\ 0 & c & s & 0 & 0 & 0 \\ 0 & 0 & 0 & c & s & 0 \\ 0 & 0 & 0 & 0 & 0 & 1 \end{bmatrix} \qquad (5.11)$$

where: $c = \dfrac{x_j - x_i}{l}$ and $s = \dfrac{y_j - y_i}{l}$

5.2.2 Modelling end anchorage

The direct rock-cable connection provided by plates and anchors change the load transfer in the cable.

To take into account the plates in the simulation of cable bolts an hypothesis was formulated : when the cable bolt is fixed with a plate and a nut, the two nodes representing the anchor head, and the adjacent rock are forced to move together, to simulate the anchoring effect (Figure 5.2).

The stiffness matrix of the cable element change and the transformation matrix became:

$$T = \begin{bmatrix} 0 & c & s & 0 & 0 & 0 \\ 0 & c & s & 0 & 0 & 0 \\ 0 & 0 & 0 & c & s & 0 \\ 0 & 0 & 0 & 0 & 0 & 1 \end{bmatrix} \qquad (5.12)$$

The load distribution along cable bolts with end plates is different from the case without plates as shown by the model. The maximum force is mobilized at the anchored end and is zero at the free end. A case study in a coal mine using cable bolts and rock bolts with plates (Bouteldja and Mitri, 1999) shows the effect of plates in the load distribution along the cable for fully and partially grouted cable bolts.

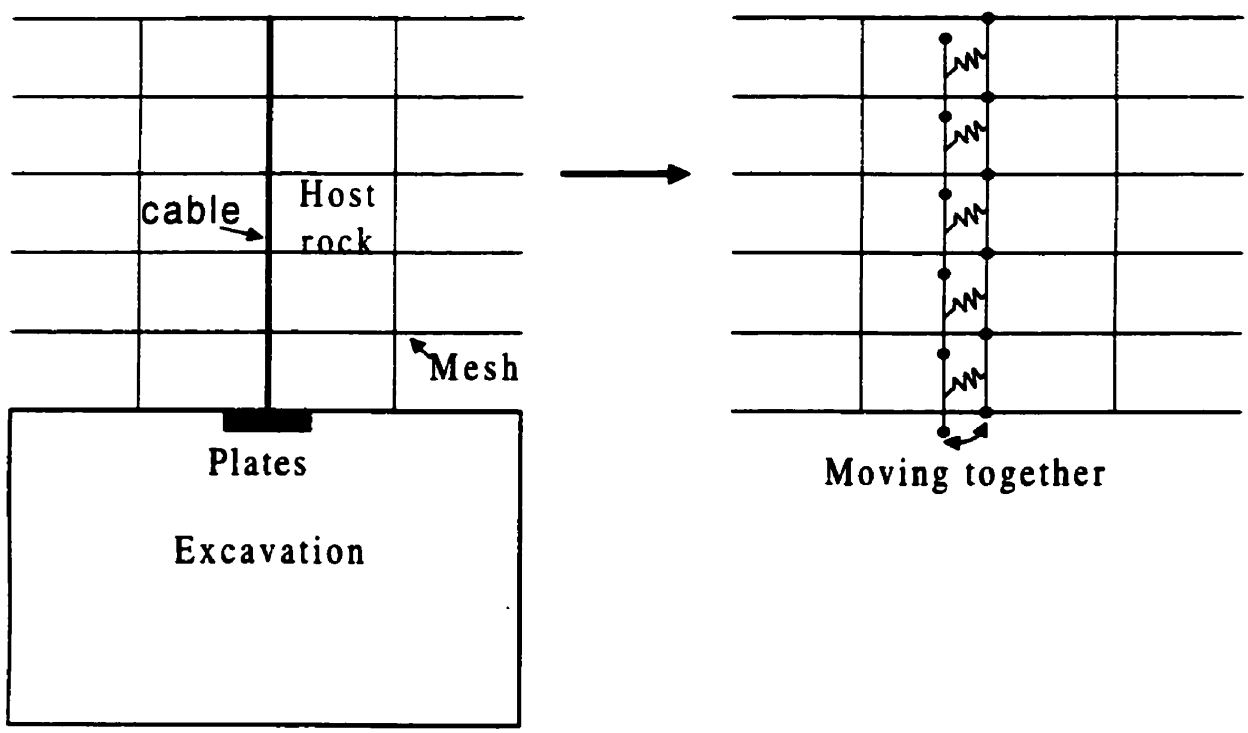

Figure 5.2: Simulation of anchored cable bolts

5.2.3 Modelling of pretension

Cable bolts are in some situations pretensioned and became active to help the rock mass to resist itself . It is apparent that pretensioning of the cable bolts is not required in the majority of underground cable bolting situations except where the horizontal stresses are low. This is not the case for rock bolts especially mechanically anchored bolts which are in most cases tensioned.

When anchor tensioning is required at the time of installation (Figure 5.3), an initial load vector, F_c^0 should be included in the formulation as:

$$F_c^0 = - \int_V B_b^T \, t \, dV \qquad (5.13)$$

Where B_b is the strain-displacement matrix of the bar element and t is the tension force.

$$\{F_c\}^0 = \{t_i \quad ct_i \quad st_i \quad ct_j \quad st_j \quad t_j\}^T \qquad (5.14)$$

With: $c = \dfrac{x_j - x_i}{l}$ and $s = \dfrac{y_j - y_i}{l}$

l: length of cable element

Figure 5.3 shows the simulation of pretension for a cable bolt.

- For element connected to plate t_i=t, t_j=0 and for the rest $t_i = t_j = 0$.
- For element connected to the cable $t_i = 0$, $t_j = -t$.
- For all the rest $t_i = t_j = 0$.

When a passive cable bolt is installed, the load vector from rock anchor element is $F_c^0 = 0$.

As the finite element model can simulate rock bolts and rock anchors. For mechanically anchored bolt the tension force is distributed uniformly along the bolt but for partially and fully grouted bolts the load from the tension force tends to zero at the free end because of the resin anchored end (Tang et al., 1999). The effect of pretension in the load distribution as computed by the model is shown in Figure 5.4.

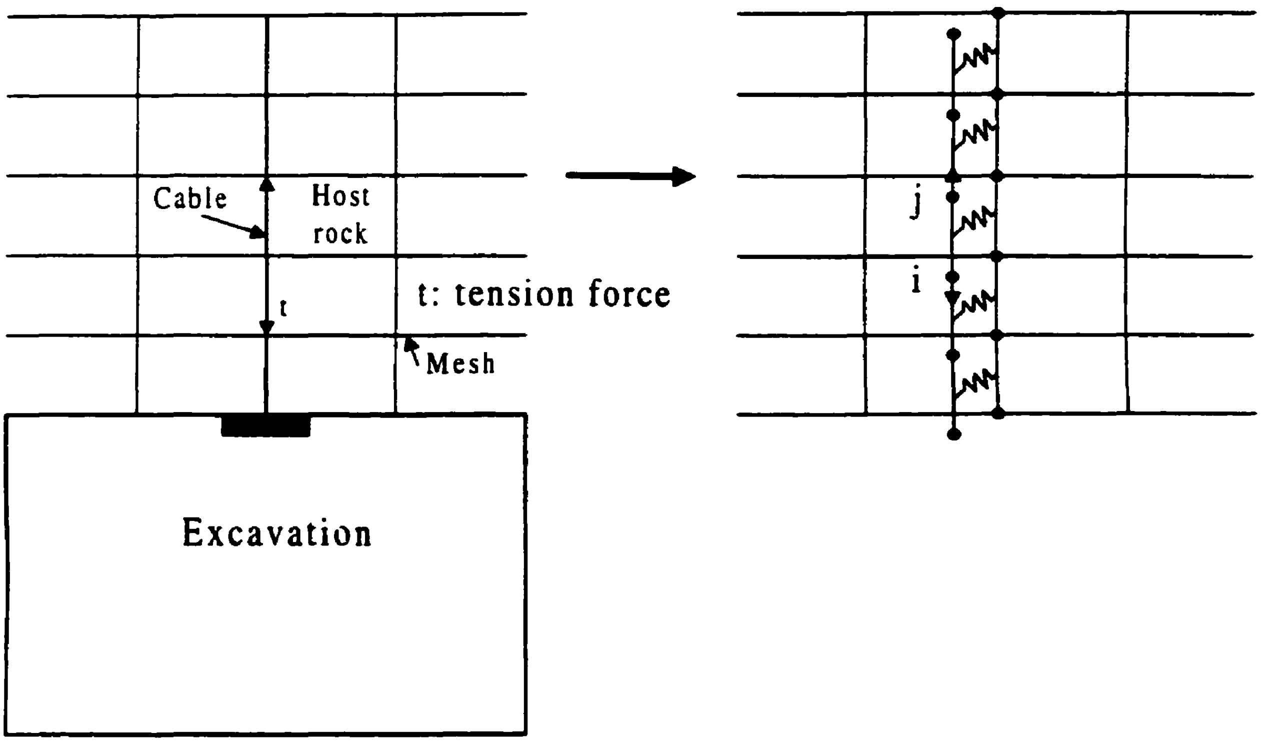

Figure 5.3: Simulation of tensioned cable bolts

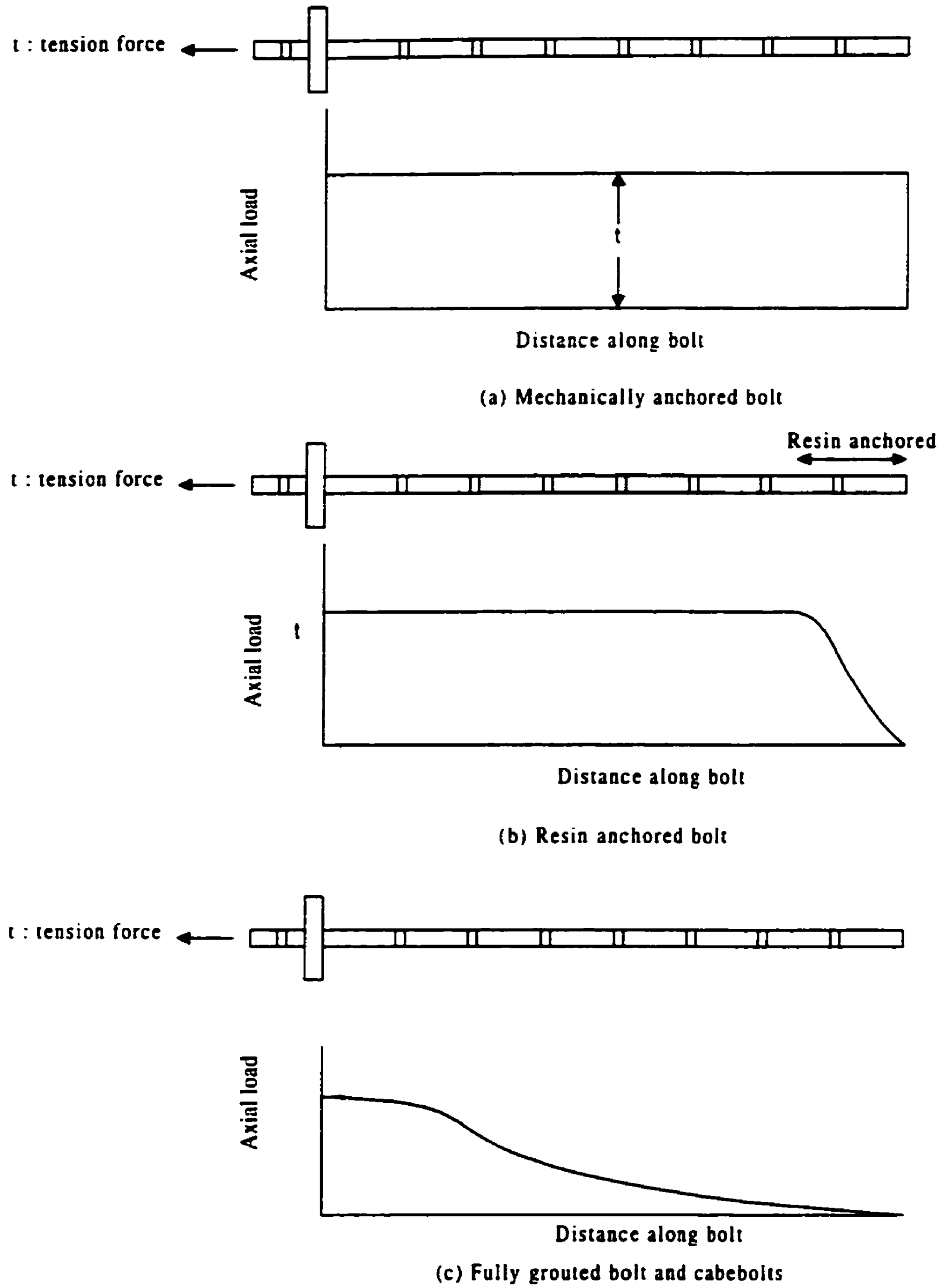

Figure 5.4: Anticipated load distribution along tensioned cable bolts

5.3 The program e-z tools

The new cable element model was implemented in e-z tools software which was previously developed at McGill University (Mitri, 1993). e-z tools is a finite element modelling software for 2-dimensional stress and stability analysis of surface and underground excavations in rock and soil materials.

The program consists of three modules (Figure 5.5), the preprocessor (ezpre), the core program (ezcor) and the postprocessor (ezpost) . In order to model cable bolts, the users needs to create a datafile with the extension CAB and will have the same name as the mesh file (.COR file). The purpose of the .CAB file is to provide such data as the mechanical properties of the cable bolt, the bond stiffness of the interface material and the locations of the cable bolts, the need for end plates and the tension force.

e-z tools uses a linear elastic model with 4-nodes isoparametric element. The program can simulate up to 8 materials. Isotropic or orthotropic materials can be simulated. The safety level of the material can be calculated using Mohr-Coulomb or Hoek-Brown failure criteria (Hoek and Brown, 1980 and 1988).

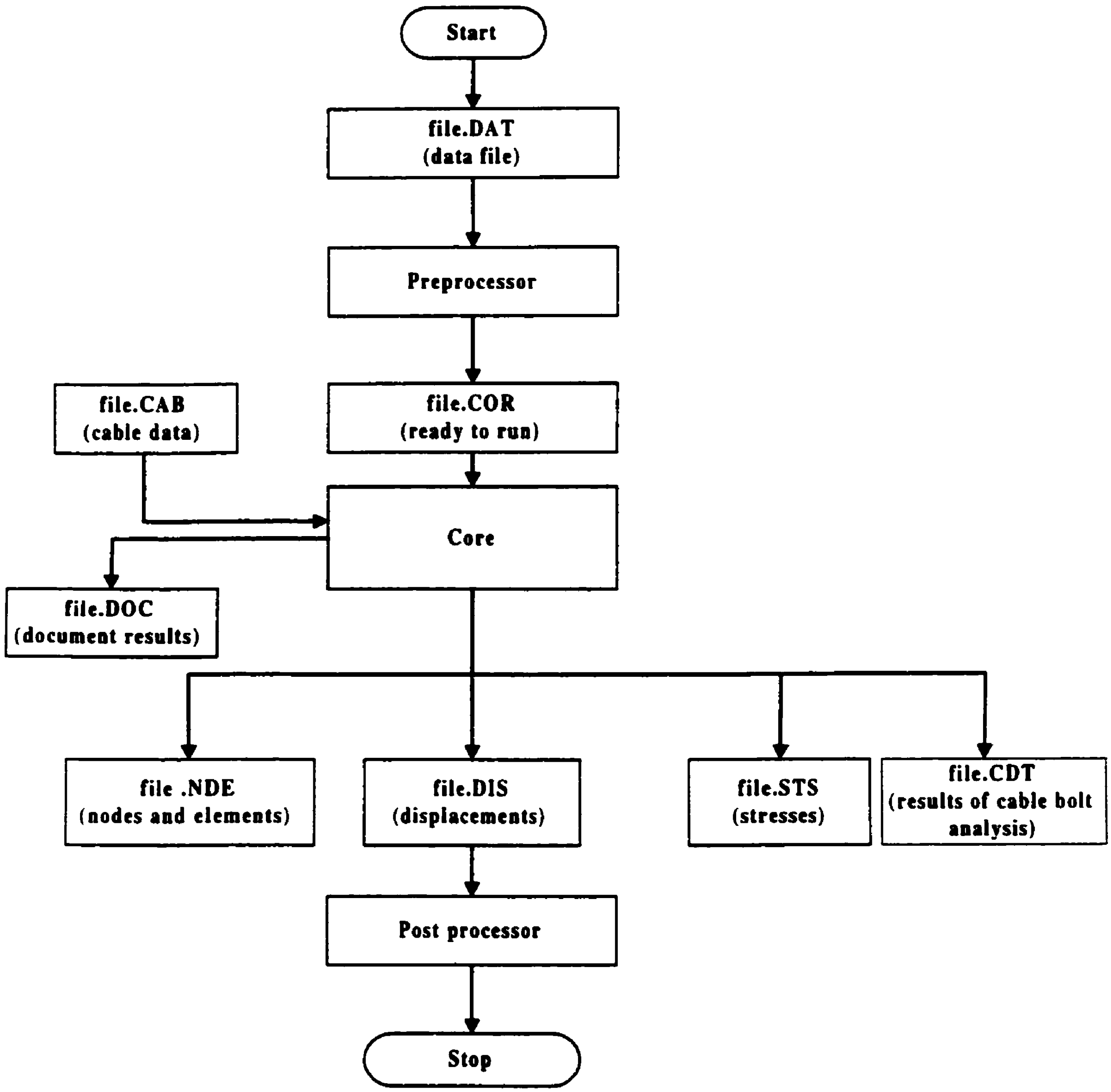

Figure 5.5: Flowchart of e-z tools

5.5 Numerical example

In order to demonstrate the capability of the proposed modelling technique in simulating cable bolts, a simple example of a rectangular, underground excavation is presented. The dimensions of the excavation are 5m wide by 3.6m high as shown in Figure 5.6 and it is situated 200m below ground surface. The vertical in situ stress is given by the depth times the unit weight of the rock, while the horizontal to vertical in situ stress ratio is 0.8. It is assumed that the immediate roof rock layer is of poor quality rock and hence requires support. The geomechanical properties of the host rock and the roof are listed in Table 5.1.

A row of six (6) 2.4m-long cable bolts with 0.9m spacing is assumed. Different cases are simulated to illustrate the effects of anchorage type, length of anchorage, and pre-tensioning on the load distribution along the cable bolt and maximum axial load attained.

A finite element model was constructed using e-z tools with 962, 4-node isoparametric elements to simulate fully grouted cable bolts and partially grouted cable bolts (Figure 5.7).

Cable bolts are simulated with the following parameters:

E_c = 200 GPa (modulus of elasticity of the cable)

A_c = 0.000138 m^2 (cable area)

k = 105 MN/m/m (for the resin anchored portion of the cable bolt)

k = 67.3 MN/m/m (for the cement grouted portion of the cable bolt)

t = 2.5 tonnes (tension force where applicable)

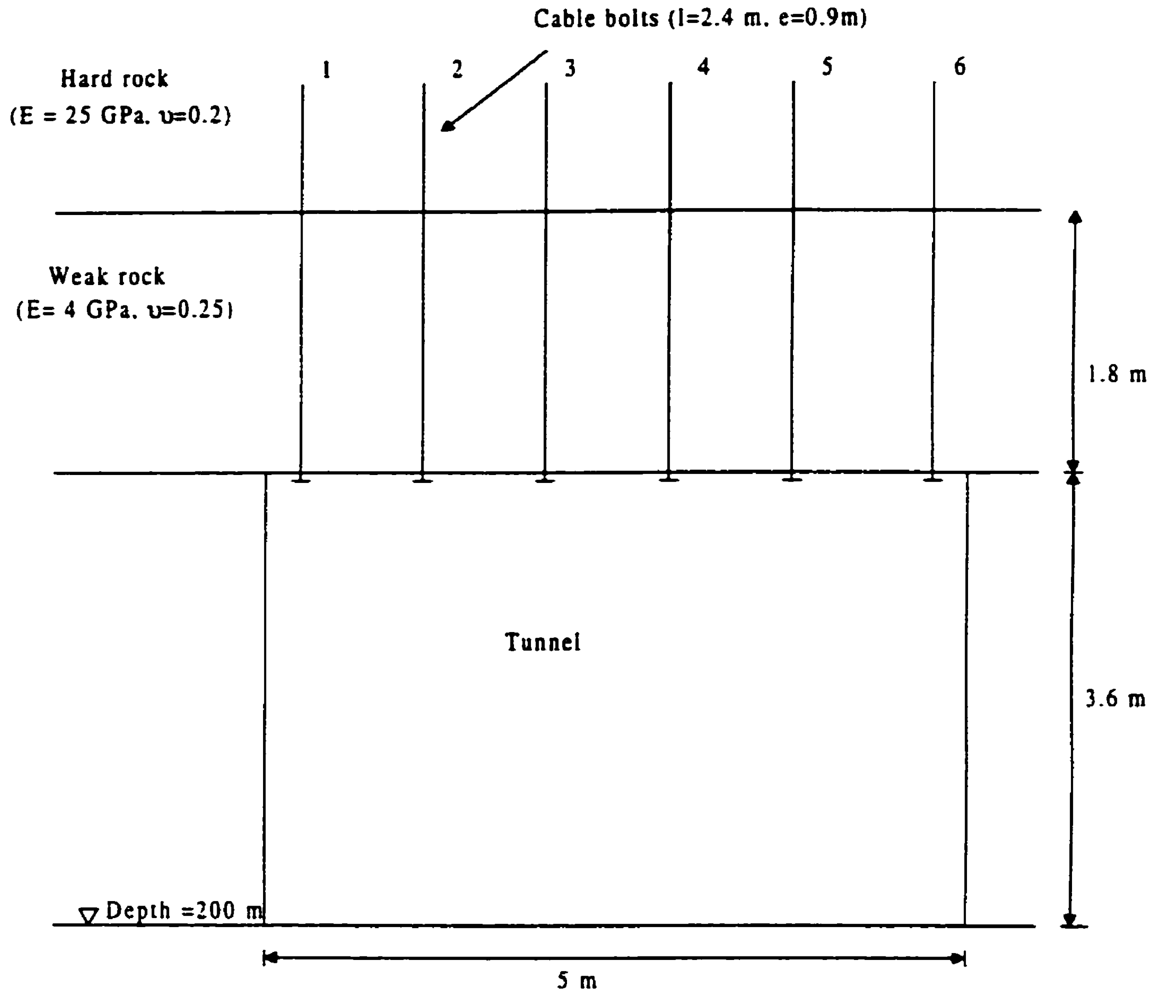

Figure 5.6: Definition of numerical example analyzed

Table 5.1: Geomechanical properties of the numerical example

Material Properties	Host rock	Roof
γ (MN/m^3)	0.027	0.025
E (MPa)	25000	4000
ν	0.2	0.25

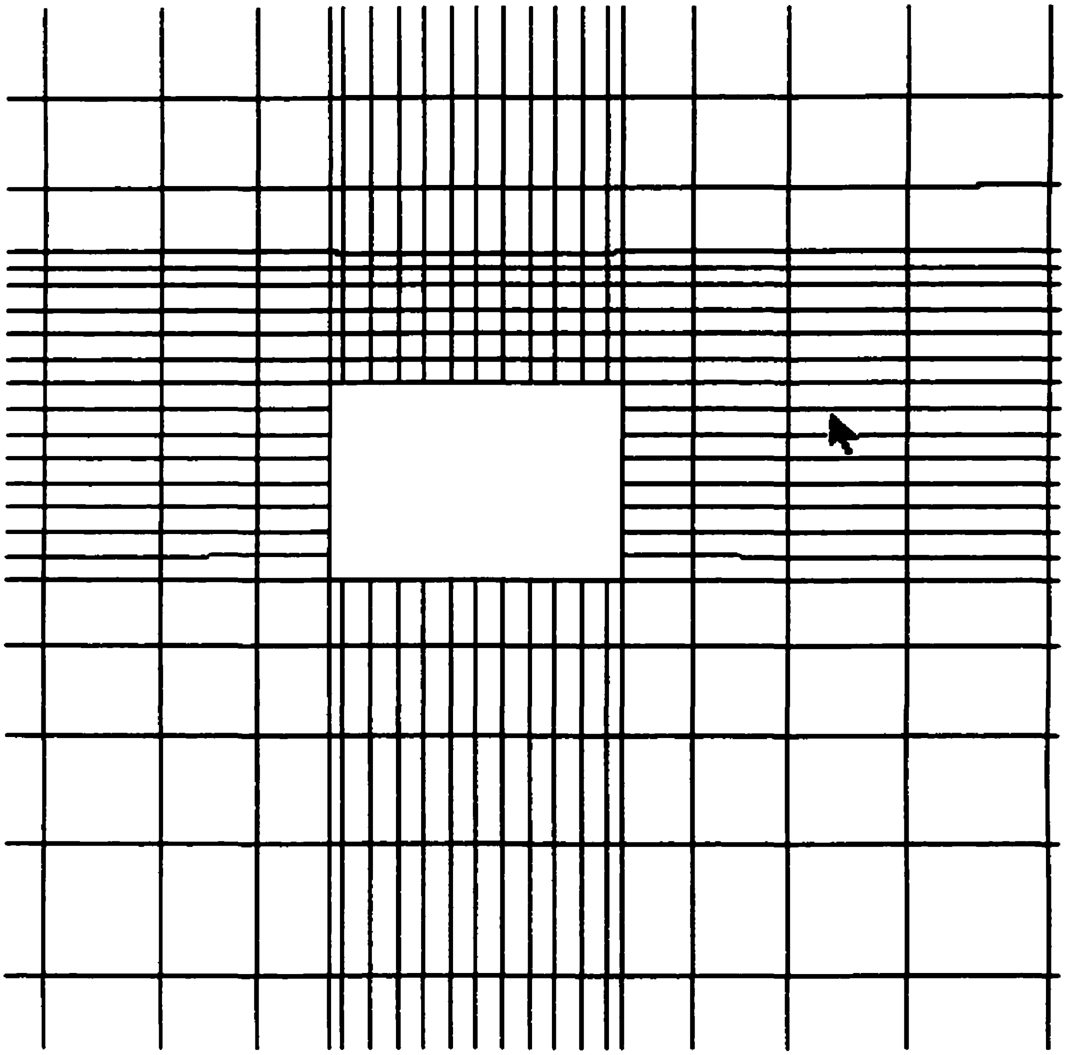

Figure 5.7: Finite element mesh of the numerical example

5.4.1 Fully grouted cable

When the cable is cement grouted over the entire length, the load distribution exhibits a consistent increase in axial load to a maximum value at the bolt head; see Figure 5.8. Cable No. 3 attained a maximum load of 4.5 tonnes. Tensioning of fully grouted cable bolts can be made possible with the help of a fast setting resin grout. Figure 5.9, shows the results of this simulation where resin grout is applied over a length of 0.6m, cement grout over the remaining length of 1.8m, and a tension load of 2.5tonnes is applied. The maximum bolt load is found at its head and is 7.0 tonnes, for cable No. 3. The third simulation is one in which the cable bolt is not anchored at both ends. In this case, the maximum load on bolt No. 3 is only 2.1 tonnes as shown in Figure 5.10.

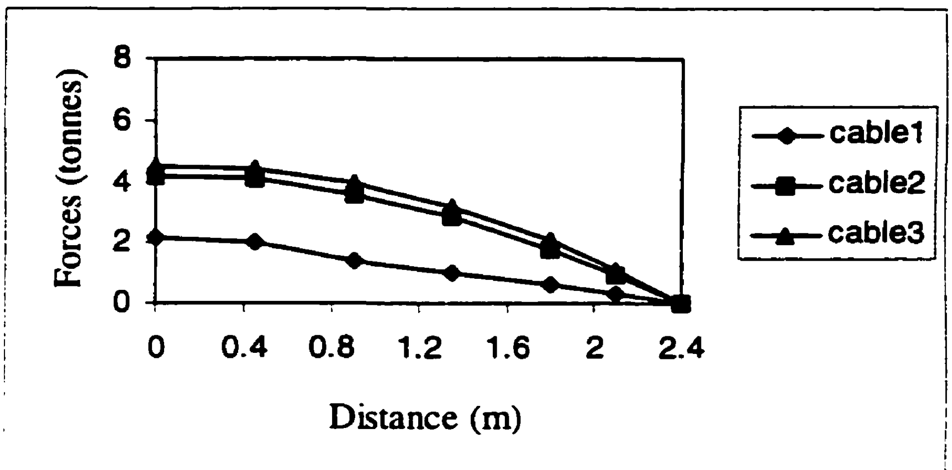

Figure 5.8: Axial load distribution along fully grouted cable bolts (with end plate)

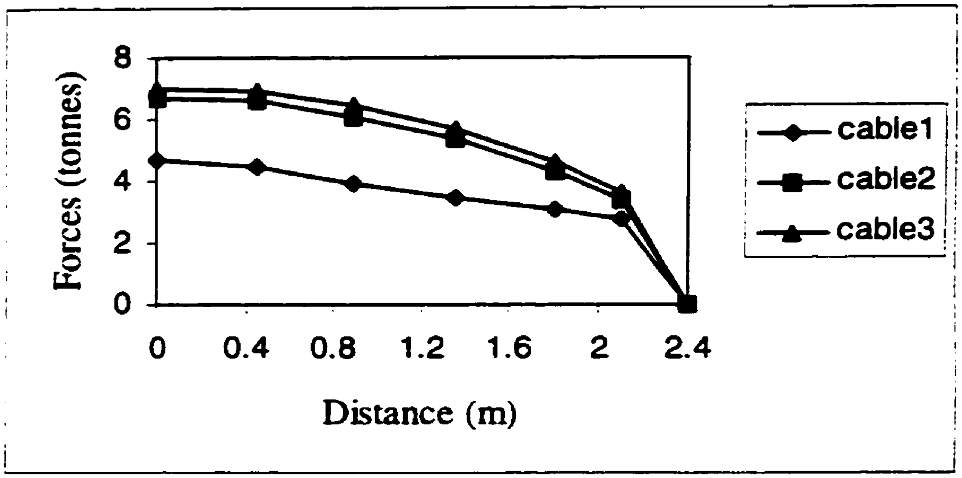

Figure 5.9: Axial load distribution along fully grouted cable bolts (with pretension)

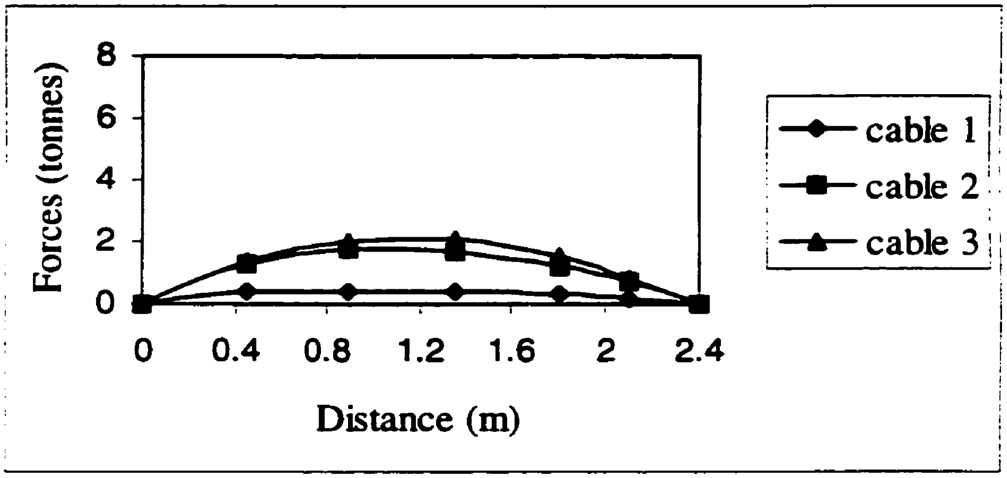

Figure 5.10: Axial load distribution along fully grouted cable bolts (no end plate)

5.5.2 Partially grouted cable (resin grout)

In this case the cable bolt is resin grouted for a length of 0.6 m. The shear bond stiffness along the ungrouted length is zero and for the grouted length k=105 MN/m/m. Two cases were simulated one with end plate and another with a tension force of 2.5 tonnes. The results are shown in Figures 5.11 and 5.12. As can be seen, the axial load distribution is uniform along the free length with a value for cable no.3 of 5.3 tonnes with plates (Figure 5.11) and 7.8 tonnes with pretension (Figure 5.12). The axial load decays to zero over the resin grouted portion. Such behaviour is also in agreement with the work reported by Hutchinson and Diederichs (1996), and Thompson (1992).

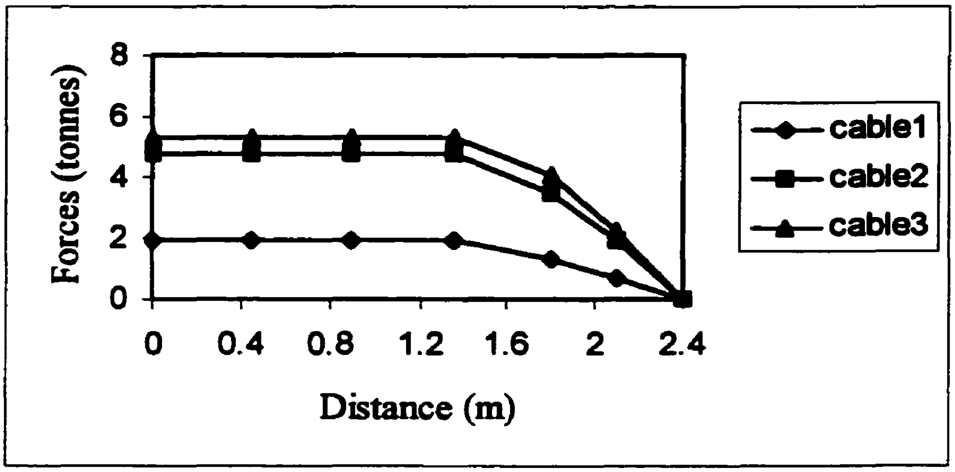

Figure 5.11: Axial force distribution in the partially grouted cable (with end plate)

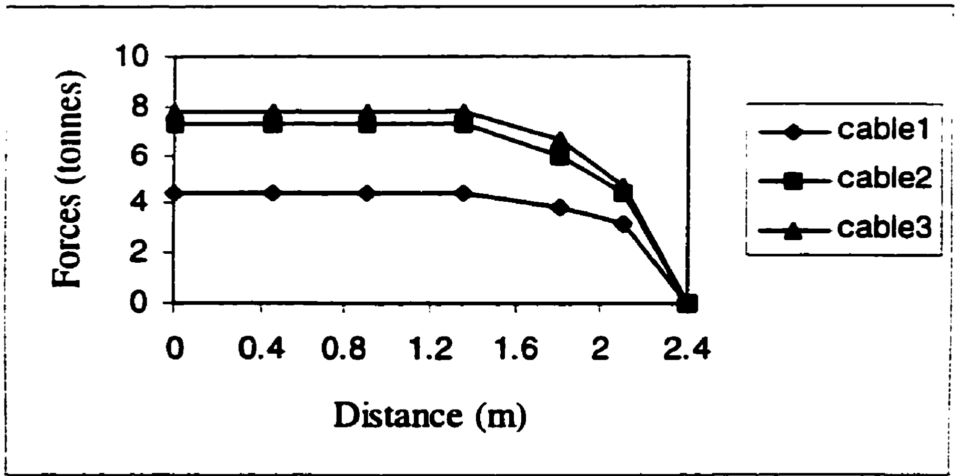

Figure 5.12: Axial force distribution in the partially grouted cable (with pretension)

5.4.3 Rockbolts

The model developed can be generalized for rock anchors other than cable bolts. For fully grouted rock bolts and resin bolts the simulation is similar as for cable bolts as shown in the numerical example. For mechanical bolts the simulation is different.

The simulation of expansion shell anchored rockbolts can be achieved with two assumptions. First, the two nodes on the bolt head and the rock surface are forced to move together, thus simulating complete anchorage. Secondly, the expansion shell is assumed to undergo some slip as the bolt works, thus, a shear bond stiffness value of 300 MN/m/m is assigned at the bolt end (toe). Simulation of mechanical bolts in the numerical example with a pretension load of 2.5 tonnes shows an uniform load distribution (Figure 5.13) The maximum mobilised load is 5.8 tonnes in bolt No.3 near the excavation mid-span.

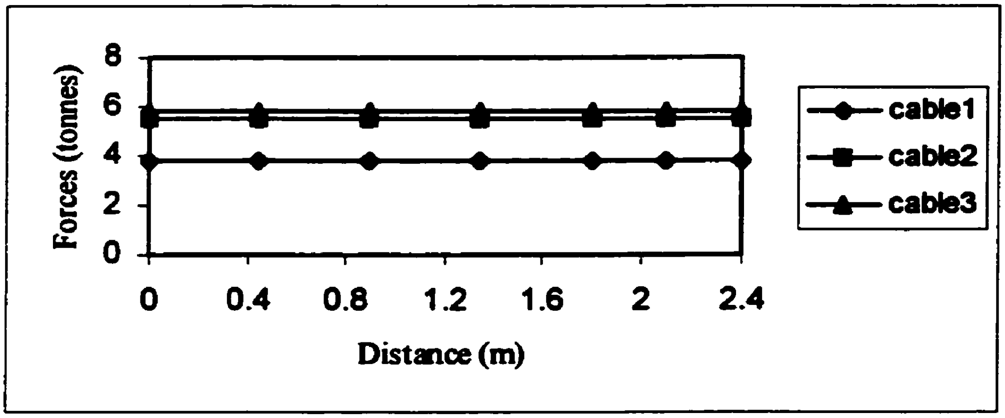

Figure 5.13: Axial load distribution along mechanically anchored bolts

5.5 Summary

The proposed numerical modelling technique is capable of representing a wide range of load and boundary conditions, like the effect of cable bolt tensioning, grouting (fully or partially), and head anchorage. More specifically, it can be noted that:

1. Head and toe anchorage causes an increase in the cable bolt load.
2. Cable bolt tensioning increases the cable bolt load.
3. Resin grout results in higher cable bolt load than cement grout.
4. When the cablebolt is not anchored at both ends, the maximum axial load develops somewhere in the middle.

CHAPTER 6
MODEL PARAMETRIC STUDY

6.1 Introduction

In this chapter, a parametric study is performed using the newly developed numerical model for cable bolt. The study examines the effect of variation of the following parameters: cable cross sectional area, cable length, stiffness of host medium, confining stress, shear bond stiffness, end anchorage and pretension. The numerical example described in Chapter 5 is adopted for the parametric study with 6 cable bolts as shown in Figure 6.1.

The dimensions of the excavation are 5m wide by 3.6m high and it is situated 200m below ground surface. It is assumed that the immediate roof rock layer is of poor quality rock and hence requires support. The modulus of elasticity and unit weight of the hard rock are: E=20 GPa and $\gamma = 0.027$ MN/m^3. For the roof rock layer: E=20 GPa and $\gamma = 0.027$ MN/m^3. The in-situ stresses are:

$\sigma_v = \gamma H = 5$ MPa (vertical stress)

$\sigma_h = K_0 \sigma v = 4.32$ MPa (horizontal stress)

Where : H is the depth below surface = 200 m.

K_0 the horizontal to vertical in-situ stress ratio = 0.8.

A row of six (6) 3.6 m-long cable bolts with 0.9m spacing and with end plates is assumed. Cable bolts are simulated with the following parameters: E_c = 200 GPa (modulus of elasticity of the cable), A_c = 0.00028 m^2 (cross sectional area) and the shear bond stiffness *k*= 20 MN/m/m.

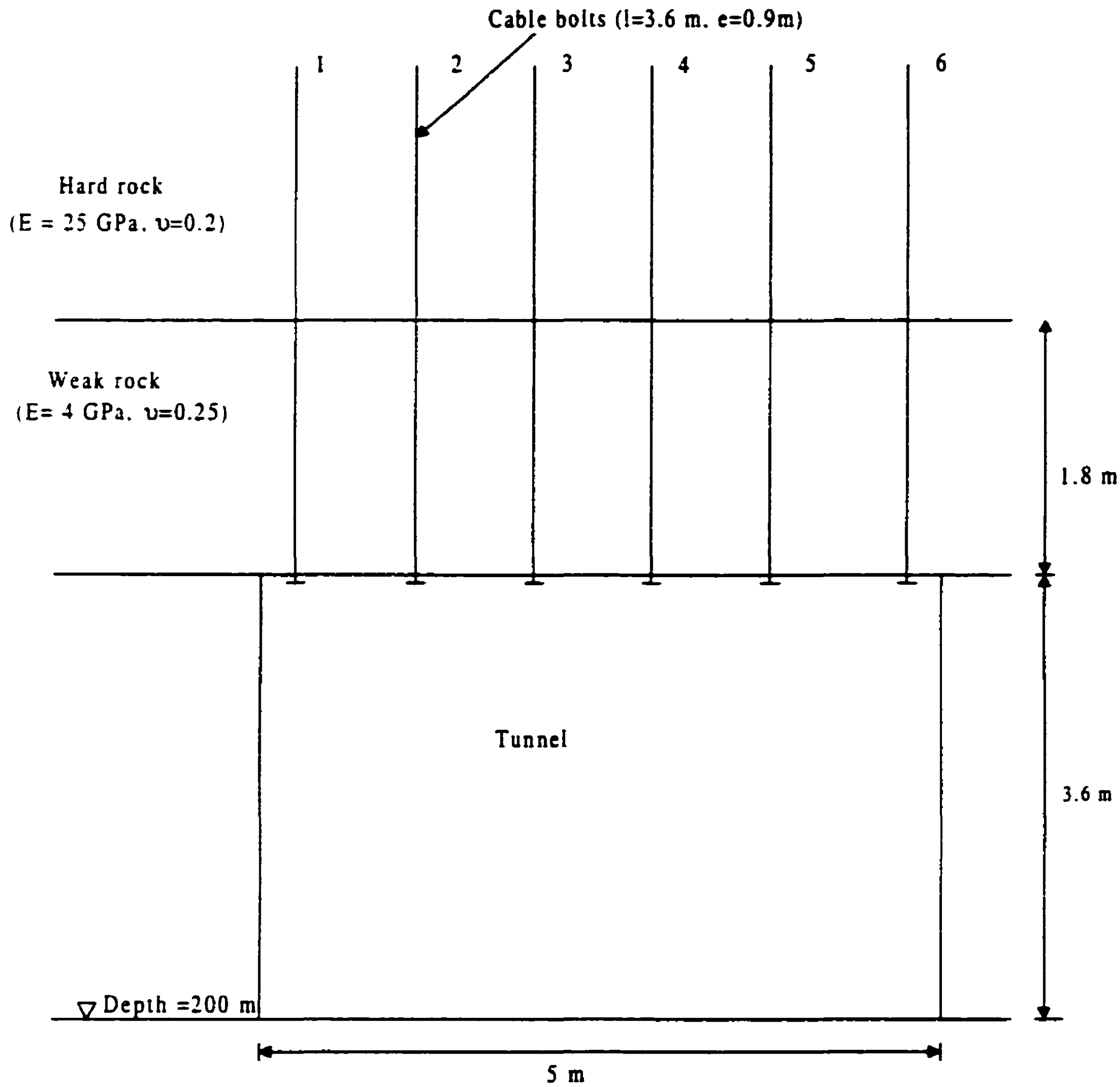

Figure 6.1: Example used for the parametric study

6.2 Effect of cross sectional area of the cable

Cable area is used as input parameter in the model and have an effect in the mobilized load in the cable. The effect of cross sectional area of the cable on the cable capacity have been studied by many authors in the laboratory and in the field (Hassani et al. 1992, Hyett et al. 1992). Since different types of cable bolts are used in the field (standard cable bolts, modified cable geometries), cross sectional area of the cable varied from 100 mm^2 to 615 mm^2.

Table 6.1 shows the different values for cross sectional area of the cable and the maximum forces computed for each cable by the model. As the problem is symmetric only forces mobilized along cables 1,2 and 3 are presented.The shear bond stiffness is kept constant with a value of 20 MN/m/m (cement grout with a water:cement ratio w:c=0.35). The cable bolt is fully grouted along the entire length of the borehole.

Figures 6.2 and 6.3 show the load distribution along cables for a cable area of 100 mm^2 and 615 mm^2 respectively. The maximum forces are computed for cable 3 with an intensity of 1.9 tonnes for A_c=100 mm^2 and 6.1 tonnes for A_c=615 mm^2.

Figure 6.4 presents the variation of the maximum forces in the cable with the cable cross sectioned area. The maximum forces mobilized increase with the increase in cross sectional area of the cable. The effect of variation in the cross sectional area of the cable as computed by the model is the same as the effect of external diameter of sample on pull-out capacity of cable in the laboratory (Hassani et al., 1992).

Table 6.1: Maximum forces computed with variation of cross sectional area of the cable

Cable area (mm2)	Diameter (inch)	Maximum axial loads (tonnes)		
		Cable1	Cable2	Cable3
100	0.5"	1.0	1.8	1.9
138	Single 5/8"	1.2	2.3	2.4
200	0.7"	1.6	3.0	3.2
280	Double 5/8"	1.9	3.7	4.0
615	1.1"	2.8	5.6	6.1

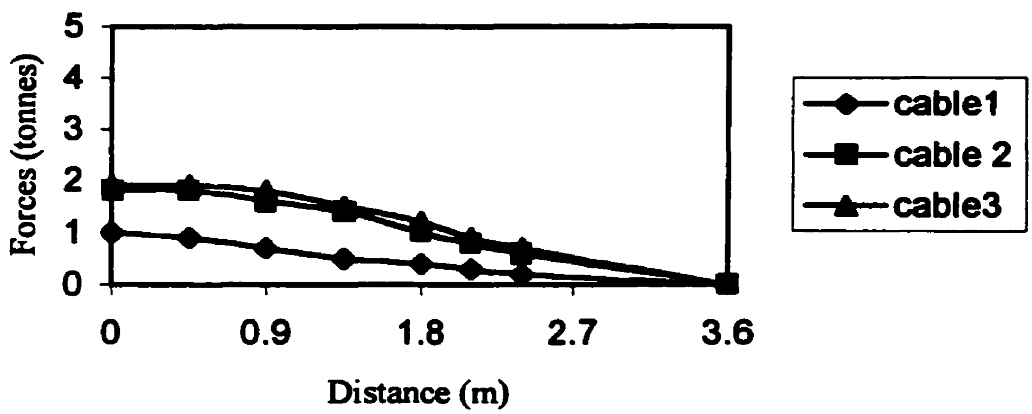

Figure 6.2: Load distribution along cables (A_c=138 mm^2)

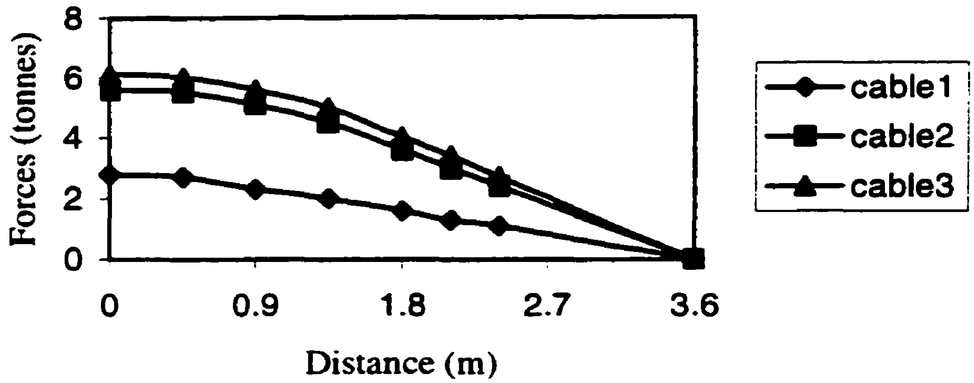

Figure 6.3: Load distribution along cables (A_c=615 mm^2)

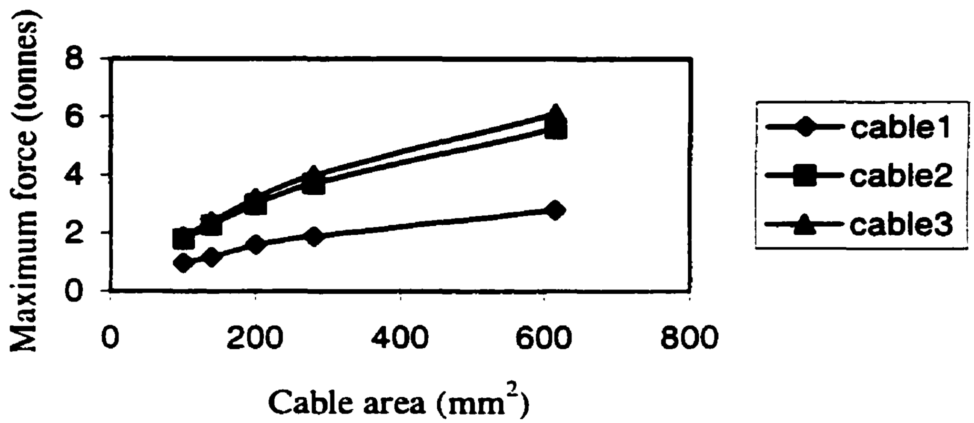

Figure 6.4: Effect of cable area on the maximum forces

6.2 Effect of embedment length

Embedment length is an important factor which have an effect on the load distribution along the cable bolt. Table 6.2 shows the different values used for the embedment length and the maximum loads computed in the cables. Embedment length varied from 1.35 m to 7.2 m and the modulus of elasticity of the weak rock is E=4 GPa.

Figures 6.5 and 6.6 show the load distribution along cables for an embedment length of 1.35 m and 7.2 m. The maximum forces mobilized in cable 3 are 1.6 tonnes for L=1.35 m and 4.3 tonnes for L=7.2 m.

Figure 6.7 shows the variation of the maximum loads mobilized in the cables with embedment length. Maximum loads increase linearly with embedment length and then become constant reaching a critical value (critical bond length). Figure 6.8 shows the maximum force mobilized in cable 3 for two values of roof rock stiffness E=4GPa and E=20 GPa, maximum forces are higher for low modulus of elasticity.

Table 6.2: Maximum forces computed with variation of embedment length

Embedment length (m)	Maximum axial load (tonnes)		
	Cable1	Cable 2	Cable3
1.35	1.0	1.5	1.6
2.4	1.6	3.1	3.2
3.6	1.9	3.7	4.0
5.2	2.0	3.9	4.3
7.2	2.0	4.0	4.3

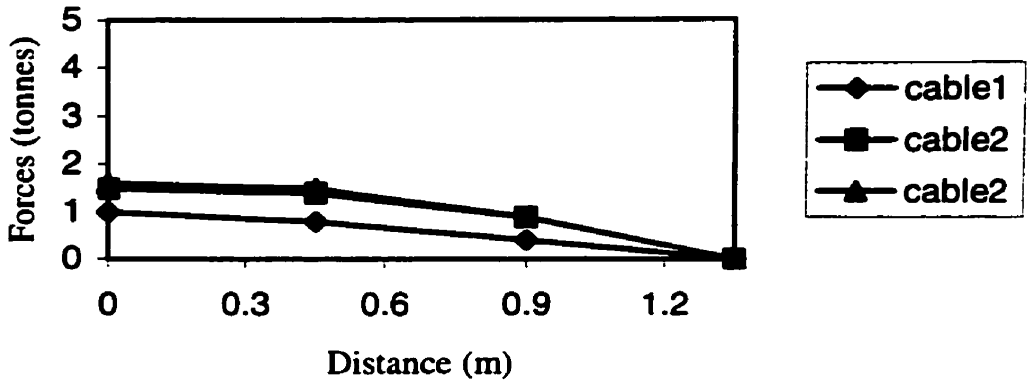

Figure 6.5: load distribution along cables (L=1.35 m)

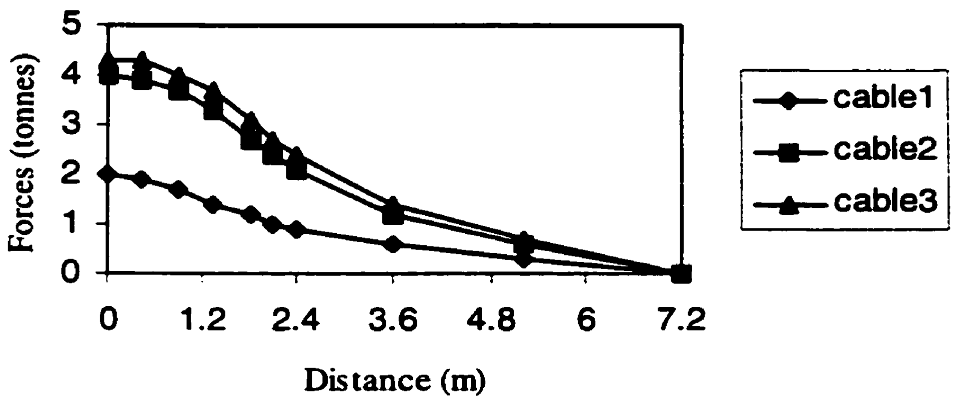

Figure 6.6: Load distribution along cables (L=7.2 m)

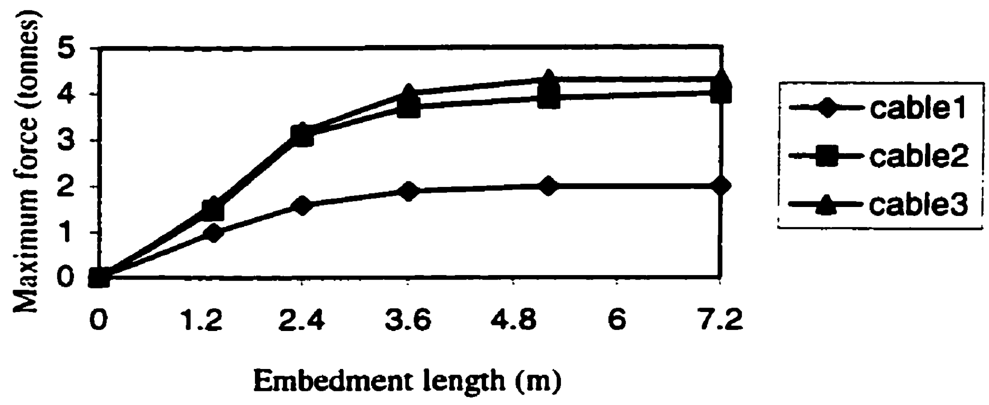

Figure 6.7: Effect of embedment length on the maximum forces

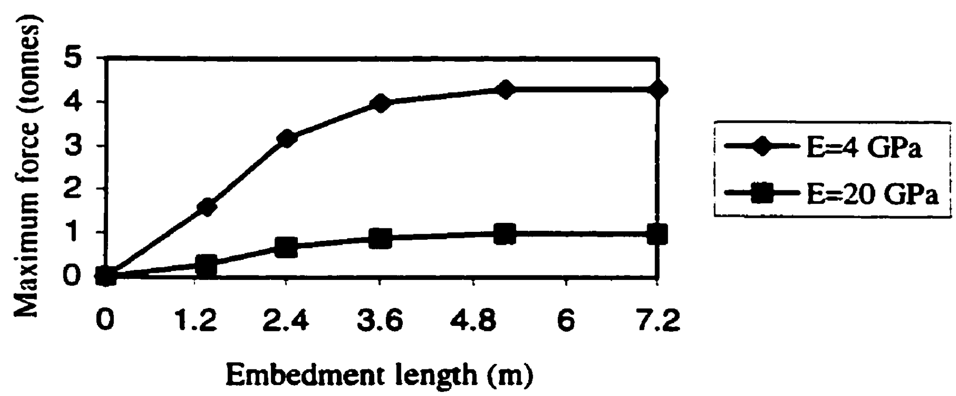

Figure 6.8: Effect of embedment length on the maximum force for cable 3 with variation of modulus of elasticity

6.3 Effect of host medium stiffness

The host medium (rock mass) is another parameter which influences the cable capacity and the load transfer.

Table 6.3 shows the different values used for the host medium stiffness, the shear bond stiffness and the maximum forces computed in the cables. For this simulation the modulus of elasticity of the weak rock varies from 2 GPa to 20 GPa.

Figures 6.9 and 6.10 show the load distribution along cables for a modulus of elasticity of 20 GPa and 2 GPa respectively. The maximum forces mobilized in cable 3 are 0.9 tonnes for E=20 GPa and 7.8 tonnes for E=2 GPa.

Figure 6.11 shows the variation of the maximum force mobilized in the cable and the modulus of elasticity of the host medium. The maximum forces mobilized in the cable decrease with increasing of modulus of elasticity. For a weak and fractured rock the maximum forces mobilized in the cable are higher than for a hard rock and this is due to large displacements on the ground for weak rock which create tension on the cable and increase the force mobilized on the cable.

Table 6.3: Maximum forces computed with variation of host medium stiffness

Modulus of elasticity E (MPa)	Forces (tonnes)		
	Cable1	Cable2	Cable3
20000	0.4	0.8	0.9
10000	0.7	1.5	1.7
4000	1.9	3.7	3.9
2000	3.9	7.3	7.8

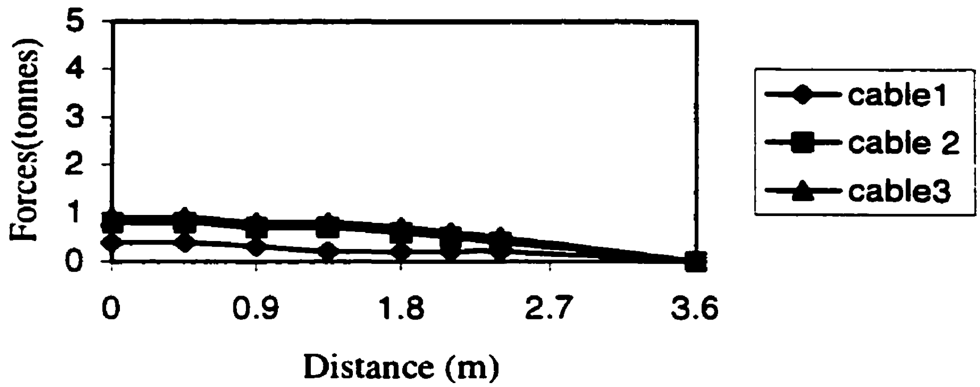

Figure 6.9: Load distribution along cables (E=20GPa)

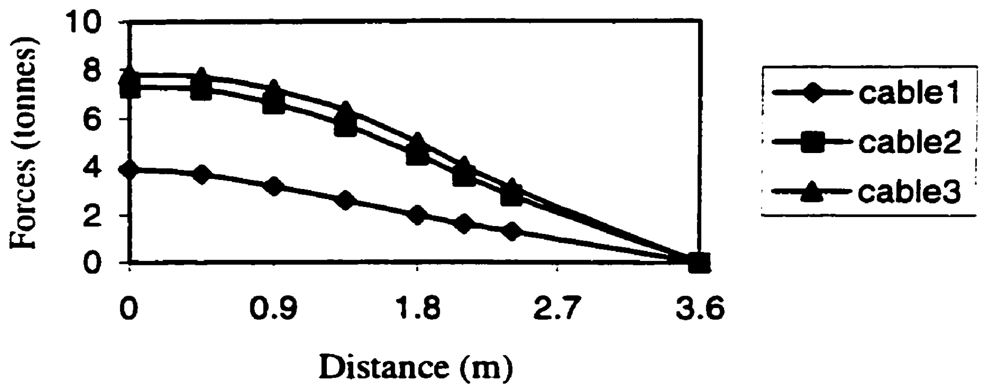

Figure 6.10: Load distribution along cables (E=2GPa)

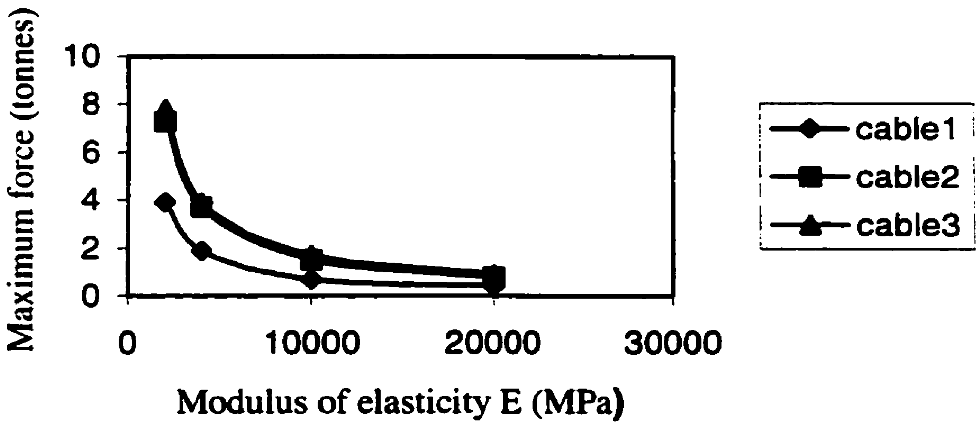

Figure 6.11: Effect of modulus of elasticity on the maximum forces

6.4 Effect of confining pressure

Variation of confining pressure in the field is the most important parameter in the design of cable bolts because this parameter leads to many failures in the field. The effect of this parameter was studied by many authors (Moossavi, 1997 ; Hyett et al., 1992; Yazici et al., 1992).

A simulation was done to see how the model takes into account this parameter. Table 6.4 shows the different values used for the confining pressure and the maximum forces in the cables as computed by the model. Variation of shear bond stiffness with confining pressure is calculated using the empirical formula for standard cable bolts developed in chapter 4:

$k = 12.31\Delta\sigma + 63.7$ $\quad 0<\Delta\sigma\leq 20$ MPa

$k = 310$ MN/m/m $\quad \Delta\sigma\geq 20$ MPa

Figures 6.12 and 6.13 show the load distribution along cables for a variation of confining pressure of 3 MPa and 15 MPa. The maximum forces computed in cable 3 are 1.9 tonnes for a stress variation of 3 MPa and a shear bond stiffness of 101 MN/m/m and 16.2 tonnes for a stress variation of 15 MPa and a shear bond stiffness of 248 MN/m/m.

Figure 6.14 presents the variation of the forces in the cable for shear bond stiffness (*k*) varying in function of confining pressure. An increase in the confining pressure causes an increase of the forces mobilized in the cable.

Keeping the shear bond stiffness constant as in the classical procedure, a simulation was done to see the difference with variable shear bond stiffness, Table 6.5 and Figure 6.15 show the results for a constant shear bond stiffness (*k*=20 MN/m/m). The maximum force mobilized in the cables increased in cable 3 from 14.4 tonnes to 22.1 tonnes for a stress variation of 20 MPa. This shows that an underestimation of shear bond stiffness in the cable can lead to a lower safety factor and may lead to failure in the cable.

Table 6.4: Maximum forces computed with variation of confining pressure (*k* variable)

Confining pressure $\Delta\sigma$ (MPa)	Calculated shear bond stiffness *k* (MN/m/m)	Forces (tonnes)		
		Cable1	Cable 2	Cable3
3.0	101	1.3	2.1	2.3
5.0	125	2.6	4.3	4.5
10.0	187	6.3	9.9	10.3
15.0	248	10.3	15.7	16.2
20.0	317	14.7	21.6	22.1

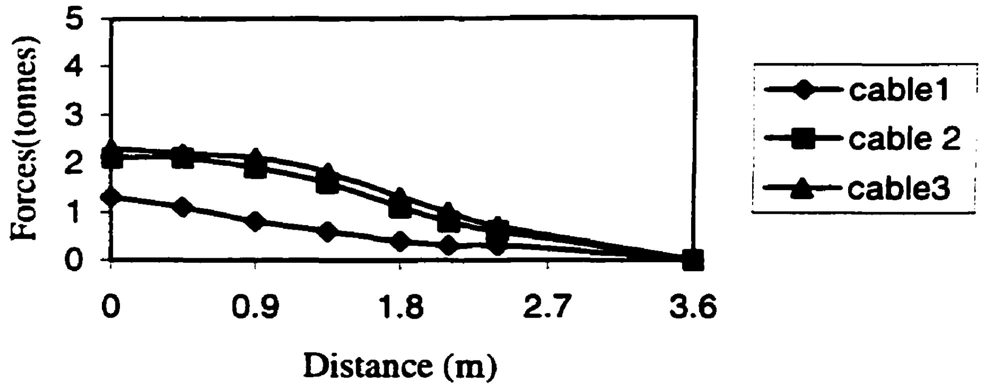

Figure 6.12: Load distribution along cables ($\Delta\sigma$=3 MPa)

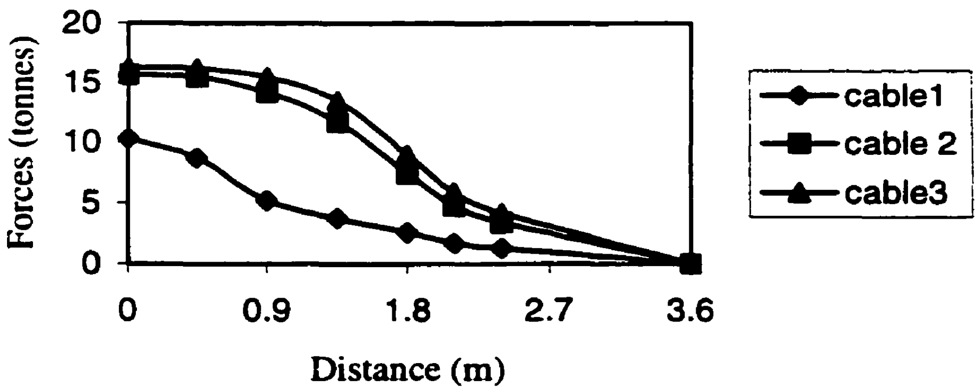

Figure 6.13: Load distribution along cables ($\Delta\sigma$=15 MPa)

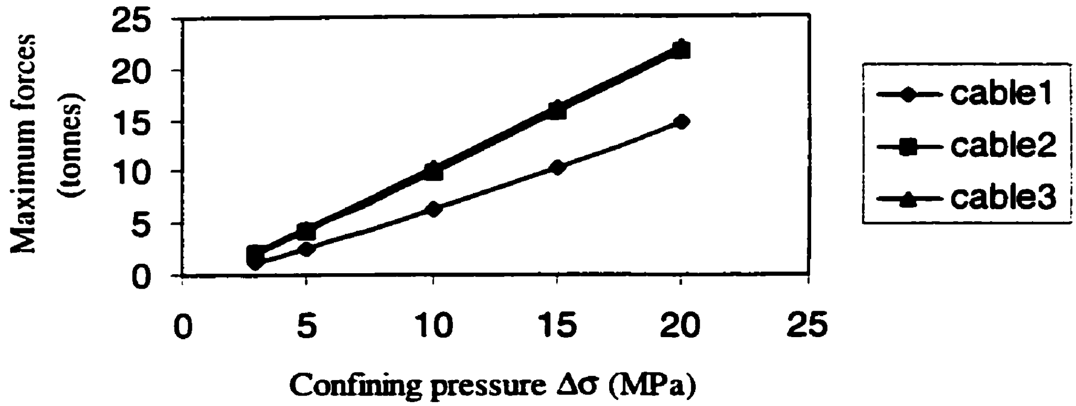

Figure 6.14: Effect of variation of confining pressure on the maximum forces (k variable)

Table 6.5: Maximum forces computed with variation of confining pressure (k constant)

Confining pressure $\Delta\sigma$ (MPa)	Forces (tonnes)		
	Cable1	Cable 2	Cable3
3.0	0.8	1.5	1.6
5.0	1.5	2.9	3.1
10.0	3.3	6.4	6.9
15.0	5.1	9.9	10.6
20.0	6.9	13.4	14.4

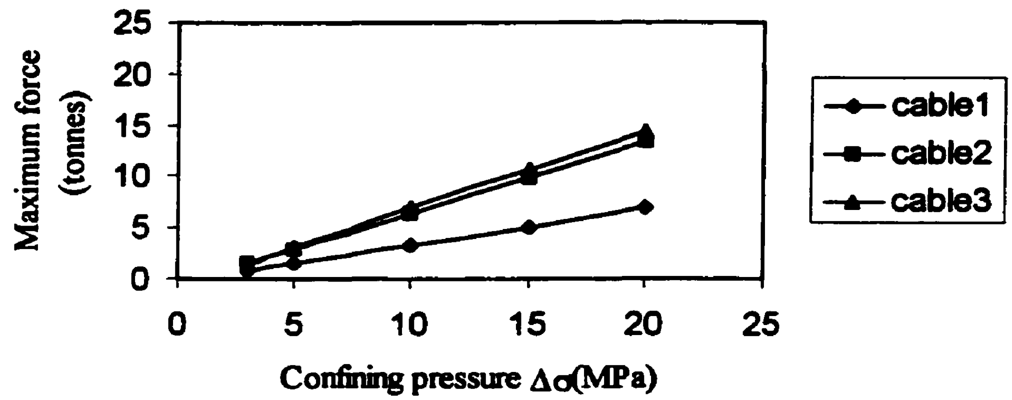

Figure 6.15: Effect of variation of confining pressure on the maximum forces (*k* constant)

6.5 Effect of shear bond stiffness

Shear bond stiffness (*k*) is one of the most important parameters affecting the behaviour of cable bolts. As shown before it's a factor which depends on water cement ratio, stiffness of host medium and variation of theconfining pressure.

Simulations were conducted by varying the shear bond stiffness and keeping constant the modulus of elasticity of host medium and the confining pressure. Table 6.6 presents the different values of shear bond stiffness, varying from 20 MN/m/m to 300 MN/m/m, and the maximum forces mobilized on the cable bolts. Figures 6.16 and 6.17 show the load distribution along the cables for a shear bond stiffness of 20 MN/m/m and 300 MN/m/m. The maximum forces computed for cable 3 are 4 tonnes for a shear bond stiffness of 20 tonnes and 6.2 tonnes for a shear bond stiffness of 350 MN/m/m.

Figure 6.18 presents the variation of the maximum forces mobilized in the cable and shear bond stiffness *k*. The mobilized load increases linearly with the shear bond stiffness but is constant for higher values of shear bond stiffness. This is in accordance with the work of Moossavi (1997) reported in his Ph.D thesis.

Table 6.6: Maximum forces computed with variation of shear bond stiffness

Shear bond stiffness (k) (MN/m/m)	Force (tonnes)		
	Cable1	Cable2	Cable3
20	1.9	3.7	4.0
50	2.6	4.8	5.1
100	3.2	5.4	5.7
200	3.7	5.8	6.0
300	4.0	6.0	6.1
350	4.2	6.0	6.2

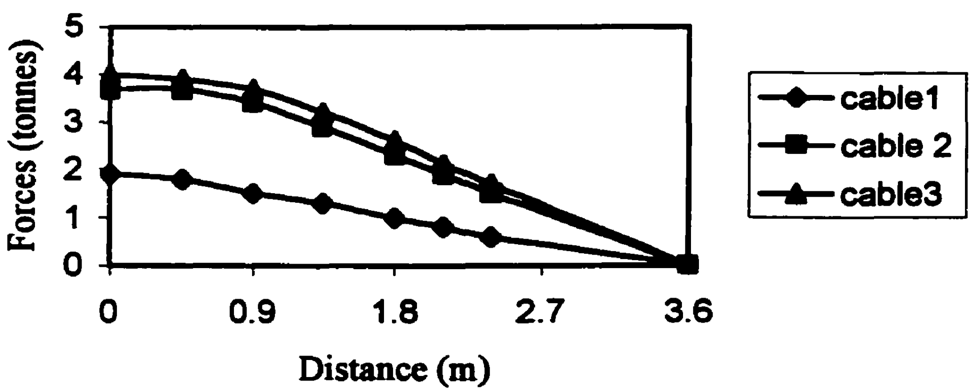

Figure 6.16: Load distribution along cables (k=20MN/m/m)

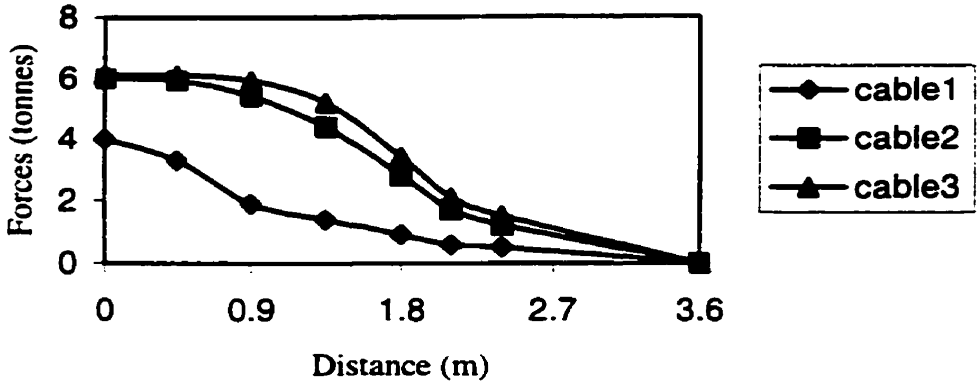

Figure 6.17: Load distribution along cables (k=300 MN/m/m)

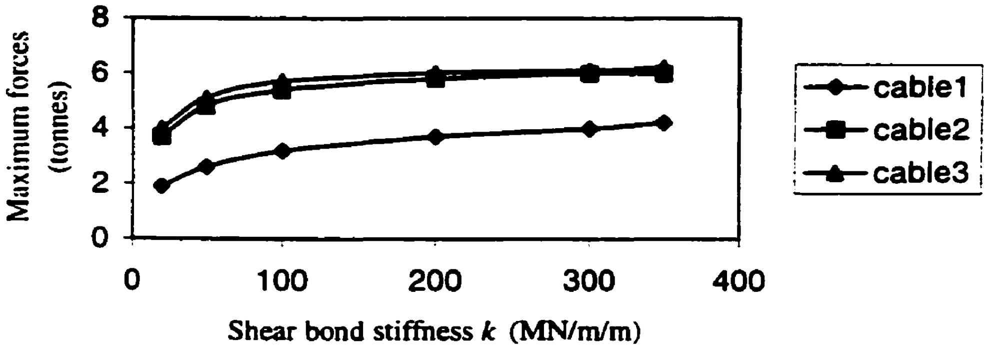

Figure 6.18: Effect of shear bond stiffness on the maximum forces

6.6 Effect of end anchorage and pretension

Load distribution along cable bolts is very sensitive to the use of end plates and pretension. The effect of end anchorage is shown on Figure 6.19. Without plates, the axial force is zero at both ends of the cable and the maximum force computed is 1.5 tonnes. However, the use of plate increased the load distribution along the cable, and the maximum force computed increased to a value of 4 tonnes at the anchored end and the force is zero at the free end.

For pretension, Figure 6.20 shows the load distribution along cable 3 taking into account the effect of pretensioning. The load distribution, using pretension shows an increase of the maximum force from 4 tonnes to 6.5 tonnes with a pretension of 2.5 tonnes. The maximum force is computed at the anchored end, the load distribution shows a decrease in the load distribution at the resin grouted part to reach zero at the free end part as the pretension is applied at the anchored end and is not uniformly distributed along the the cable. The load distribution along tensioned cable bolts and rock bolts depend on the type of grout and the type of anchor used.

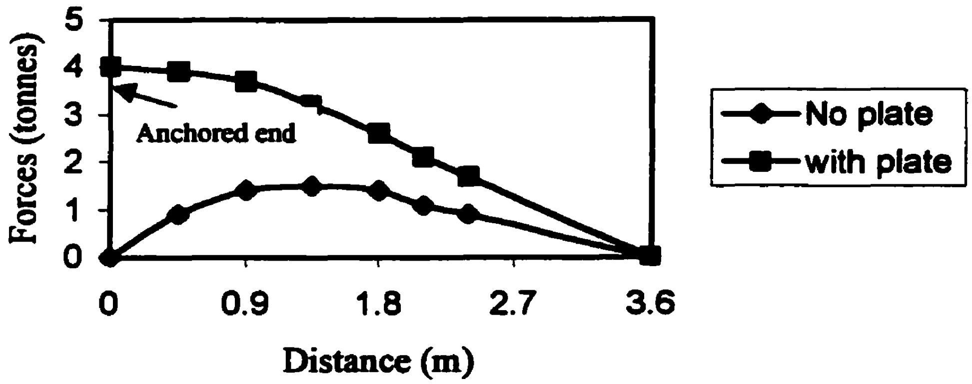

Figure 6.19: Effect of plates in the load distribution along the cable

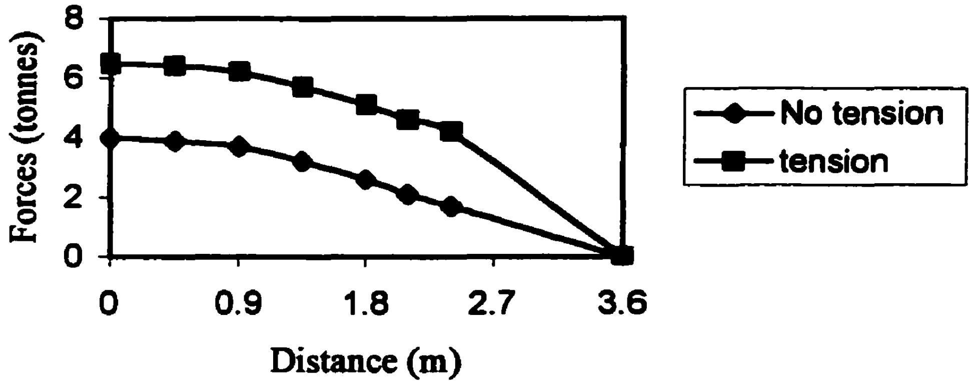

Figure 6.20: Effect of pretension in the load distribution for grouted cable bolts

6.7 Summary

The parametric study has led to the following conclusions:

- Cross sectional area of the cable: The model is sensitive to the variation of cross sectional area of the cable. The forces mobilized in the cable increase linearly with the cross sectional area of the cable.
- Embedment length: Maximum loads in the cable increases with the embedment length and become constant reaching a critical value (critical bond length).
- Stiffness of host medium: fractured and weak rocks mobilized more loads on the cable than hard rock and this can be attributed to large displacement in case of weak rocks which increases the forces in the cable.
- Confining pressure: The model is very sensitive to the variation of confining pressure. The shear bond stiffness depends on the variation of confining pressure and the empirical model was used to compute the shear bond stiffness. The forces mobilized in the cable increase linearly with the confining pressure.
- Shear bond stiffness: This is the most important parameter which affect the load distribution along cable bolts. The mobilized loads increase linearly with shear bond stiffness. For higher values the model is less sensitive to the variation of shear bond stiffness and the forces reach a constant value.
- Plates: End plates change the load distribution along cables and the model is very sensitive to this effect. The maximum force in the cable is computed at the anchored end and is zero at the free end.
- Pretension: Pretension increases the load distribution along cable bolts. The load increases at the anchored end and is zero at the free end for grouted cable bolts.

CHAPTER 7
PROPOSED DESIGN METHODOLOGY AND CASE STUDIES

7.1 Proposed design methodology

An adequate procedure for the designing a cable bolt system must take into consideration a number of important parameters be considered including cable bolting pattern, density, orientation, length and grout performance.

Any design procedure consists of the following conceptual stages:

- Problem definition.
- Establishing the design criteria.
- Determining a possible solution.
- Evaluation of the prospective solution and to ensure objectives have been met.

Following this design philosophy a design approach may be proposed. The proposed design method uses an empirical model for the evaluation of shear bond stiffness k which simulates cable-rock interface and a new finite element model developed and implemented in e-z tools for the determination of the load distribution along the cable bolt.

The proposed design methodology (Figure 7.1) consists of three steps:

1) Preliminary analysis: Carry out a preliminary stress analysis of the mine opening. This requires the knowledge of the following input parameters:

a) Geometry of the openings: A finite element model is constructed with the boundary conditions associated with the problem.

b) In situ stresses:

The in-situ stresses are given by :

$\sigma_v = \gamma H$ (Vertical stress) (7.1)

$\sigma_H = K_0 \sigma_v$ (Horizontal stress) (7.2)

Where γ is the average unit weight of the rock mass, H the depth below surface and K_0 the horizontal to vertical stress coefficient.

c) Geomechanical data of the rock mass:

For the elastic model, two parameters used are the deformation modulus of the rockmass E_{RM} and the Poisson's ratio ν. The deformation modulus of the rock mass may be calculated by knowing either the rock mass rating RMR or the rock mass quality Q, by using one of the following empirical equations:

$E_{RM} = 2RMR - 100$ (GPa) (7.3) (Bieniawski, 1978)

$E_{RM} = 10^{\frac{RMR-10}{40}}$ (GPa) (7.4) (Serafim and Pereira, 1983)

$E_{RM} = 25\log_{10} Q$ (GPa) (7.5) (Serafim and Pereira, 1983)

$$E_{RM} = E\left[0.0028RMR^2 + 0.9\exp(\frac{RMR}{22.82})\right] \quad (7.6) \text{ (Nicholson and Bieniawski, 1990)}$$

$$E_{RM} = \frac{E}{2}\left[1 - \cos\frac{\pi(RMR)}{100}\right] \quad (7.7) \text{ (Mitri, Edrissi and Henning, 1996)}$$

where E is the Young's modulus of intact rock material.

Equation 7.3 is limited to values of RMR greater than 50, or else it produces negative values for E_{RM}. According to Serafim and Pereira (1983), equation 7.4, or its equivalent 7.5, in terms of Q, are valid only for the range of E_{RM} between 1 and 10 GPa. This leaves equations 7.6 and 7.7 to choose from, for all practical purposes. According to Mohammad et al. (1997), equation 7.7 was found to provide a much better fit with field data, than equation 7.6, as it provides more realistic reductions of E_{RM} in the low RMR and stiffness range.

For Mohr-coulomb criterion the parameters used are:

(c, ϕ) : cohesion and internal friction of the rock mass.

For Hoek-Brown criterion:

σ_c : uniaxial compressive strength of the intact rock.
m and s: values depending on the type of rock mass.

Hoek and Brown (1988) proposed a revised set of relations between Bieniawski's rock mass rating (RMR) and the parameters m and s.

$$m = m_i \exp\left(\frac{RMR-100}{28}\right) \qquad (7.8)$$

$$s = \exp\left(\frac{RMR-100}{9}\right) \qquad (7.9)$$

where m_i is the value of m for intact rock.

With this information, a finite element model can be constructed and the mining-induced stresses and deformations are calculated.

2) Determination of the need for cable bolt support: This step consists of the delineation of any potentially unstable zones, thus requiring support. In this context, unstable zones may be defined as those areas where failure is induced by high stress concentration, or high stress relief thus creating a zone of ground relaxation and possible sloughing/caving. In elastic model, the zone of ground relaxation is identified with tensile zone. The safety level can be calculated using the equations (7.12) and (7.15).

- For shear failure:

The safety level of the material can be calculated using Mohr-Coulomb or Hoek-Brown failure criteria. Given the principal stresses (σ_1,σ_2 and σ_3) at a point, the quantities with subscripts "all" and "max" representing the strength and the existing stress of the material respectively.

For Mohr-Coulomb criterion:

$$\tau_{all} = c - \left[\frac{\sigma_1 + \sigma_3}{2} - \left(\frac{\sigma_1 - \sigma_3}{2}\right)\sin\phi\right]\tan\Phi \qquad (7.10)$$

$$\tau_{max} = \frac{\sigma_1 - \sigma_3}{2}\cos\Phi \qquad (7.11)$$

The safety factor is defined as $F = \tau_{all} / \tau_{max}$ (7.12)

For Hoek-Brown criterion:

$$\sigma_{all} = \sigma_3 + (m\sigma_c\sigma_3 + s\sigma_c^{\,2})^{1/2} \qquad (7.13)$$

$\sigma_{max} = \sigma_1$ (positive in compression) (7.14)

$$F = \sigma_{all} / \sigma_{max} \qquad (7.15)$$

According to Brady and Brown (1993), experimental rock failure envelopes are generally non linear and therefore Coulomb's linear criterion is not a particularly satisfactory peak strength criterion for rocks.

- For tension failure:

$\sigma > \sigma_t$: tension failure (7.16)

σ_t : tensile strength of the rockmass.

In case of heavily jointed rockmass, the tensile stress may be taken as zero, on the assumption that the joints will open under the smallest tensile stress.

If the results of the preliminary analysis are indicative of unstable zones around the excavation, the method suggests the use of cable bolt support and it proceeds to the next step.

3) Selection of a cable bolting system: A proposed cable bolting pattern, with specified cable geometry, grout mix, etc. is proposed at this stage. A second stress analysis can then be carried out to examine the effectiveness of the selected cable bolting system using the new numerical model to compute the load distribution along cable bolts. Based on the stress results obtained from the preliminary analysis, a value for the shear bond stiffness of the cable bolts is calculated using the empirical model described in chapter 4.

$$k = a \ \Delta\sigma + b \qquad (7.17)$$

k : Shear bond stiffness (MN/m/m)

$\Delta\sigma$: Variation of confining pressure (MPa)

a, b: parameters depending on type of cable, water:cement ratio and host medium stiffness.

In the second analysis, both the cable bolts and unstable zones are simulated. Unstable zones are simulated by reducing the elastic properties of the rock mass in the unstable area and using a corrected rock mass modulus $E_R = R.\ E_{RM}$ where R is the reduction factor (10 to 20 %) and E_{RM} the deformation modulus of the rockmass. Different cable systems may be tried out, in an iterative process, as shown in Figure 7.1, until a satisfactory system is reached. The type of cable support system used should be suitable to the ground conditions and the maximum load computed along the cable should not exceed the cable capacity divided by an appropriate safety factor.

The parameters that are taken into account by the proposed design approach are:

- Cable length, orientation, geometry and density.
- Grout mix properties.
- Rock mass properties.
- Mining induced effects (stresses, deformations).

• Surface fixtures (end plates).

• Pretension at point of installation.

To demonstrate the application of the proposed design methodology in the field, two case studies are presented using cable bolts as ground support: one for a hard rock Canadian mine and another for a Western U.S coal mine.

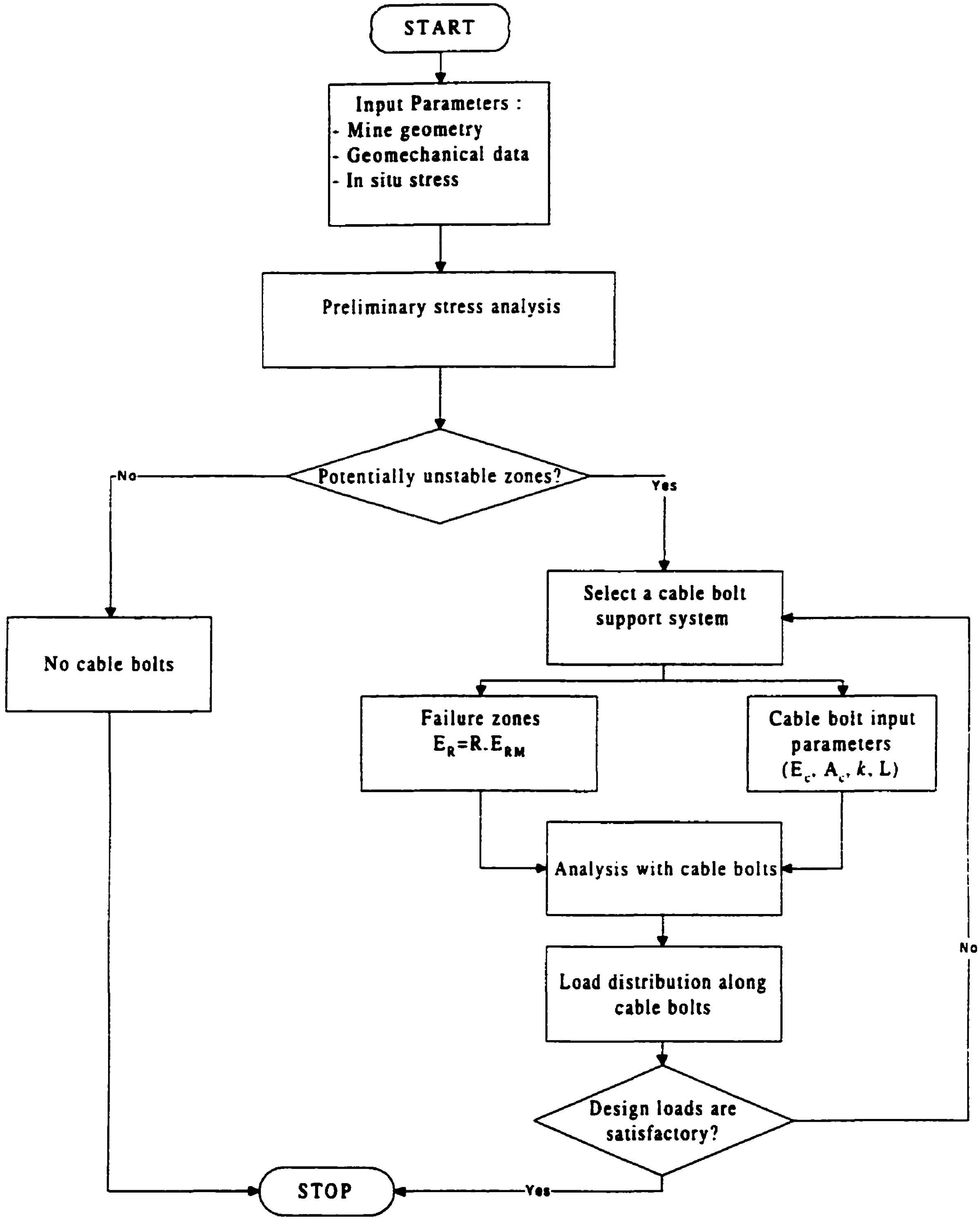

Figure 7.1: Proposed design methodology for cable bolted mining excavations

7.2 Case study 1: Stope hanging-wall support by cable bolts

7.2.1 Description of the case study

An open stope in a Canadian underground mine (Bousquet mine) using sublevel, longhole mining method (Figure 7.2) is analyzed. The stope, located 1170m below surface, is 30m high and 7m wide. The orebody is a stiff, massive sulphide, sandwiched between soft, schistose host walls. As a result, ore extraction causes significant stress relief in the walls, which can result in significant wall caving into the stope (or ore dilution) when the walls are not supported. To remedy the situation, cable bolts are installed, prior to stope mining, from a hanging wall drift in a fanning pattern as shown in Figure 7.2. This pattern is repeated every 1.5 meters in the strike direction of the orebody. The geomechanical data are listed in Table 7.1. The in situ stresses are given by:

$\sigma_y{}^0 = \gamma H$, (vertical stress) MPa

$\sigma_x{}^0 = 2.26\,\gamma H$ (horizontal stress perpendicular to the strike) MPa

$\sigma_z{}^0 = 1.52\,\gamma H$ (horizontal stress parallel to the strike) MPa,

where, H is the depth below surface(1170m) and γ is the average unit weight of the rock mass (0.027 MN/m^3).

The deformation modulus of the rock mass reported in Table 7.1 was calculated in terms of its Young's modulus of elasticity (of intact rock material) and rock mass rating RMR using equation 7.7.

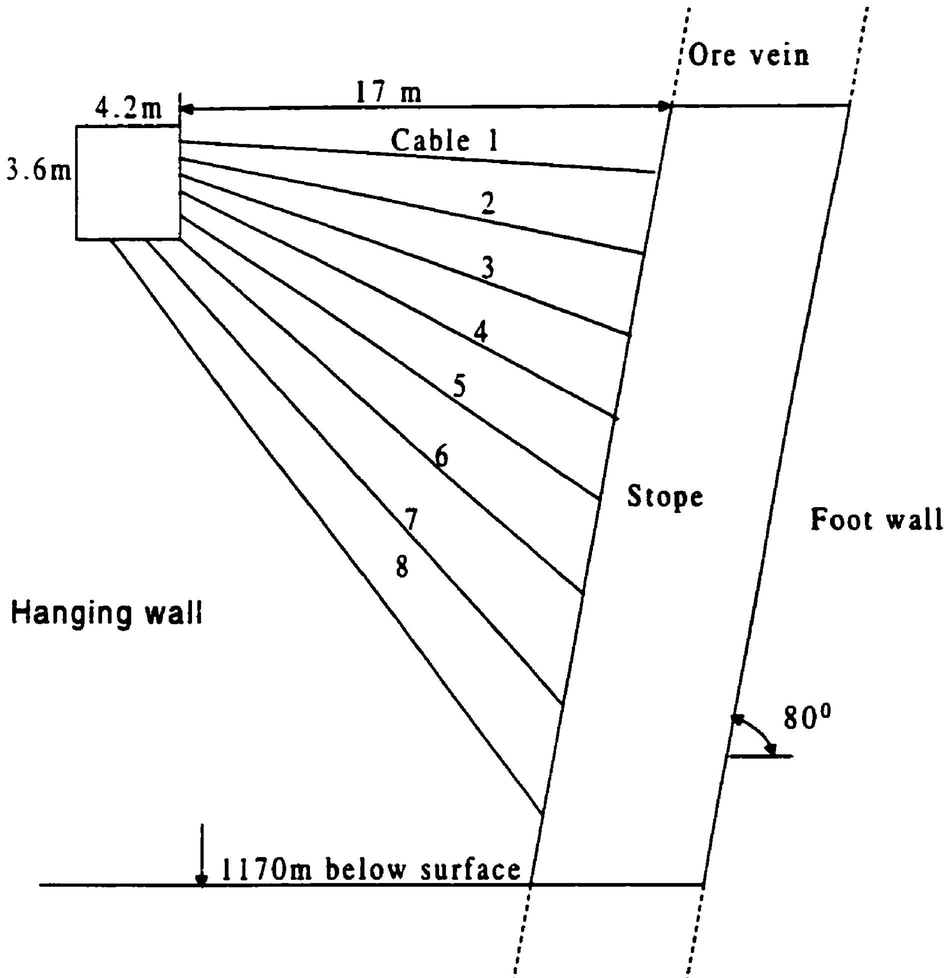

Figure 7.2: Sublevel open stope supported by 8 cable bolts

7.2.2 Preliminary analysis and delineation of hanging wall weak rock

A finite element model was constructed with a dense, graded mesh in the hanging wall to examine the stress levels around the mine stope (Figure 7.3). The results of the preliminary analysis show high stress concentration reaching up to 183 MPa in top and bottom corners of the stope (Figure 7.4). It also shows significant stress relief zone both in the hanging wall and footwall with relief or tensile stresses reaching up to 41 MPa. Before a cable bolt analysis is carried out, it is important to delineate the area in the hanging wall requiring support. To do so, the elements having tensile stresses in the hanging wall are identified as the weak rock zone. These are modelled in the final analysis with lower mechanical properties than the hanging wall rock. The treatment of the hanging wall rock as a no-tension material was shown to give better results than other rock failure criteria, it appears to give more realistic results and conforms more closely with the Cavity Monitoring System measurements of the mined stope (Diakité, 1998; Mitri et al. 1998). It is therefore adopted for the case study presented herein.

Table 7.1: Rock mass properties used for preliminary modelling (case study 1)

	Hanging wall (HW)	Footwall (FW)	Sulphide Orebody	Weak rock (HW)
γ (MN/m^3)	0.027	0.027	0.027	0.025
E(MPa)	54000	75000	125000	
RMR	50	55	75	
E_R(MPa)	31000	49000	115000	5270
ν	0.21	0.15	0.1	0.3

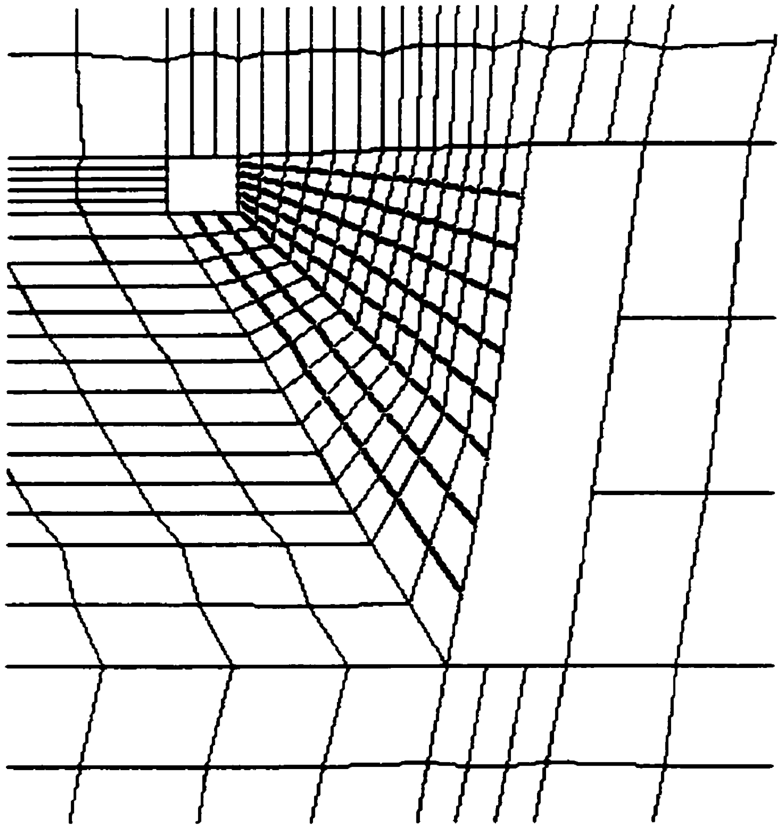

Figure 7.3: Finite element mesh of the stope with cable bolts

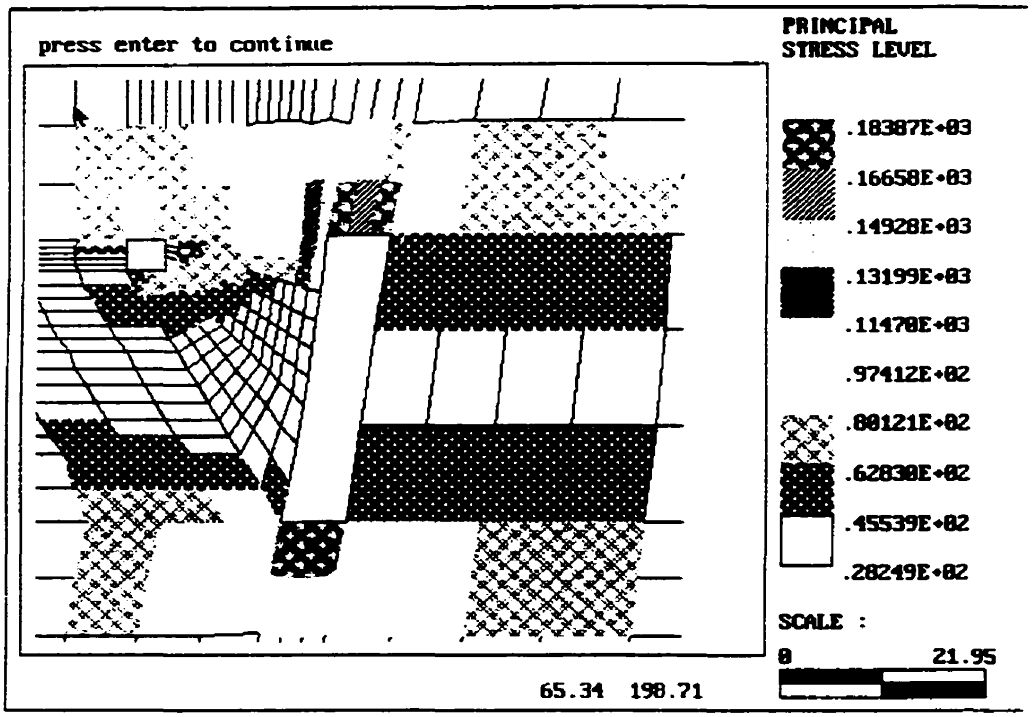

Figure 7.4: Principal stress levels for the case study 1

7.2.3 Analysis with cable bolts and model validation

The analysis with cable bolts is conducted with the cable bolting pattern shown in Figure 7.2. A total of eight, standard 7-wire, 15.875 mm diameter, cable bolts are used. These cables have a tensile strength capacity of 26 tonnes each. The following input parameters were used in modelling of cable bolts:

A_c=139 mm^2 (cross sectional area).
E_c=200 GPa (modulus of elasticity).

The shear bond stiffness is determined using the empirical model. For standard cable bolt with a water cement:ratio of 0.35 and no variation of confining pressure: k=63.7 MN/m/m.

The deformation modulus of the weak rock mass was determined from a sensitivity analysis and comparison of model results with field observations (Figure 7.5). The selected deformation modulus for the cable bolt analysis is equal to 17% of that of the hanging wall rock mass, i.e. 5270 MPa. The cable bolt analysis was then carried out and the axial load distribution in each of the cables was computed. The load distribution results are plotted in Figure 7.6. As can be seen, the axial load is zero at both ends of all cables. This is because the cables are not anchored, neither at the drift nor at the stope face. The cables, which appear to take more load are Nos. 1, 2 and 3 with peak axial loads of 22.34, 24.75 and 22.16 tonnes, respectively (Figure 7.7). This may be attributed to the effect of the angle between the cable and the stope face. When such angle is near 90 degrees, the cable support appears to be more effective.

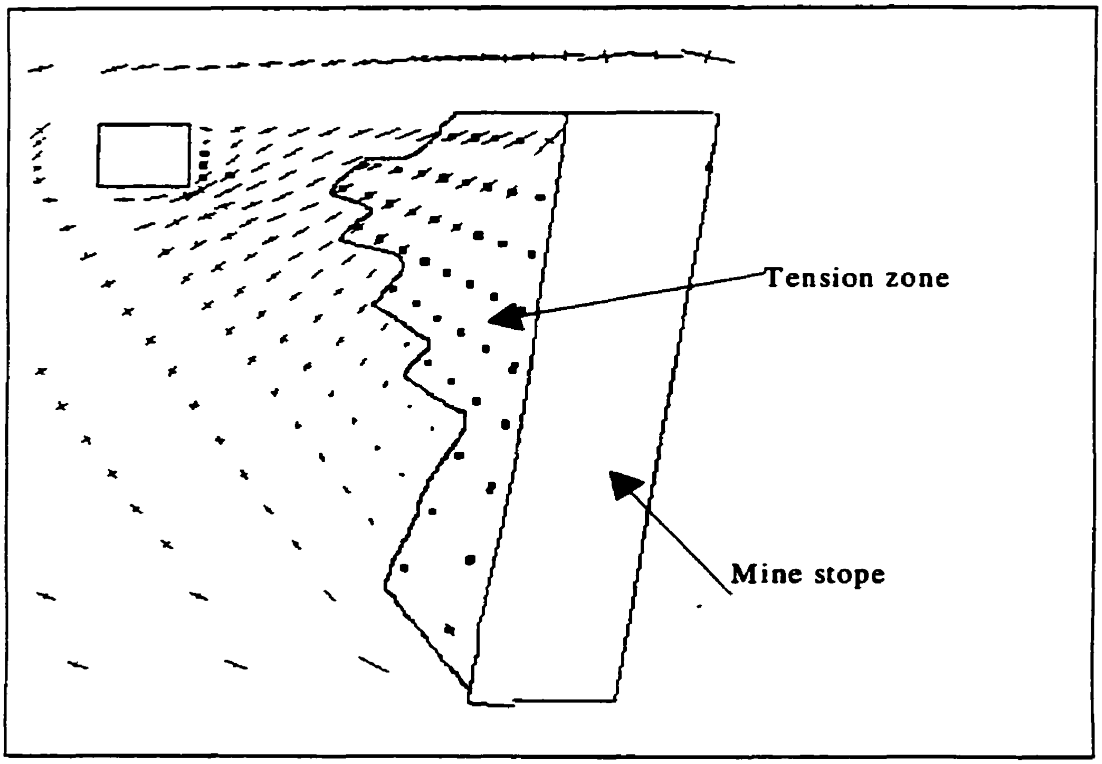

Figure 7.5: Delineation of potentially unstable zones

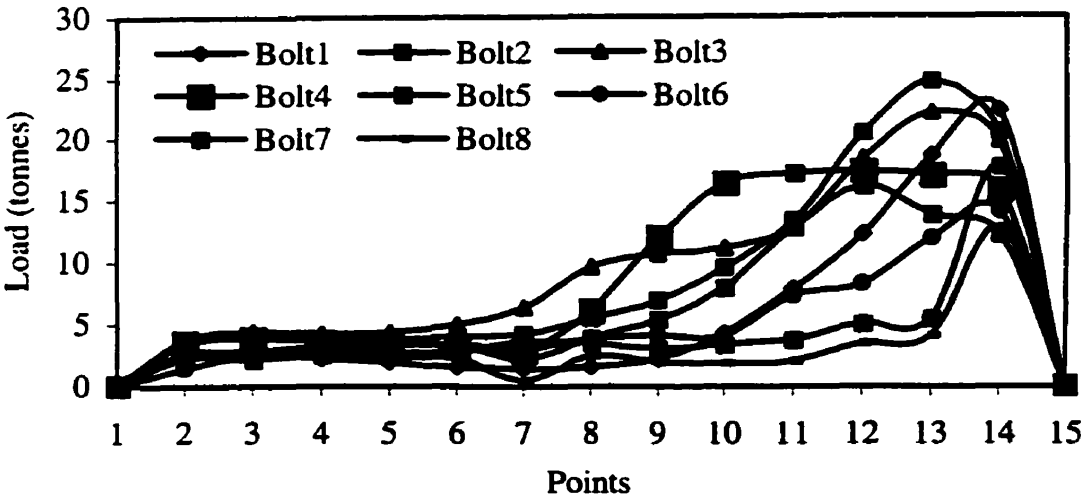

Figure 7.6: Axial force distribution in the cable bolts

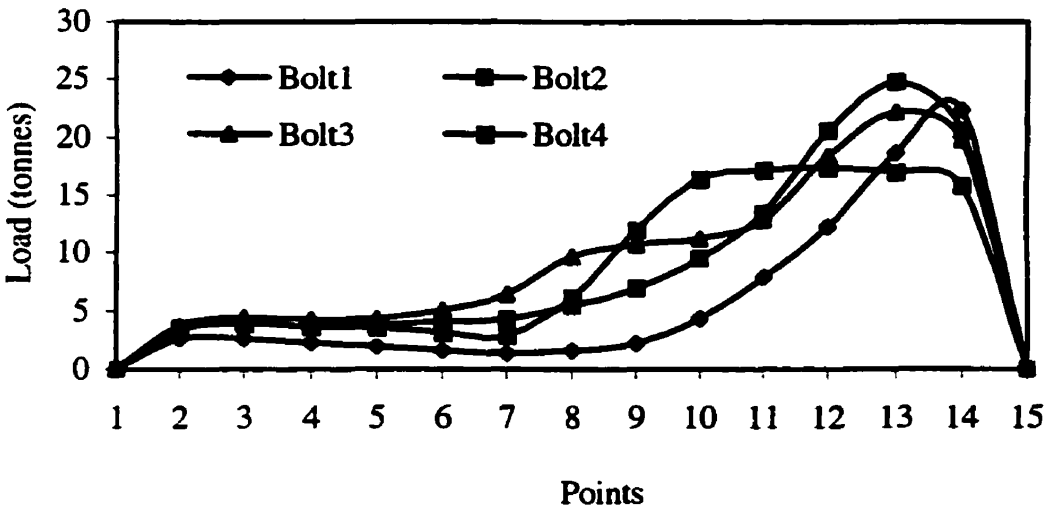

Figure 7.7: Axial force distribution in the cable bolts (cables 1,2,3 and 4)

The same mine stope of this case study was the subject of a field investigation by Bawden et al. (1997). In their study, the axial displacements in selected cables were monitored at six anchor points along the cable from the time of their installation prior to mining to the time when stope blasts were completed and the stope was completely mined out (as shown in Figure 7.2). Knowing the axial stretch between two anchor points along the cable, the strains were calculated and hence the average cable axial load for that segment. The results and observations reported by Bawden et al. served to validate the present model. First, it was reported that the cable loads were negligible in the lower holes; an observation, which substantiates the numerical results obtained here, e.g. for cables 7 and 8. Secondly, the cables in the upper holes attained maximum loads of nearly 250kN (or 25 tonnes); which correlates very well with the computed maximum loads in cables 1, 2 and 3 (22.16 to 24 tonnes).

7.3 Case study 2: Tailgate secondary supports

Cable bolting is becoming widely used as secondary support in coal mines. The use of cablebolting in coal mines was initially developed in Australian coal mines (O'Grady et al., 1993) and now it is used in United Kingdom, U.S.A and Canada. The cables are generally placed in critical areas (gate roads, belt roads and travelling roads) to assure safety in the mine. Resin-grouted cable bolts are now the most commonly used in coal mines, as resin grouts provide an excellent mechanical interlock thus creating a high degree of cable anchorage.

7.3.1 Description of the case study

This case study describes the installation and evaluation of resin-grouted cables for secondary support in a longwall gate road in a Western U.S coal mine (Tadolini, 1999). Cable support systems were designed to provide stability in a gate road that was utilized for two longwall panels, first as headgate and then a tailgate (Figure 7.8).

The mining depth is approximately 365 m and the initial mining height is 2.8 m. The abutment pillar designed to absorb the first panel abutment stresses and protect the integrity of the yield pillar measured 30.5 m wide by 40 m long. The yield pillar measures 11.2 m wide by 40 m long. The geology consisted of top coal, shale and sandstone. Rock mass properties of different materials are presented in Table 7.2.

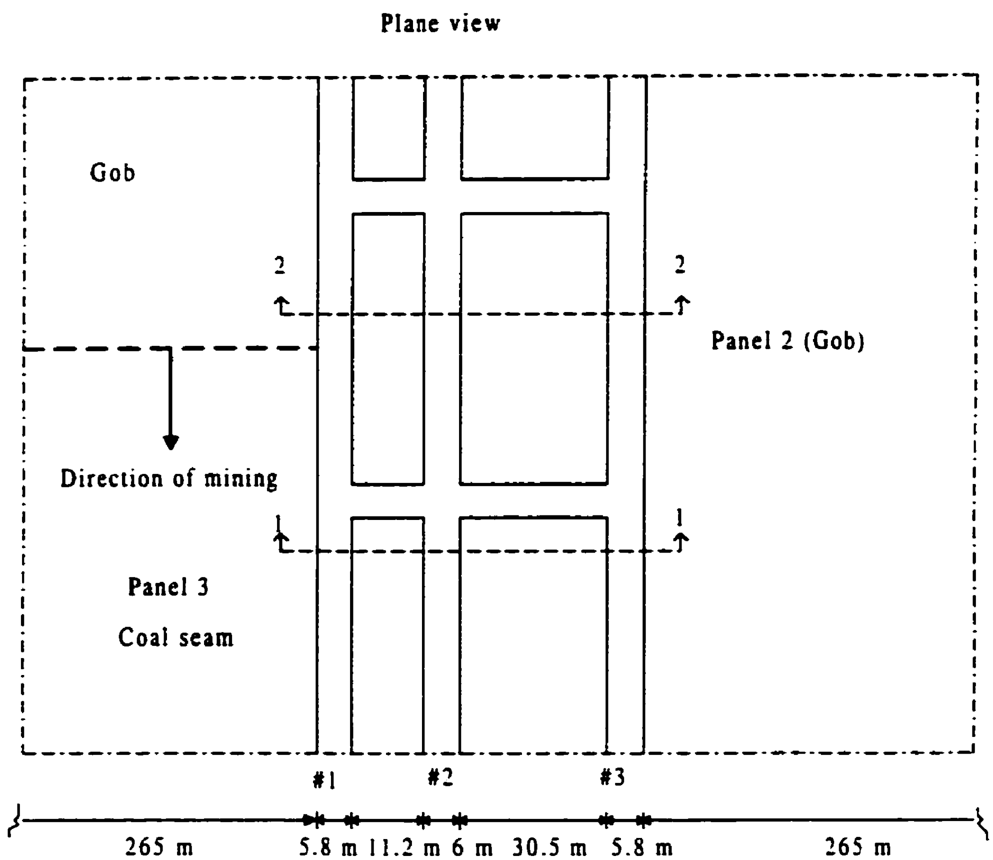

Figure 7.8: Plan view of the mining area under study (case study 2)

Table 7.2: Material properties of the coal mine case study

Property	Coal	Shale	Sandstone	Gob
γ (MN/m^3)	0.012	0.0224	0.0256	0.016
E (MPa)	3378	14410	33784	1441
ν	0.4	0.37	0.3	0.4

7.3.2 Descripton of the finite element model

To model rock bolts and cablebolts in the mine two modelling scenarios, namely model A and B, were adopted (Bouteldja and Mitri, 1999). For model A, panel 2 is mined out and panel 3 is not (Figure 7.9), which correspond to mining of panel 2 and only rock bolts were used . For model B, both panel 2 and panel 3 are mined out. Here, the cable bolts are used to support the tailgate (Figure 7.10).

A finite element mesh was constructed with 2598, 4-node isoparametric elements (Figure 7.11). A preliminary analysis without bolts was done to examine the stress distribution in the mine and delineate the tensile stress zones in the roof. For the model A, both panel 2 (gob) and the tensile stress zone were modeled with a weak material (E=1.44 GPa, ν=0.40). For the model B, panels 2 and 3 as well as the tensile stress zone in the roof were modeled with the same weak material (Figure 7.12).

Section 1-1

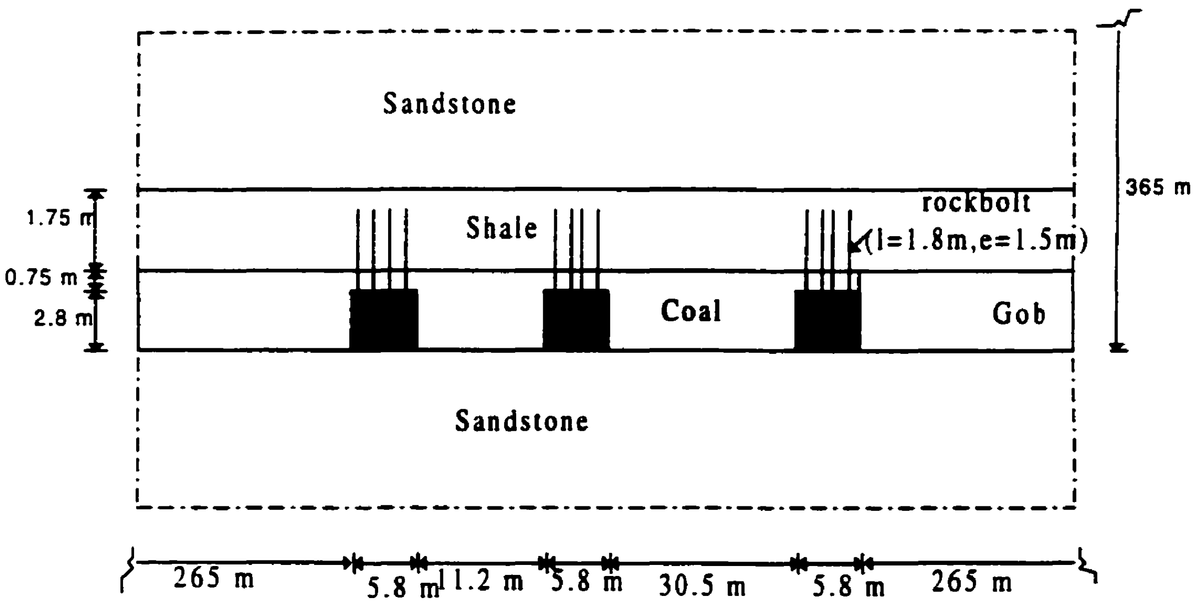

Figure 7.9: Coal mine case study - Model A

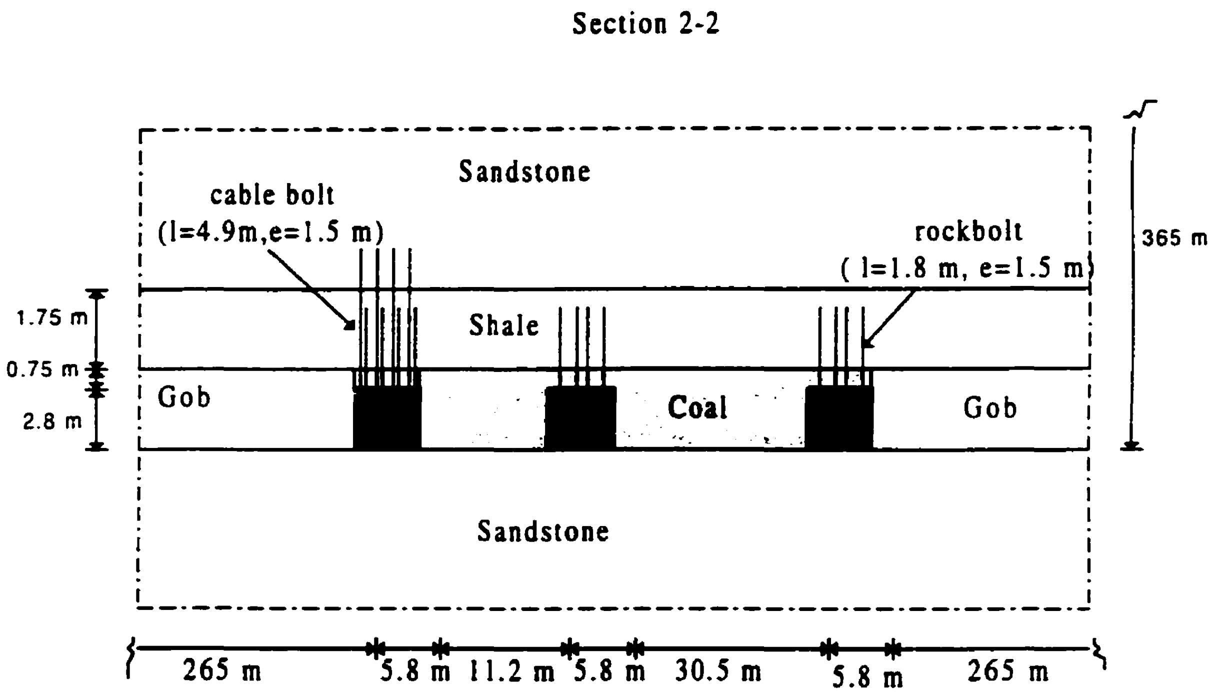

Figure 7.10: Coal mine case study - Model B

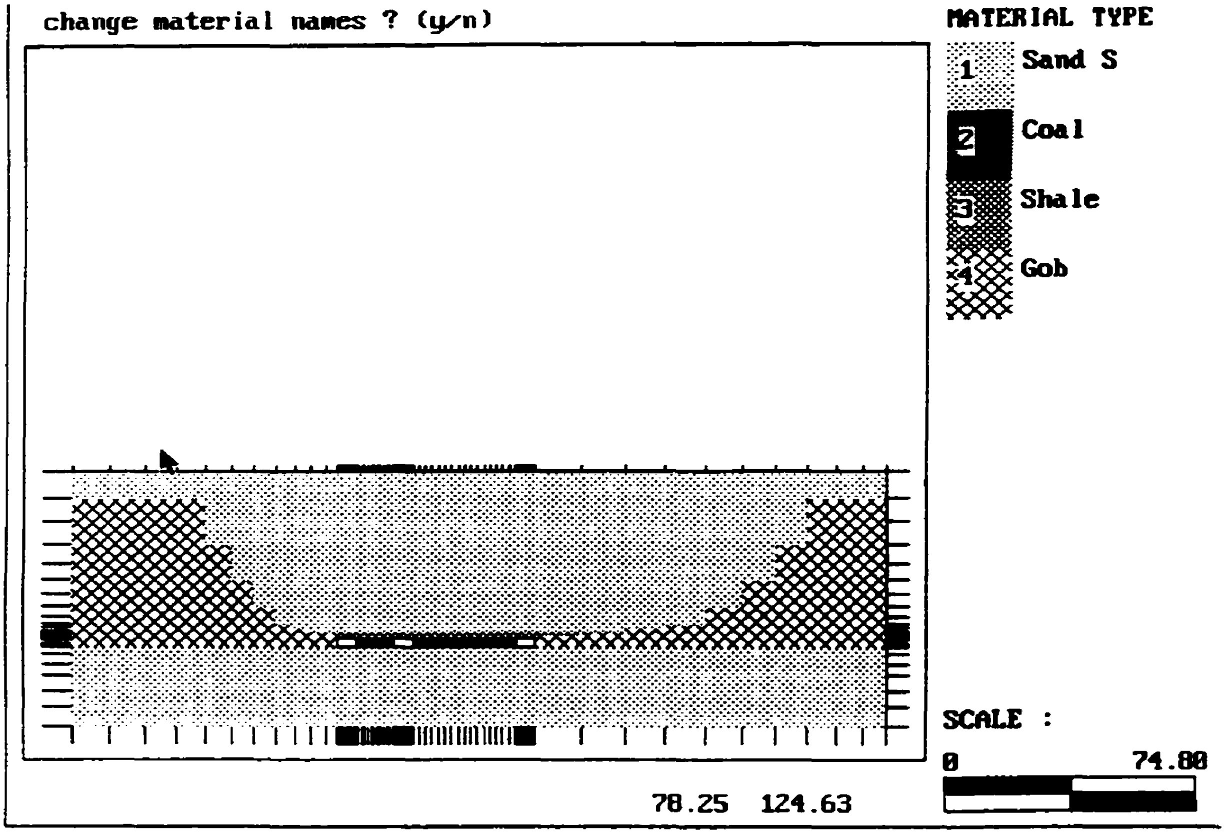

Figure 7.11: Finite Element mesh and geological materials modeled

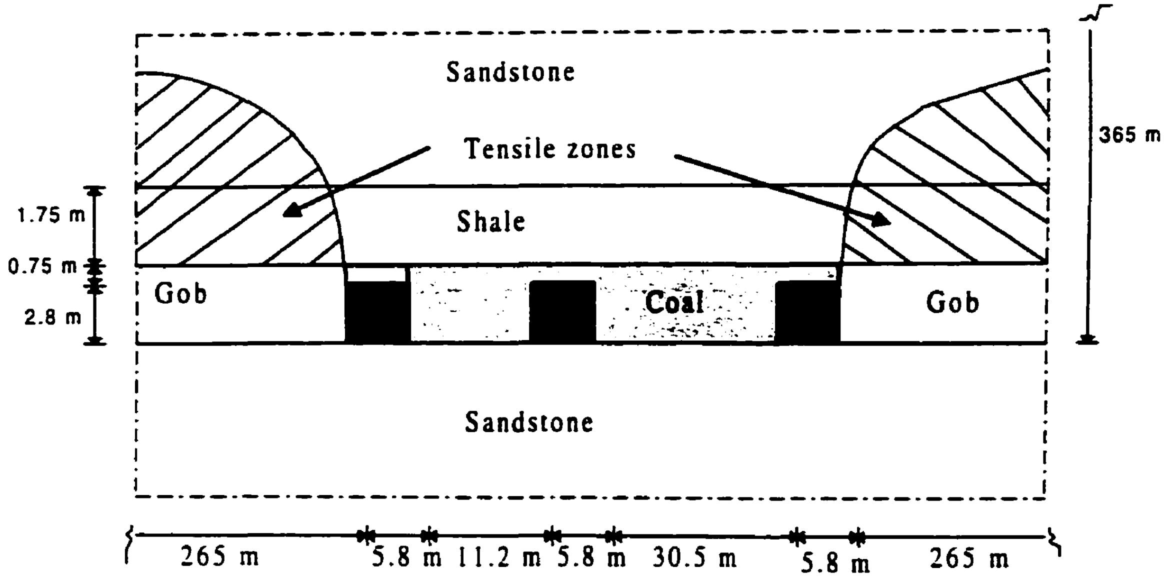

Figure 7.12: Delineation of tensile stress zones in the roofs of panels 2 and 3

The instrumented test area was initially supported with 1.9 m full column resin-grouted bolts as primary support on a 1.5 m row spacing as shown in Figure 7.13. Resin grouted cable bolts supports were installed after mining panel 2 as a secondary support with end bearing plates to support the tailgate (Figure 7.13) with a length of 4.9 m and 1.5 m spacing. Standard 7-wire, 15.2 mm diameter cables were used. These cables have a load bearing capacity of 26 tonnes, a modulus of elasticity of 200 GPa and are partially grouted (1.7 m resin).

Shear bond stiffness *k*:

As the empirical model developed for shear bond stiffness is available only for cement grout, shear bond stiffness for resin grout was determined from the results of laboratory pull-out tests. A shear bond stiffness *k* of 300 MN/m/m for the cable bolts in the grouted length was taken and for rock bolts *k*=105 MN/m/m . These results are based on the pull-out tests reported by Tadolini (1998).

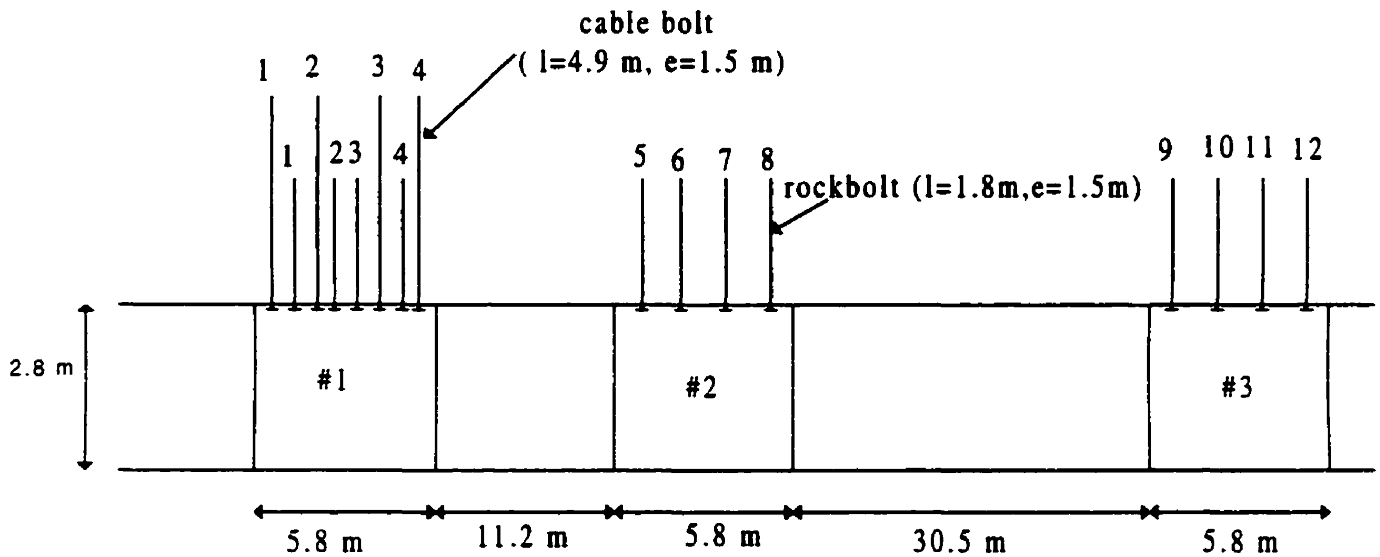

Figure 7.13: Location of cable bolts and rock bolts

7.3.3 Discussion of the results

For the first analysis, the maximum forces in the bolts as computed by e-z tools are shown in Table 7.3. The forces decrease to reach zero at the free end (Figure 7.14). The maximum force computed is 5.3 tonnes and is mobilized by the rock bolt 12 which is near the panel 2, that is mined out and filled with gob.

Table 7.3: Maximum forces in the rockbolts

Bolts	1	2	3	4
Forces (tonnes) Model A	5.0	4.1	4.1	5.0
Forces (tonnes) Model B	4.3	4.1	4.1	4.3

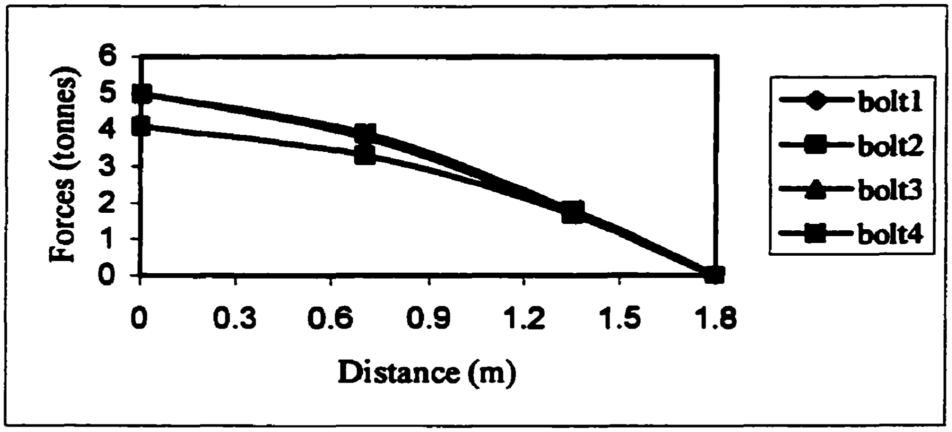

Figure 7.14: Axial force distribution in the resin- grouted rock bolts (Model A)

7.3.3 Discussion of the results

For the first analysis, the maximum forces in the bolts as computed by e-z tools are shown in Table 7.3. The forces decrease to reach zero at the free end (Figure 7.14). The maximum force computed is 5.3 tonnes. We see that the maximum force is mobilized by the rock bolt 12 which is near the panel 2, that is mined out and filled with gob.

Table 7.3: Maximum forces in the rockbolts

Bolts	1	2	3	4
Forces (tonnes) Model A	5.0	4.1	4.1	5.0
Forces (tonnes) Model B	4.3	4.1	4.1	4.3

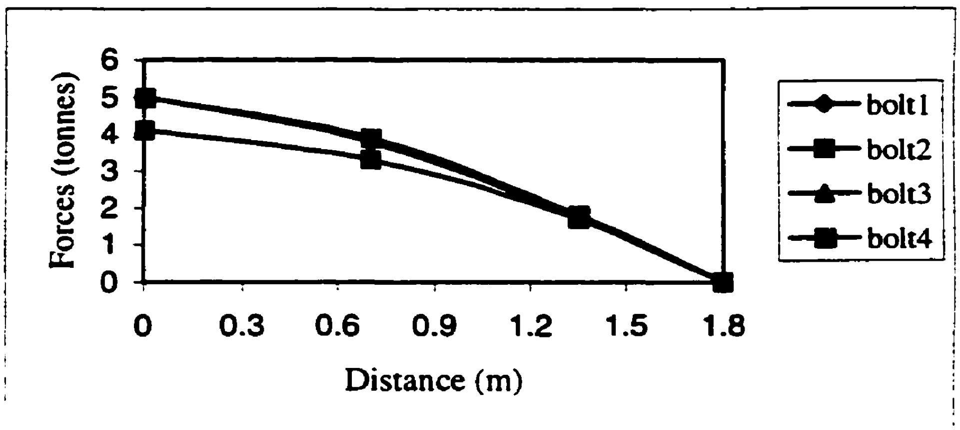

Figure 7.14: Axial force distribution in the resin- grouted rock bolts (Model A)

For the second analysis, rock bolts and cable bolts were used. The maximum forces in the rockbolts are shown in Table 7.3 and in Table 7.4 for cablebolts. The load distribution in the rockbolts which support gates 2 and 3 (bolts 5 to 12) is the same as for model A and the maximum force is 5.3 tonnes (rock bolt 12) but for the gate 1, the load distribution is different and for the rock bolts the maximum force is 4.3 tonnes (bolts 1 and 4). For the cablebolts, the maximum force mobilized is 13.6 tonnes (cable 1) at the plated face and the minimum force is zero at the toe of the cables (Figure 7.15).

Table 7.4: Maximum forces in the cables (Model B)

Cable	1	2	3	4
Forces (tonnes)	13.6	13.5	13.5	13.5

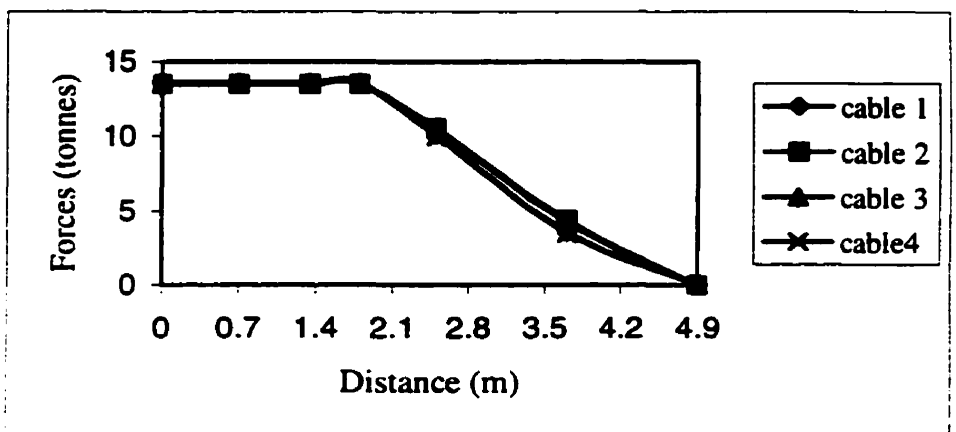

Figure 7.15: Axial force distribution in the cable bolts

The monitoring results from measured field instrumentation indicated that the maximum cable bolt force was 14.8 tonnes (Tadolini, 1999). This is in accordance with the forces computed by the model where the maximum force was 13.6 tonnes (Figure 7.13). When comparing load values, cable bolts mobilized more forces than rock bolts.

7.4 Summary

A design methodology is proposed and applied to two case studies. The case studies are: stope hanging-wall support by cable bolts in hardrock mine and tailgate secondary supports in a coal mine. It appears from the first case study (hardrock mine) that hanging-wall cable bolts are quite effective, particularly those which are nearly perpendicular to the stope face (cables No. 1, 2 and 3) and that that the cablebolting pattern could be optimized by moving more of the cable bolts towards the upper end of the stope. This would result in more evenly shared loads on the cable bolts and would reduce overall cost. From the second case study, it is shown that the maximum cable bolt force is at the anchored end with forces reaching 5 tonnes in the resin-grouted rockbolts and 13.3 tonnes in the resin grouted cable bolts. This compares favourably with field measurement of 14.8 tonnes for the maximum axial force in the cable bolts. The use of the design methodology as a design tool for cable bolts has been demonstrated by the two case studies.

CHAPTER 8
CONCLUSIONS

8.1 Summary and Conclusions

Cable bolts have been used for many years for the support of underground excavations and new type of cables, grout, pumps and installation methods has been successfully developed. The design of cable bolts became a real challenge for the ground control engineer even with the existing empirical, analytical and numerical design methods (Yazici et al., 1992; Hyett et al. 1992; Mitri, 1993). This thesis investigates a new numerical model and proposes a design approach for cable bolts.

An empirical model for the evaluation of shear bond stiffness which simulates the interface cable-grout and grout-rock was developed using a collection of data assembled in a database from laboratory and field pull-out tests . The shear bond stiffness varied depending on the type of cable, stiffness of host medium and confining pressure. The empirical model showed that the shear bond stiffness is proportional to the modulus of elasticity of host medium and variation of confining pressure depending on type of cable and water:cement ratio. Shear bond stiffness is higher for modified geometry cable bolts (garford bulb and nutcase) than for standard cable bolts. This is in accordance with the work of Moossavi reported in his Ph.D thesis (1997).

Load distribution along cable bolts was investigated numerically using the finite element method and a new numerical model was developed. The numerical model take into account the important parameters affecting the behaviour of cable bolts as the type of cable, the type of grout, the stiffness of host medium and variation of confining pressure. Fully and partially grouted cable bolts can be simulated varying the shear bond stiffness along the cables. End anchored cable bolts with attached plates and tensioned can be simulated.

A model parametric study varying including parameters like cable area, embedment length, modulus of elasticity of host medium and variation of confining pressure was conducted. For cable area, maximum forces mobilized in the cable increased with cable area and modified geometry cables and twin standard cable mobilized more loads than standard cable. The embedment length is another parameter which has a great influence on load distribution along cable bolts. The loads increase linearly with embedment length but reaching a critical value (critical bond length), the loads mobilized become constant. Varying the modulus of elasticity of host medium causes a decrease in the cable bolt with stiffness of host medium. Weak rocks mobilized more forces than hard rock. Another important parameter is the variation of confining pressure and simulation of different variation of confining pressure show that maximum forces on the cable increase with an increase of confining pressure.

Using the numerical and empirical models developed, a new design methodology was proposed. In this new approach unstable zones were simulated by reducing the elastic properties of the rock mass in the unstable area and using the empirical model for the evaluation of shear bond stiffness.

To test the application of the model in the field two case studies with instrumented cables were presented. The first case study was a hanging wall support in an underground mine (Bousquet mine, Val D'or, Québec) where the use of cable bolts are very efficient to limit ore dilution. The computed load distribution along the cable bolts computed by the model correlated well with the results obtained from the instrumentation in the field. The second case study was a gateroad support in a Western U.S coal mine using cable bolts as secondary support with resin grout and plates. A comparison with measurements in the field (Bawden, 1997; Tadolini, 1999) shows a good accordance with computed forces.

The model developed in this thesis may be generalized for other internal ground supports such as rock bolts even though it was developed for cable bolts. Some limitations of the model are:

- The model is a linear elastic. No elastoplasticity or viscoplasticity is accounted for.
- A maximum of 9 isotropic or orthotropic materials can be modelled.
- 2-dimensional problems, plane stress or plane strain analysis are modelled. 3-dimensional problems are not simulated.
- Static analysis only are performed and dynamic loads are not simulated. Dynamic loading effect might be simulated using the concept of equivalent static loading.

8.2 Further Research Studies:

The research work presented in this thesis can be further extended in the following directions:

1- Implementation of a visco-plastic model in the program to simulate large deformations and the effect of time.

2- Further calibration studies are recommended to enhance the model reliability in underground mining applications.

3- Development of a 3-dimensional formulation for the model to handle 3D mining applications. Three dimensional analyses are required in such situations as drift intersections and room and pillar mining.

4- Investigation of new type of materials for cable bolts to reduce the cost and increase the cable capacity.

STATEMENT OF CONTRIBUTION

A finite element model for the design of cable bolts was developed. This model computes the load distribution along cable bolts taking into-account the important parameters affecting the behaviour of cables as cable type, stiffness of host medium, confining pressure, attached plates and pretension.

The numerical model is used with an empirical model developed for the evaluation of shear bond stiffness for cable bolts. A database with a collection of data from pull-out tests was constructed and integrated with the new model.

A design methodology is proposed for the design of cable bolts and applied for two cases studies using cable bolts as ground support: one for an underground hardrock mine and another for a coal mine.

REFERENCES

Anwyll, D. (1996). The cable bolt – grout displacement meter an innovation in cable bolt monitoring. M.Eng Thesis, Department of Mining and Metallurgical Engineering, McGill University, Montréal, Canada.

Aydan, O., Ichikawa, Y. and Kawamoto, T. (1985). Load bearing capacity and stress distribution in/along rockbolts with inelastic behaviour of interfaces. Proc. of the 5th Int. Conf. On Num. Meth. In Geomechanics, Nagoya, Japan, 2, pp. 1281-1292.

Bandis, S., Lumsden, A.C. and Barton, N. (1983). Fundamentals of rock joint deformation. Int. J. Rock Mech. Min. Sci., Vol.20, 249-268.

Barton, N., Lien, R., and Lunde, J. (1974). Engineering classification of rockmasses for the design of tunnel support. Rock Mech., May, 189-236.

Barton, N. (1988). Rock mass classification and tunnel reinforcement selection using the Q-system. Rock classification systems for Engineering Purposes, A.S.T.M. 984, (ed.Kirkaldie), American Society for Testing and Materials, 59 - 88.

Bawden, W.F., Hyett, A.J. and Lausch, P. (1992). An experimental procedure for the in situ testing of cable bolts. Int. J. Rock. Mech. Min. Sci. & Geomech. Abstr., 29, (5), 525-533.

Bawden, W.F., Hyett, A.J. and Cortolezzis, D. (1992). Towards a methodology for performance assessment in cable bolt design. Rock support (eds. Kaiser and McCreath), Rotterdam: A.A. Balkema, 277-284.

Bawden, W.F. and Hyett, A.J. (1992). A field cable bolt pull test programme for lac minerals at Bousquet division – mineshaft 2. Internal report, Department of Mining Engineering, Queen's University, Kingston, Ontario.

Bawden, W.F., Hyett, A.J, Laush P., Moosavi M., deGraaf P.J.H. and Ruest M. (1997). The S.M.A.R.T cable bolt: Results from two initial field trials. In Proc. of the Annual General Meeting of the Canadian Institute of Mining-Rock Mechanics Division, pp. 245-255.

Bawden, W.F., de Graaf, P.J.H., Hyett A.J., Lausch P. and Yao M. (1999). Trout lake and Callinan mines: Case sudies of cable bolt support design improvement through multifaceted design, including 'SMART' technology as an aid to ground support design performance evaluation. 14e colloque en contrôle de terrain, Val-d'Or, Québec, 23-24 mars 1999.

Benmokrane, B., Chennouf, A. and Balivy, G. (1992). Study of bond strength behaviour of steel cables and bars anchored with different cement grout. Proc. Rock support in mining and underground construction, eds. Kaiser and McCreath, Rotterdam: A.A. Balkema, 293-301.

Bieniawski, Z.T. (1973). Engineering classification of jointed rock masses. Transaction of the South African Institute of Civil Engineers, 15, pp.335-344.

Bieniawski, Z.T. (1978). Determination of rock mass deformability: Experience from case histories. . Int. J. Rock Mech. Min. Sci. & Geomech. Abstr., 15, pp. 237-247.

Bieniawski, Z.T. (1989). Engineering rock mass classifications. John Wiley & Sons, Inc., New York.

Bieniawski, Z.T. (1993). Classification of rock masses for engineering : The RMR system and future trends. Comprehensive Rock Engineering, (ed.Hudson), Oxford: Pergamon, 3, 553-573.

Bouteldja, M. and Mitri, H.S. (1999). Analysis of cable bolts performance using numerical modeling. 18th International Conference on Ground Control in Mining, Morgantown, West Virginia, U.S.A., 3-5 August 1999, pp. 248-255.

Bouteldja, M. and Mitri, H.S. (2000). Empirical evaluation of shear bond stiffness of cable bolts. Ground Improvement Journal, Publication of ISSMFE, London (to be submitted).

Brady, B.H.G. and Brown, E.T. (1993). Rock mechanics for underground mining. London: Chapman and Hall, 571p.

Brady, B. and Lorig, L. (1988). Analysis of rock reinforcment using finite difference methods. Computers and Geotechnics 5, 123-149.

Campoli, A., Mills, P., Todd, P. and Dever, K. (1999). Resin annulus size effects on rebar bolt pull strength and resin loss to fractured rock. 18th International Conference on Ground Control in Mining, Morgantown, West Virginia, U.S.A., 3-5 August 1999, pp. 222-231.

Chekired, M., Benmokrane, B. and Mitri, H.S. (1997). Laboratory evaluation of a new cable bolt tension measuring device. Int. J. Rock Mech & Min. Sci. Vol. 34: 3-4, paper No. 203.

Choquet, P., Miller, F. (1988). Development and field testing of a tension measuring gauge for cable bolts used as ground support. CIM Bulletin. 81:915, 53-59.

Cook, R.D. (1995). Finite element modelling for stress analysis. John Wiley&Sons, Inc., New York.

Cundall, P., Board, M. (1988). A microcomputer program for modelling large-strain plasticity problems. Proc. of Numerical Methods in Geomechanics (Innsbruck), Swoboda (ed.), Balkema, pp. 2101-2108.

Diakité, O. (1998). Ore dilution in sublevel open stope mining. M. Sc. Thesis, Mining Engineering Department, McGill University, Montréal, Canada.

Drouhin, M. (1935). Consolidation du barrage de Cheurfas par tirants métalliques mis en tension. Annales des Ponts et chaussées, Paris, France.

Douglas. T.H., and Arthur, L.J. 1983. Aguide to the use of rock reinforcement in underground excavations. CIRI Report No. 101, London, 74p.

Farmer, I.W. (1975). Stress distribution along a resin grouted rock anchor. International Journal of Rock Mechanics and Mining Sciences, Vol.12, pp. 347-351.

Fuller, P.G. (1983). Cable support in mining: A keynote lecture. RockBolting, Rotterdam: A.A. Balkema, 511-522.

Gambarova, P.G. and Karakoç, C. 1982. Shear-confinement interaction in the bar-to-concrete interface. Proc. Int. Conf. on Bond in Concrete, Edited by P.Bartos, Applied Science Publishers, London, pp.82-96.

Goodman, R. and Boyle, W. 1985. Non linear analysis for calculating the support of a block with dilatant joint surfaces. 34th Geomechanics Colloquium, Salzburg, Austria.

Goris, J.M. (1990). Laboratory evaluation of cable bolt supports. 92nd Canadian Institute of Mining Annual General Meeting, Ottawa, Ontario, Canada, paper #163.

Goris, J.M. (1991). Laboratory evaluation of cable supports. CIM bulletin, Volume 84, N0. 948, pp. 44- 50.

Gramoli. L. (1975). Tensioned cable rock anchorage at Geco Division of Noranda mines Ltd. CIM first underground operators conference, Sudbury, Ontario.

Grimstad, E., and Barton, N. 1993. Updating the Q-system for NMT. Proc. Int. Symp. On sprayed concrete, Fagermes, (eds. Kompen, Ospahl and Berg), Oslo: Norwegian Concrete Association.

Hassani, F.P., Mitri, H.S., Khan, U.H., and Rajaie, H. (1992). Experimental and numerical studies of the cable bolt support system. Rock Support, (eds. Kaiser and McCreath). Rotterdam: A.A. Balkema, 411- 417.

Hadjigeorgiou, J., Leclair, J.G and Potvin, Y. (1995). An update of the stability graph method for open stope design. CIM-AGM, Halifax.

Hoek, E. and Brown, E.T. (1980). Underground excavation in rock. The Institution of Mining and Metallurgy, London, England.

Hoek, E. and Brown, E.T. (1988). The Hoek-Brown failure criterion - a 1988 update. Proc. 15th Can. Rock Mech. Symp., 31-38.

Hoek. E. 1981. Geotechnical design of large openings at depth. Proc. Conf. Rapid Excavation Tunnelling, New York: AIME.

Hoek, E., Grabinsky, M.W., Fiederichs, M.S. (1991). Numerical modelling for underground excavation design. Trans. Inst Min. Metall., 100, A22-A30.

Hoek, E. (1998). Practical Rock Engineering. Course notes. Rocscience site web (http:\\www.rocscience.com).

Hollingshead, G.W. (1971). Stress distribution in rock anchors. Canadian Geotechnical Journal, Vol.8, No. 4, pp. 588-592.

Hutchinson, D.J. and Diederichs, M.S. (1996). Cablebolting in underground mines. BiTech Publishers Ltd., Richmond, BC.

Hutchinson, D.J. and Diederichs, M.S. (1996). The cablebolting cycle-underground support engineering. CIM Bulletin, 89 , (1001), June 96, 117-122.

Hutchinson, D.J. (1992). A field investigation of cablebolt reinforcement of open stopes at Ansil mine. Ph.D thesis, Departement of civil engineering, University of Toronto, Ontario, Canada, 470p.

Hutchinson, D.J., and Grabinsky, M.W. (1992). Back analysis of slope stability at Ansil mine using instrumentation data and numerical modelling. Proc. Rock support, (eds. Kaiser and McCreath), Rotterdam: A.A. Balkema, pp. 167-176.

Hyett, A.J, Bawden, W.F, Lausch, P., Ruest, M., Hennings, J. and Baillargeon, M. (1997). The S.M.A.R.T cable bolt, An instrument for the determination of tension in 7-wire strand cable bolts. 12e Colloque en contrôle de terrain, Val-d'Or , 25-26 Mars 1997.

Hyett, A. J., Bawden, W.F., and Reichert, R.D. (1992). The effect of rock mass confinement on the bond strength of fully grouted cable bolts. Int. J. Rock Mech. Min. Sci. & Geomech. Abstr., 29, (5), 503 -524.

Hyett, A.J., Bawden, W.F., MacSporran, G.R., and Moosavi, M. (1995). A constitutive law for bond failure of fully-grouted cable bolts using a modified Hoek cell. Int. J. of Rock Mech. Min. Sci. & Geomech. Abstr., 32, (1), 11 - 36.

Hyett, A.J., Moosavi, M. and Bawden, W.F. (1996). Load distribution along fully grouted bolts, with emphasis on cable bolt reinforcement. Int. J. for Numer. Anal. Methods. in Geomech., 20, 517-544.

Hyett, A.J., Bawden, W.F., Laush, P., Ruest.M., Henning, J. and Baillargeon, M. 1997. The S.M.A.R.T. cable bolt: an instrument for the determination of tension in 7-wire strand cable bolts. 12e colloque en contrôle de terrain, Val-d'Or, Québec, 25-26 mars 1997.

Itasca Consulting Group (1995). FLAC user manual version 3.3. Minneapolis: Itasca Consulting Group.

Itasca Consulting Group (1993). UDEC : Universal Distinct Element Code (version 2.0). User's manual, Itasca Consulting Group.

Kafarkis, M.G., Kan., S.W, Wilson, R. and Zelanco, J. (1998). Characterization of polyester grouts for ground control. Mining Engineering, September 1998, pp. 69- 74.

Kaiser, P.K., Diederichs, M. and Yazici, S. (1992). Cable bolt performance during mining induced stress change- Three case examples. Proc. Rock support, (eds. Kaiser and Mcreath), Rotterdam: Balkema, 377-384.

Kaiser, P.K., Maloney, S.M., and Yazici, S. (1992). A new perspective on cable bolt design. CIM Bulletin, 85, (962), 103 - 109.

Kaiser, P.K., Yazici, S. and Nosé, J. (1992). Effect of stress change on the bond strength of fully grouted cables. Int. J. Rock Mech. Min. Sci. & Geomech. Abstr., 29, (3), 293 - 306.

Khan, U. (1995). Laboratory investigation of steel and composite material tendons. Ph.D Thesis, Department of Mining and Metallurgical Engineering, McGill University, Montréal, Canada.

Ladany, B. and Dominique, D. (1980). Analysis of bond strength for rock socketed piers. Int. Conf. on Structural Foundations on Rock, Sydney, pp. 363-373.

Laubscher, D.H. (1977). Geomechanics classification of jointed rock masses - mining applications. Trans. Inst. Min. Metall., 86, A1 - A8.

Littlejohn, G.S. (1992). Keynote lecture: Rock anchorage practice in civil engineering. Proc. Rock Support in Mining and Underground Construction, Kaiser&McCreath(eds), Balkema, Rotterdam, pp. 257-258.

MacSporran, G.R. (1992). An empirical investigation into the effects of mine induced stress change on standard cable bolt capacity. M.Sc.thesis, Queen's University, Kingston, Ontario, Canada.

Marence, M. and Swoboda, G.(1995). Numerical model for rock bolts with consideration of rock joint movements. Rock Mechanics and Rock Engineering, 28(3), pp. 145-165.

Mathews, K.E, Hoek, E., Wyllie, D.C and Stewart, S.B.V (1981). Prediction of stable excavation spans for mining at depths below 1000m in hard rock mines. CANMET Report DSS Serial N. OSQ 80-00081, April 1981.

Miller, S.M. and Ward, D.C. (1998). Evaluation of pullout resistance and direct-shear strength of grouted fiberglass cable bolts. Int. J. of Rock Mech.& Min. Sci. , Vol. 35, Nos. 4-5, Paper No. 66.

Mitri, H.S. and Rajaie, H. (1990). Stress analysis of rockmass with cable bolt support - a finite element approach. CANMET: stresses in underground structures, Ottawa, 2-3 October, pp. 110 -119.

Mitri, H.S. (1993). Ez tools: 2-dimensional finite element modeling software. Users's manual, Numerical Modelling Laboratory, McGill University, Montréal.

Mitri, H.S, Edrissi, R. and Henning, J. (1996). Finite element modelling of cable-bolted stopes in hard rock underground mines. Transaction of the Society for Mining, Metallurgy, and Exploration Inc., vol.298, pp. 1897-1902.

Mitri, H.S., Ma, J., Mohammed, M. and Diakite, O. (1998). Design of cable bolts using numerical modelling. Proc. 5th South American Congress on Rock Mechanics, ISRM Regional Symposium , Sao Paulo, Brazil, 22-25 November 98.

Mitri, H.S., Mohammed, M. and Bouteldja, M. (1999). Recent advances in cable bolting technology. Proc. 6th International Mining, Petroleum, and Metallurgical Engineering Conference, Cairo, Egypt, Vol.1-A, pp. 168-179.

Mohammad, N., Reddish, D.J. and Stace, L.R. (1997). The relation between in situ and laboratory rock properties used in numerical modelling. Int. J. of Rock Mech.& Min. Sci. , Vol. 34, No. 2, pp. 289-297.

Moosavi, M. (1997). Load distribution along fully grouted cable bolts based on constitutive models obtained from modified Hoek cells. Ph.D Thesis, Dept. of Mining Engineering, Queens University, Kingston, Ontario, 287 p.

Nicholson, G.A. and Bieniawski, Z.T. (1990). A non linear deformation modulus based on rock mass classification. Int. J. Min.& Geological Engng, 8, pp. 181-202.

Nickson, S.D. (1992). Cable support guidelines for underground hard rock mines operations. M.A.Sc. Thesis, Dept. of Mining and Mineral Processing, University of British Columbia, 223p.

Obert, L., and Duvall, W.I. (1967). Rock Mechanics and the Design of Structures in Rock. New York: John Wiley and Sons, 650 p.

O'Grady, P., Fuller, P. and Dight, P. (1993). Cablebolting in Australian coal mines-current practice and design considerations. Meeting of the South Western Branch of IminE, Hengoed, Australia.

Pakalnis, R., Peterson, D.A. and Peter Mah G. (1994). Glass fibre cable bolts an alternative. CIM Bulletin, 87, (175), 53-57.

Pande, G.N., Beer, G. and Williams, J.R. (1990). Numerical Methods in Rock Mechanics. John Wiley & Sons, New York.

Peng, S.S. and Guo, S. 1992, An improved numerical model of grouted bolt – roof rock interaction in undergrounds openings. Proc. Rock Support in Mining and Underground Construction, eds. Kaiser and McCreath, Rotterdam: A.A. Balkema, 67-74.

Popov, E.P. (1978). Mechanics of Materials. New Jersey: Prentice-Hall Inc., 590 p.

Potvin, Y. (1988). Empirical open stope design in Canada. Ph.D. Thesis, Dept. Mining and Mineral Processing, University of British Columbia, 343 p.

Potvin, Y., Hudyma, M.R., and Miller, H.D.S. (1989). Design guidelines for open stope support. CIM bulletin, 82, (926), 53 -62.

Potvin, Y., and Milne, D. (1992). " Empirical cable bolt support design". Rock support, (eds. Kaiser and McCreath), Rotterdam: A.A. Balkema, 269-275.

Rajaie, H. (1990). Experimental and numerical investigation of cable bolt support systems. Ph.D Thesis, Department of Mining and Metallurgical Engineering, McGill University, Montréal, Canada.

Reichert, R.D. 1991. A laboratory and field investigation of the major factors influencing bond capacity of grouted cable bolts. M.A.Sc. Thesis, Queen's University, Kingston, Canada, 225 pages.

Reichert, R.D., Bawden, W.F., and Hyett, A.J. (1992). Evaluation of design bond strength for fully grouted cable bolts. CIM Bulletin, 85, 110 - 118.

Rocscience (1998). Phase^2 : Finite element anlysis of excavation, version 4.0.

Saeb S. and Amadei B. (1983). Modelling rock joints under shear and normal loading. Int. J. Rock Mech. Min. Sci. & Geomech. Abstr. 29, 267-278.

Scott, J.J. 1976. Friction rock stabilizers - a new rock reinforcement method. In Monograph on rock mechanics applications in mining, (eds. W.S.Brown, S.J. Green and W.M.Hustrulid). New York: Soc. Min. Engrs, A.I.M.M.P.E., 242-249.

Serafim, J.L. and Pereira, J.P. (1983). Consideration of the geomechanical classification of Bieniawski. Proc. Int. Symp. on Engineering Geology and Underground Construction, Lisbon, 33-44.

Stewart, S.B.V. and Forsyth, W.W. (1995). The Mathew's method for open stope design. CIM Bulletin, 88, (992), 45-53.

Stillborg, B. (1984). Experimental investigation of steel cables for rock reinforcement in hard rock. Ph.D Thesis, University of Lulea.

Stillborg, B. (1994). Professional Users Handbook for Rock Bolting, 2nd edition. Clausthal-Zellerfield : Trans Tech Publications.

St.John, C.M. and Van Dillen, D.F (1983). Rock bolts: A new numerical representation and its applications in tunnel design. Pro. Of the 24th US Symposium on Rock Mechanics, pp. 13-25.

Tadolini, S.C., Gallagher, J.L. and Goris, J.M. (1999). Resin grouted cable supports for coal mine ground control. CIM Bulletin, 92, (1028), March 99, 135-139.

Tadolini, S. (1998). The effects of reduced annulus in roof bolting performance. Proc. Of the 17th Conference on Ground Control in Mining, Morgantown, WV, 231-236.

Tan, G., Bawden, W.F. and Pelley C. (1993). A cable bolt model and its implementation into UDEC and FLAC. Proc. First Canadian symposium on Numerical Modelling Applications in Mining and Geomechanics, Montreal, Quebec, March 27-30, 240-252.

Tan, G. (1993). A new cable bolt load-displacement relationship and its implementation into FLAC and UDEC. Doctoral Thesis, Queen's University, Kingston, Ontario.

Tang, B., Mitri, H.S. and Bouteldja, M. (1999). A finite element approach for the simulation of rock anchors. Ground Improvement Journal, Publication of ISSMFE, London.

Thompson, A.G. (1992). Tensioning reinforcing cables. Proc. Rock Support in Mining and Underground Construction, Kaiser&McCreath(eds), Balkema, Rotterdam, pp. 285-291.

Tognon, G.P. and Cangiano, S. 1982. Stength and interface bond in concrete. Proc. Int. Conf. on Bond in Concrete, Edited by P.Bartos, Applied Science Publishers, London, pp.4-14.

Unal, E. 1983. Design guidelines and roof control standard for coal mine roofs. Ph.D Thesis, Pennsylvania State University, 355 p.

Wang, B. and Garga, V.K. (1992). A numerical model for rockbolts. Proc. Rock Support in Mining and Underground Construction, eds Kaiser and McCreath, Rotterdam: A.A.Balkema, 57-66.

Windsor, C.R. (1992). Invited lecture: Cable bolting for underground and surface excavations. Rock Support, (eds. P.K. Kaiser and D. McCreath), Rotterdam: A.A. Balkema, 349-376.

Yap, L.P. and Rodger, A.A. (1984). A study of the behavior of vertical rock anchors using the finite element method. Int. J. of Rock Mech. And Min. Sci,, Vol. 22, No.2, pp. 47-61.

Yazici, S., and Kaiser, P.K. (1992). Bond strength of grouted cable bolts. Int. J. Rock Mech. Min. Sci. & Geomech. Abstr., 29, (3), 279 - 292.

APPENDIX A
Modelling of Cable Bolts with e-z tools

In order to model internal ground supports in a given problem, the user needs to create a datafile in accrodance with the instructions given in this section. This file, should be designated with the extension CAB (Figure A1) and will have the same name as the mesh file (.COR file).

Creating a .CABfile

In the following, the sequence of input data required to construct the .CAB file is explained. Use any text editor to type the data file. The purpose of the CAB file is to provide such data as the mechanical properties of the cable bolt, the bond stiffness of the interface material and the locations of the cable bolts. The latter is determined by specifying the nodes on the mesh which are located along the cable bolt. Therefore, it is important to have the mesh with the nodes marked on it before starting to write the .CAB file. Only 4 cards of data are needed for each cable bolt to be simulated. The program will then automatically divide each bolt into a number of cable bolting elements according to the nodes specified along the cable bolt.

Card 1: Cable Bolt Properties

Variable	*Entry*
'N'	Enter cable bolt number between quotation marks e.g.'1'
EB	Modulus of elasticity of the cable bolt material
AB	Cross sectional area of the cable bolt
NB	Number of nodes defining the bolt length.
R	Factor for resin anchor (=1 in case of pretension, =0 without pretension)
T	Intensity of tension force

Card 2: Cable Bolt Properties

Variable	*Entry*
	Enter the letter n between quotes, i.e. 'n'
(NOB(I),I=1,NB)	Enter an array of NB node numbers that define the bolt length and orientation. Refer to the actual finite element mesh (not the zone model) for node numbers (.COR file).

Card 3: Data of Interface

Variable	*Entry*
	Enter the letter s between quotes, i.e. 's'
(SOB(I),I=I,NB)	Enter an array of NB stiffness values define the shear bond stiffness per Unit length between the cable bolt and solid material domain. Note that the units Should be in force per unit area i.e. like stress units.

Card 4: Need for attached plates

Variable	*Entry*
	Enter the letter p between quote, i.e. 'p'
(POB(I),I=1,NB)	Enter number 1 or 0 (=1 in case of attached plates, =0 without plates)

Repeat the sequence of cards 1,2,3, 4 until all cable bolt data is entered. Enter END on the last line.

Example

The following are the contents of an example .CAB file. It gives the data of 3 cable bolts that all have a modulus of elasticity of 200,000 MPa, and a cross sectional area of 0. 0014 m2. Each of the 3 cable bolts is defined by 4 nodes. and the shear bond stiffness of the bonding material is 90 MPa.

- Cable bolts are not attached with plates and not tensioned :

```
'1' 200000 .0014 4 0 0
'n' 17 18 19 20
's' 90 90 90 90
'p' 0 0 0 0
'2' 200000 .0014 4 0 0
'n' 5 6 7 8
's' 90 90 90 90
'p' 0 0 0 0
'3' 200000 .0014 4 0 0
'n' 1 2 3 4
's' 90 90 90 90
'p' 0 0 0 0
END
```

In the above example, the number of cable bolts simulated is 3 but the resulting number of bolting elements is 3 x 3 = 9.

- Cable bolts are end anchored with attached plates:

```
'1' 200000 .0014 4 0 0
'n' 17 18 19 20
's' 90 90 90 90
'p' 1 0 0 0
'2' 200000 .0014 4 0 0
'n' 5 6 7 8
's' 90 90 90 90
'p' 1 0 0 0
'3' 200000 .0014 4 0 0
'n' 1 2 3 4
's' 90 90 90 90
'p' 1 0 0 0
END
```

- Cable bolts are tensioned with a pretension of 2.5 tonnes:

```
'1' 200000 .0014 4 1 0.025
'n' 17 18 19 20
's' 90 90 90 90
'p' 1 0 0 0
'2' 200000 .0014 4 1 0.025
'n' 5 6 7 8
's' 90 90 90 90
'p' 1 0 0 0
'3' 200000 .0014 4 1 0.025
'n' 1 2 3 4
's' 90 90 90 90
'p' 1 0 0 0
END
```

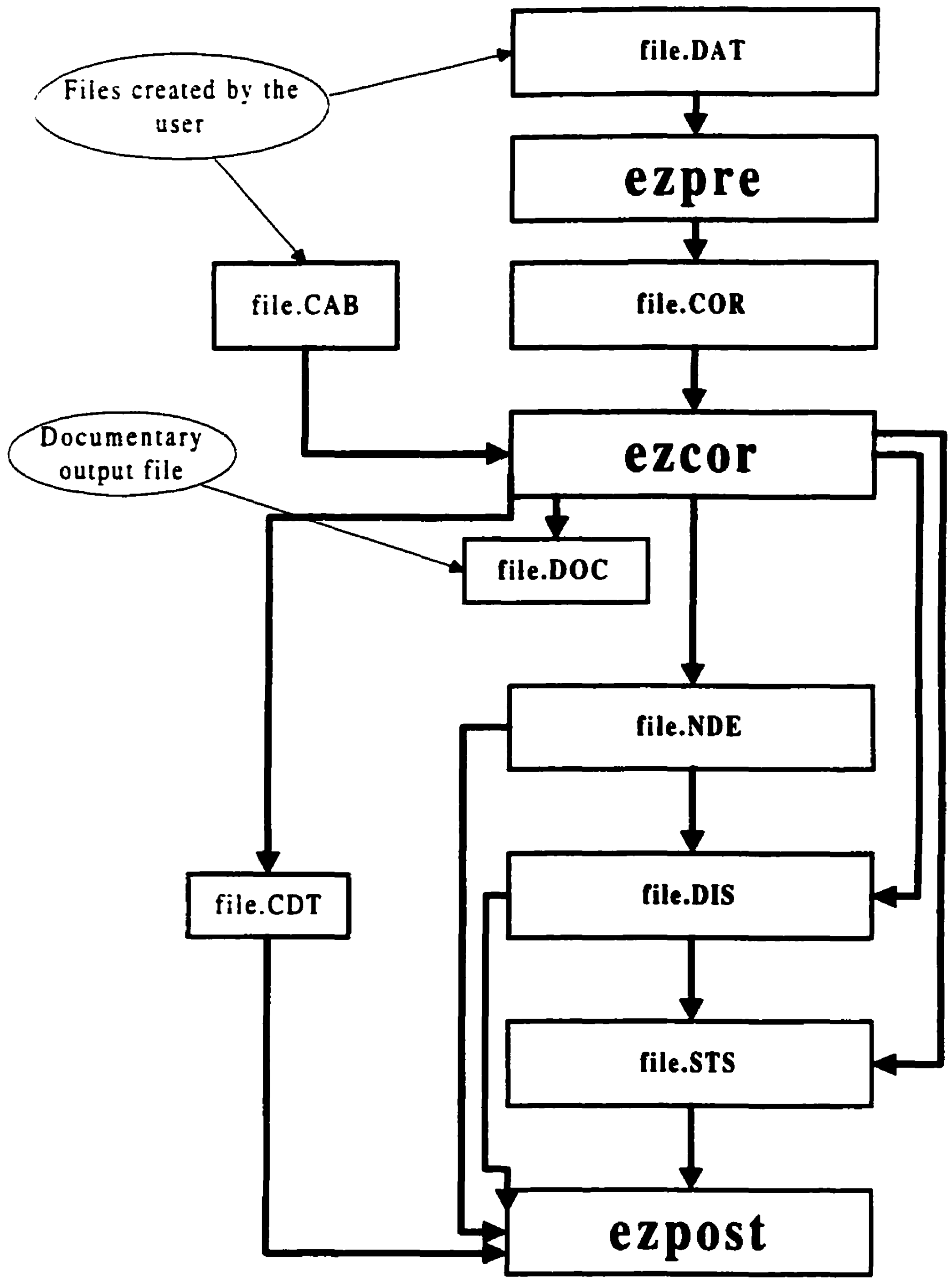

Figure A1a: Flowchart of e-z tools (Modelling of cable bolts)

APPENDIX B
Database

Field and laboratory pull-out test results

Test	Cable type	Medium	E(GPa)	Length(m)	w:c ratio	Stress (MPa)	k(MN/m/m)	Source
Laboratory	Standard	Steel	200.00	0.25	0.30	0.00	101.00	Hyett (92)
Laboratory	Standard	Aluminum	72.00	0.25	0.30	0.00	80.00	"
Laboratory	Standard	PVC	3.00	0.25	0.30	0.00	32.40	"
Field	Standard	Granite	23.30	0.25	0.30	0.00	96.00	"
Field	Standard	Limestone	32.30	0.25	0.30	0.00	37.32	"
Field	Standard	Shale	13.50	0.25	0.30	0.00	41.68	"
Laboratory	Standard	Steel	200.00	0.25	0.40	0.00	79.80	"
Laboratory	Standard	PVC	3.00	0.25	0.40	0.00	30.80	"
Laboratory	Standard	Steel	200.00	0.25	0.50	0.00	64.60	"
Laboratory	Standard	PVC	3.00	0.25	0.50	0.00	27.00	"
Field	Standard	Granite	23.00	0.25	0.40	0.00	82.80	"
Field	Standard	Shale	14.00	0.25	0.40	0.00	71.20	"
Field	Standard	limestone	32.00	0.25	0.40	0.00	72.00	"
Field	Standard	Granite	23.00	0.25	0.50	0.00	59.20	"
Field	Standard	Shale	14.00	0.25	0.50	0.00	66.80	"
Field	Standard	Limestone	32.00	0.25	0.50	0.00	87.60	"
Field	Standard	Granite	23.00	0.38	0.30	0.00	60.00	"
Field	Standard	Shale	14.00	0.38	0.30	0.00	36.30	"
Field	Standard	Granite	23.00	0.50	0.30	0.00	54.40	"
Field	Standard	Shale	13.50	0.50	0.30	0.00	34.00	"
Field	Standard	Schist	14.90	0.25	0.35	0.00	86.80	Bawden (92)
Field	Standard	Schist	14.90	0.25	0.35	0.00	86.80	"
Field	Standard	Schist	14.90	0.25	0.35	0.00	86.80	"
Field	Standard	Schist	14.90	0.25	0.35	0.00	86.80	"
Field	Standard	Schist	14.90	0.25	0.35	0.00	86.80	"

Field and laboratory pull-out test results

Test	Cable type	Medium	E(GPa)	Length(m)	w:c ratio	Stress (MPa)	*k*(MN/m/m)	Source
Field	Birdcage	Schist	14.90	0.30	0.35	0.00	43.33	"
Field	Birdcage	Schist	14.90	0.30	0.35	0.00	54.30	"
Field	Birdcage	Schist	14.90	0.30	0.35	0.00	54.30	"
Field	Birdcage	Schist	14.90	0.30	0.35	0.00	54.30	"
Field	Birdcage	Schist	14.90	0.30	0.35	0.00	54.30	"
Field	Nutcase	Schist	14.90	0.30	0.35	0.00	50.00	"
Field	Nutcase	Schist	14.90	0.30	0.35	0.00	50.00	"
Field	Nutcase	Schist	14.90	0.30	0.35	0.00	50.00	"
Field	Nutcase	Schist	14.90	0.30	0.35	0.00	50.00	"
Field	Standard	Ryolite	10.60	0.25	0.35	0.00	58.80	"
Field	Standard	Ryolite	10.60	0.25	0.35	0.00	58.80	"
Field	Standard	Ryolite	10.60	0.25	0.35	0.00	58.80	"
Field	Standard	Ryolite	10.60	0.25	0.35	0.00	58.80	"
Field	Standard	Ryolite	10.60	0.25	0.35	0.00	58.80	"
Field	Birdcage	Ryolite	10.60	0.30	0.35	0.00	38.70	"
Field	Birdcage	Ryolite	10.60	0.30	0.35	0.00	38.70	"
Field	Birdcage	Ryolite	10.60	0.30	0.35	0.00	38.70	"
Field	Nutcase	Ryolite	10.60	0.30	0.35	0.00	37.50	"
Field	Nutcase	Ryolite	10.60	0.30	0.35	0.00	37.50	"
Field	Nutcase	Ryolite	10.60	0.30	0.35	0.00	37.50	"
Field	Nutcase	Ryolite	10.60	0.30	0.35	0.00	37.50	"
Field	Standard	Ryolite	10.60	0.30	0.35	0.00	8.33	"
Field	Birdcage	Ryolite	10.60	0.30	0.35	0.00	27.80	"
Field	Birdcage	Ryolite	10.60	0.30	0.35		27.80	"
Field	Nutcase	Ryolite	10.60	0.30	0.35		54.20	"

Field and laboratory pull-out test results

Test	Cable type	Medium	E(GPa)	Length(m)	W/c ratio	Stress(MPa)	k(MN/m/m)	Source
Field	Nutcase	Ryolite	10.60	0.30	0.35		54.20	"
Field	Nutcase	Ryolite	10.60	0.30	0.35		54.20	"
Laboratory	Standard	Steel	200.00	0.30	0.45	0.00	16.67	Goris (91)
Laboratory	Standard	Steel	200.00	0.30	0.45	0.00	116.65	"
Laboratory	Standard	Steel	200.00	0.25	0.45	0.00	104.96	"
Laboratory	Standard	Steel	200.00	0.30	0.45	0.00	110.17	"
Laboratory	Standard	Steel	200.00	0.36	0.45	0.00	97.20	"
Laboratory	Standard	Steel	200.00	0.40	0.45	0.00	97.25	"
Laboratory	Standard	Steel	200.00	0.46	0.45	0.00	105.60	"
Laboratory	Standard	Steel	200.00	0.50	0.45	0.00	108.80	"
Laboratory	Standard	Steel	200.00	0.56	0.45	0.00	96.90	"
Laboratory	Standard	Steel	200.00	0.60	0.45	0.00	99.20	"
Laboratory	Standard	Steel	200.00	0.66	0.45	0.00	95.45	"
Laboratory	Standard	Steel	200.00	0.70	0.45	0.00	97.50	"
Laboratory	Standard	Steel	200.00	0.76	0.45	0.00	89.80	"
Laboratory	Standard	Steel	200.00	0.25	0.30	0.00	65.88	"
Laboratory	Standard	Steel	200.00	0.25	0.35	0.00	62.12	"
Laboratory	Standard	Steel	200.00	0.25	0.40	0.00	21.60	"
Laboratory	Standard	Steel	200.00	0.25	0.45	0.00	13.96	"
Laboratory	Standard(twin)	Steel	200.00	0.25	0.45	0.00	230.70	"
Laboratory	Standard(twin)	Steel	200.00	0.25	0.45	0.00	163.40	"
Laboratory	Birdcage	Steel	200.00	0.25	0.45	0.00	175.00	"
Laboratory	Birdcage	Steel	200.00	0.25	0.45	0.00	220.80	"
Laboratory	Standard	concrete	12.00	0.15	0.40	0.00	33.30	Rajaie (90)
Laboratory	standard	concrete	12.00	0.20	0.40	0.00	40.60	"

Field and laboratory pull-out test results

Test	Cable type	Medium	E(GPa)	Length(m)	w:c ratio	Stress (MPa)	k(MN/m/m)	Source
Laboratory	standard	concrete	12.00	0.30	0.40	0.00	35.40	"
Laboratory	standard	concrete	12.00	0.40	0.40	0.00	34.40	"
Laboratory	standard	concrete	12.00	0.50	0.40	0.00	33.30	"
Laboratory	standard	concrete	12.00	0.60	0.40	0.00	30.80	"
Laboratory	standard	concrete	12.00	0.75	0.40	0.00	30.70	"
Laboratory	standard	Steel	200.00	0.25	0.30	1.00	80.48	McSporran(93)
Laboratory	standard	Steel	200.00	0.25	0.30	1.00	80.48	"
Laboratory	standard	"	200.00	0.25	0.30	1.00	80.48	"
Laboratory	standard	"	200.00	0.25	0.30	3.00	80.12	"
Laboratory	standard	"	200.00	0.25	0.30	3.00	80.12	"
Laboratory	standard	"	200.00	0.25	0.30	3.00	80.12	"
Laboratory	standard	"	200.00	0.25	0.30	3.00	80.12	"
Laboratory	standard	"	200.00	0.25	0.30	3.00	80.12	"
Laboratory	standard	"	200.00	0.25	0.30	5.00	144.80	"
Laboratory	standard	"	200.00	0.25	0.30	5.00	144.80	"
Laboratory	standard	"	200.00	0.25	0.30	5.00	144.80	"
Laboratory	standard	"	200.00	0.25	0.30	10.00	193.20	"
Laboratory	standard	"	200.00	0.25	0.30	10.00	193.20	"
Laboratory	standard	"	200.00	0.25	0.30	10.00	193.20	"
Laboratory	standard	"	200.00	0.25	0.30	15.00	265.60	"
Laboratory	standard	"	200.00	0.25	0.30	15.00	265.60	"
Laboratory	standard	"	200.00	0.25	0.30	15.00	265.60	"
Laboratory	standard	"	200.00	0.25	0.30	15.00	265.60	"
Laboratory	standard	"	200.00	0.25	0.30			"
Laboratory	standard	"	200.00	0.25	0.30			"

Field and laboratory pull-out test results

Test	Cable type	Medium	E(GPa)	Length(m)	w:c ratio	Stress (MPa)	k(MN/m/m)	Source
Laboratory	standard	"	200.00	0.25	0.40	2.00	96.56	"
Laboratory	standard	"	200.00	0.25	0.40	2.00	96.56	"
Laboratory	standard	"	200.00	0.25	0.40	5.00	144.80	"
Laboratory	standard	"	200.00	0.25	0.40	5.00	144.80	"
Laboratory	standard	"	200.00	0.25	0.40	5.00	144.80	"
Laboratory	standard	"	200.00	0.25	0.40	10.00	185.12	"
Laboratory	standard	"	200.00	0.25	0.40	10.00	185.12	"
Laboratory	standard	"	200.00	0.25	0.40	10.00	185.12	"
Laboratory	standard	"	200.00	0.25	0.40	10.00	185.12	"
Laboratory	standard	"	200.00	0.25	0.40	15.00	241.40	"
Laboratory	standard	"	200.00	0.25	0.40	15.00	241.40	"
Laboratory	standard	"	200.00	0.25	0.40	15.00	241.40	"
Laboratory	standard	"	200.00	0.25	0.40	15.00	241.40	"
Laboratory	standard	"	200.00	0.25	0.50	2.00	64.40	"
Laboratory	standard	"	200.00	0.25	0.50	2.00	64.40	"
Laboratory	standard	"	200.00	0.25	0.50	2.00	64.40	"
Laboratory	standard	"	200.00	0.25	0.50	5.00	112.16	"
Laboratory	standard	"	200.00	0.25	0.50	5.00	112.16	"
Laboratory	standard	"	200.00	0.25	0.50	5.00	112.16	"
Laboratory	standard	"	200.00	0.25	0.50	5.00	112.16	"
Laboratory	standard	"	200.00	0.25	0.50	10.00	165.60	"
Laboratory	standard	"	200.00	0.25	0.50	10.00	165.60	"
Laboratory	standard	"	200.00	0.25	0.50	10.00	165.60	"
Laboratory	garford bulb	"	200.00	0.30	0.40	2.00	183.70	"
Laboratory	garford bulb	"	200.00	0.30	0.40	2.00	115.70	"

Field and laboratory pull-out test results

Test	Cable type	Medium	E(GPa)	Length(m)	w:c ratio	Stress (MPa)	k(MN/m/m)	Source
Laboratory	garford bulb	"	200.00	0.30	0.40	2.00	183.70	Moossavi(97)
Laboratory	garford bulb	"	200.00	0.30	0.40	2.00	183.70	"
Laboratory	nutcase	"	200.00	0.30	0.40	2.00	226.00	"
Laboratory	nutcase	"	200.00	0.30	0.40	2.00	226.00	"
Laboratory	nutcase	"	200.00	0.30	0.40	2.00	226.00	"
Laboratory	nutcase	"	200.00	0.30	0.40	2.00	226.00	"
Laboratory	garford bulb	"	200.00	0.30	0.40	5.00	205.30	"
Laboratory	garford bulb	"	200.00	0.30	0.40	5.00	205.30	"
Laboratory	garford bulb	"	200.00	0.30	0.40	5.00	205.30	"
Laboratory	garford bulb	"	200.00	0.30	0.40	5.00	205.30	"
Laboratory	garford bulb	"	200.00	0.30	0.40	5.00	218.00	"
Laboratory	nutcase	"	200.00	0.30	0.40	5.00	211.70	"
Laboratory	nutcase	"	200.00	0.30	0.40	5.00	211.70	"
Laboratory	nutcase	"	200.00	0.30	0.40	5.00	211.70	"
Laboratory	nutcase	"	200.00	0.30	0.40	5.00	211.70	"
Laboratory	garford bulb	"	200.00	0.30	0.40	10.00	224.00	"
Laboratory	garford bulb	"	200.00	0.30	0.40	10.00	224.00	"
Laboratory	garford bulb	"	200.00	0.30	0.40	10.00	224.00	"
Laboratory	garford bulb	"	200.00	0.30	0.40	10.00	224.00	"
Laboratory	nutcase	"	200.00	0.30	0.40	10.00	261.70	"
Laboratory	nutcase	"	200.00	0.30	0.40	10.00	261.70	"
Laboratory	nutcase	"	200.00	0.30	0.40	10.00	261.70	"
Laboratory	nutcase	"	200.00	0.30	0.40	10.00	261.70	"
Laboratory	garford bulb	"	200.00	0.30	0.40	15.00	230.00	"
Laboratory	garford bulb	"	200.00	0.30	0.40	15.00	230.00	"

Field and laboratory pull-out test results

Test	Cable type	Medium	E(GPa)	Length(m)	w:c ratio	Stress (MPa)	k(MN/m/m)	Source
Laboratory	garford bulb	"	200.00	0.30	0.40	15.00	230.00	"
Laboratory	garford bulb	"	200.00	0.30	0.40	15.00	230.00	"
Laboratory	nutcase	"	200.00	0.30	0.40	15.00	297.70	"
Laboratory	nutcase	"	200.00	0.30	0.40	15.00	297.70	"
Laboratory	nutcase	"	200.00	0.30	0.40	15.00	297.70	"
Laboratory	nutcase	"	200.00	0.30	0.40	15.00	297.70	"
Laboratory	nutcase	"	200.00	0.30	0.40	15.00	297.70	"
Laboratory	garford bulb	"	200.00	0.30	0.40	20.00	291.30	"
Laboratory	garford bulb	"	200.00	0.30	0.40	20.00	291.30	"
Laboratory	garford bulb	"	200.00	0.30	0.40	20.00	291.30	"
Laboratory	garford bulb	"	200.00	0.30	0.40	20.00	291.30	"
Laboratory	nutcase	"	200.00	0.30	0.40	20.00	311.50	"
Laboratory	nutcase	"	200.00	0.30	0.40	20.00	311.50	"
Laboratory	nutcase	"	200.00	0.30	0.40	20.00	311.50	"
Laboratory	nutcase	"	200.00	0.30	0.40	20.00	311.50	"
Laboratory	garford bulb	"	200.00	0.30	0.40	30.00	291.30	"
Laboratory	garford bulb	"	200.00	0.30	0.40	30.00	291.30	"
Laboratory	garford bulb	"	200.00	0.30	0.40	30.00	291.30	"
Laboratory	nutcase	"	200.00	0.30	0.40	30.00	291.30	"
Laboratory	nutcase	"	200.00	0.30	0.40	30.00	291.30	"
Laboratory	nutcase	"	200.00	0.30	0.40	30.00	291.30	"
Laboratory	Standard	Steel	200.00	0.24	0.40	0.00	57.30	Khan (1995)
Laboratory	Standard	Concrete	12.00	0.24	0.40	0.00	52.10	"
Laboratory	Standard	PVC	3.00	0.24	0.40	0.00	18.75	"
Laboratory	Standard	Charnockle	60.00	0.20	0.40	0.00	26.00	"

Field and laboratory pull-out test results

Test	Cable type	Medium	E(GPa)	Length(m)	w:c ratio	Stress (MPa)	k(MN/m/m)	Source
Laboratory	Standard	Granite	65.00	0.20	0.40	0.00	15.00	"
Laboratory	standard	Gabbro	60.00	0.20	0.40	0.00	21.10	"
Laboratory	Standard	PVC	3.00	0.14	0.40	2.00	17.00	"
Laboratory	Standard	PVC	3.00	0.14	0.40	5.00	20.40	"
Laboratory	Standard	PVC	3.00	0.14	0.40	7.00	17.00	"